Università Campus Bio-Medico di Roma

Corso di dottorato di ricerca in Bioingegneria e Bioscienze
XXXII ciclo a.a. 2016-2017

A bio-cooperative approach for upper limb robot-aided rehabilitation

Francesco Scotto di Luzio

Coordinatore:
Prof. Giulio Iannello

Tutore:
Prof. Loredana Zollo
Co-Tutore:
Dott. Francesca Cordella

12 Marzo 2020

Ai miei Genitori,
sempre accanto a me ad ogni traguardo raggiunto,
perché grazie ai loro Sacrifici ed al loro Amore
mi hanno aperto nuovi orizzonti.

Acknowledgements

In the beginning, I would say thanks to my supervisor Prof. Loredana Zollo to guide me well throughout the research work from title's selection to finding the results. Apart from my Supervisor, I won't forget to express the gratitude to Dr. Francesca Cordella, for giving the encouragement and sharing insightful suggestions. They all have played a major role in polishing my research writing skills.

I would always remember my fellow lab-mates too for the fun-time we spent together, sleepless nights that gave us the courage to complete tasks before deadlines and for stimulating the discussions.

In the end, I am grateful to my parents Giuseppe and Angela and my brother Gennaro who gave me enough moral support, encouragement and motivation to accomplish the personal goals. I consider myself nothing without them. They have always supported me financially so that I only pay attention to the studies and achieving my objective without any obstacle on the way.

Abstract

The design of patient-tailored rehabilitative protocols has a crucial role both in the clinical and research fields. Moreover, the inclusion of the patient in the robot control loop and a control strategy adaptable to the user's requirements are expected to significantly improve functional recovery in robot-aided rehabilitation.

Ambition of this thesis is to design and develop of a bio-cooperative platform for upper limb robot-aided rehabilitation based on human-in-the-loop approach. The proposed platform is composed of an end-effector robot arm, a purposely developed arm-weight support of patient limb and a multimodal interface to constantly monitor patient status. It is equipped with sensors that allow recording kinematic, kinetic and physiological data both during the evaluation phase of the patient and during the rehabilitation treatment. It is capable of adapting therapy characteristics to specific patient needs, thanks to biomechanical and physiological measurements, and thus closing the subject in the control loop. The level of arm-weight support and the level of the assistance provided by the end-effector robot are varied on the basis of muscular fatigue and biomechanical indicators. An assistance-as-needed approach is applied to provide the appropriate amount of assistance.

An overview of the validated tools for patient evaluation, used both in the clinical setting and in research, was presented. In addition, sensory systems, such as position/force, magneto-inertial (M-IMU) and electromyographic (EMG) sensors, and indicators extracted from these signals, presented in the state-of-the-art, were analyzed. Among these, muscular hand synergies in chronic stroke patients have been investigated in combination with robot-aided rehabilitation. The results show a good similarity of muscle patterns between the affected and the healthy hand of the same subject. Furthermore, following the robot-mediated rehabilitation, the muscular synergies of the affected hand they tend to look like those of the healthy limb. Muscle synergies can also be a useful tool for assessing the patient's status, especially in patients with mild and moderate impairment.

The platform and the adopted control strategy have been tested on 8 healthy subjects performing point-to-point 3D movements. The trajectory executed by the forearm support has been monitored to assess the performance of the chosen control approach. Moreover, a questionnaire based on the Likert rating scale has been submitted to the subjects to evaluate

the overall platform. Preliminary results showed that the proposed control algorithm allowed to follow the arm movement in 3D space with a reduced position error. Moreover the subjects felt their arm completely supported, free to move in any direction of the space and judged the platform easy to use.

The proposed bio-cooperative approach has been experimentally validated on 10 healthy subjects; they performed 3D point-to-point tasks in two different conditions, i.e., with and without assistance-as-needed. The results have demonstrated the capability of the proposed system to properly adapt to real needs of the patients. Moreover, the provided assistance was shown to reduce the muscular fatigue without negatively influencing motion execution.

Repetitive and intensive exercises are the main features of robot-aided rehabilitation, but they may expose patients to inappropriate and unsafe postures. The introduction of a sensory feedback can help the subject to perform the rehabilitation task with an ergonomic posture. A preliminary evaluation on eight healthy subjects shows that the use of the proposed platform allowed subjects to execute highly controlled movements while maintaining an ergonomic posture able to limit the trunk compensatory movements during reaching. The introduction of visual and vibrotactile feedback in the proposed robotic platform for upper limb rehabilitation has been proposed to ensure ergonomic posture during rehabilitation. The two feedback modalities have been used to provide information about incorrect neck and trunk posture. Ten healthy subjects have been involved in this study. Each of them performed 3D reaching movements with the aid of the robotic platform in three different conditions, i.e. without feedback, with visual feedback and with vibrotactile feedback, and a comparative analysis has been carried out to evaluate feedback effectiveness, acceptance and performance. Experimental results show that in case of no feedback the subjects reach and maintain configurations that can lead to incorrect neck and trunk configurations and therefore, if repeated, to musculoskeletal disorders. Conversely, with visual or vibrotactile feedback, the subjects tend to correct inappropriate posture with both trunk and head during task performing.

The proposed bio-cooperative platform is currently adopted in a clinical trial on 10 workers suffering from humerus fracture and subjects in aftermath of surgical repair of rotator cuff injury. The objective is to verify the efficacy of the proposed platform for robot-aided rehabilitation of the upper limb in workers affected by musculoskeletal pathologies.

Table of contents

List of figures

List of tables

Chapter 1

Introduction

Robot-aided rehabilitation is a technique of using robotic platforms to administer physical therapy to patients, able to provide repetitive, intensive and task-specific training for recovering limb functionality. In the last decades, the development of novel platforms for robot-aided rehabilitation provided fundamental tools to allow objectifying therapy, repeating exercises many times and objectively evaluating subject performance.
Several platforms for robot-mediated rehabilitation are present in the state-of-the-art, for motor deficits in both upper and lower limbs due to various diseases, such as stroke, cerebral palsy [47], multiple sclerosis [10], spinal cord injury [109], and others. Moreover, robotics and novel technologies might represent a new frontier of devices able to treat musculoskeletal disorders (MSDs) to accelerate recovery of work-injured people for a quick reinsertion in their workplace [33, 106].
Important requirements to be addressed by robots for rehabilitation are: i) safety of the patient, which has to closely interact with the system [9]; ii) not hampering patient movements; iii) maximization of patient involvement; iv) adaptation of the robot control architecture, i.e. of the robot behaviour, to patient needs.
In the field of rehabilitation robotics, *bio-cooperative* robotic systems represent a novel generation of robotic platforms that promote a mutual human-robot interaction based on multimodal interfaces [95]. An overview of bio-cooperative robotic platform is shown in Fig. 1.1. More in detail, the patient is the crucial part of the control loop: he/she interacts with a robotic platform and/or a virtual environment and sensors are used to estimate subject state and adapt the level of assistance on the basis of patient performance (the so-called human-in-the-loop approach). The peculiarity of a bio-cooperative robotic platform is the inclusion of physiological and psychological measurements of the patient state into the control loop together with biomechanical data. Data coming from sensory information provided by biomechanical, physiological and psychological measurements, as well as intentions and

environmental factors, may contribute to provide a continuous feedback on patients' global conditions [78]. As a result, robotic assistance can be dynamically changed on the basis of the subject's needs according to global measures of his/her state provided by multisensory monitoring systems [65]. Strategies based on this approach provide the so called assistance-as-needed to the patients. In [77], biomechanical and psychophysiological measurements are used for including the human-in-the-loop; in [32], psychophysiological feedback has been used to develop a human-centered approach aimed to customize the therapy on patient requirements and state, without affecting stress level and health. In [80], psychophysiological measurements have been used for improving the challenge/skill ratio experienced by the user during the interaction with a multimodal interface in a cooperative scenario. Trajectory error with respect to a desired motion path are used in [48] to measure motion accuracy and accordingly adjust the level of robot assistance. Other online approaches vary the amount of assistance depending on the obtained performance [60] or the application scenario [24, 112]. Although the bio-cooperative platforms presented in the state-of-the-art demonstrate the need to investigate this approach in order to provide the correct level of assistance to the patient, is evident the lack of a complete picture of the subject state and his/her complete integration inside the control loop of the robotic platform taking into account the performance of the patient during the execution of the task.

In this perspective, the design and development of a bio-cooperative platform for upper limb robot-aided rehabilitation based on human-in-the-loop approach is the main ambition of this work.

These platforms use multisensory monitoring systems to control their multiple degrees of freedom, ensure maximum safety conditions during interaction with humans, objectively assess patient performance during therapy and correspondingly dynamically adapt robot behavior. The bio-cooperative platforms are equipped with internal sensors that allow recording kinematic and kinetic data both during the evaluation phase of the patient and during the rehabilitation treatment. They are also enriched with additional wearable sensors such as surface electromyographic sensors (sEMG), magneto-inertial sensors (M-IMU), electroencephalography (EEG), Electrooculography (EOG), eye-tracking and physiological sensors to measure, for instance, respiration (RR) and heart rate (HR). Evidently, the so-called *multimodal interface* plays a key role in the design and development of the bio-cooperative platform. It consists of several sensor subsystems that allow continuous monitoring of the user, recording and providing data during the therapy, feedback to the user, maximizing his/her involvement.

The main limitation in the state-of-the-art is the lack of a standard in the determination of indicators that allow to delineate the patient state during the interaction with the robot. This

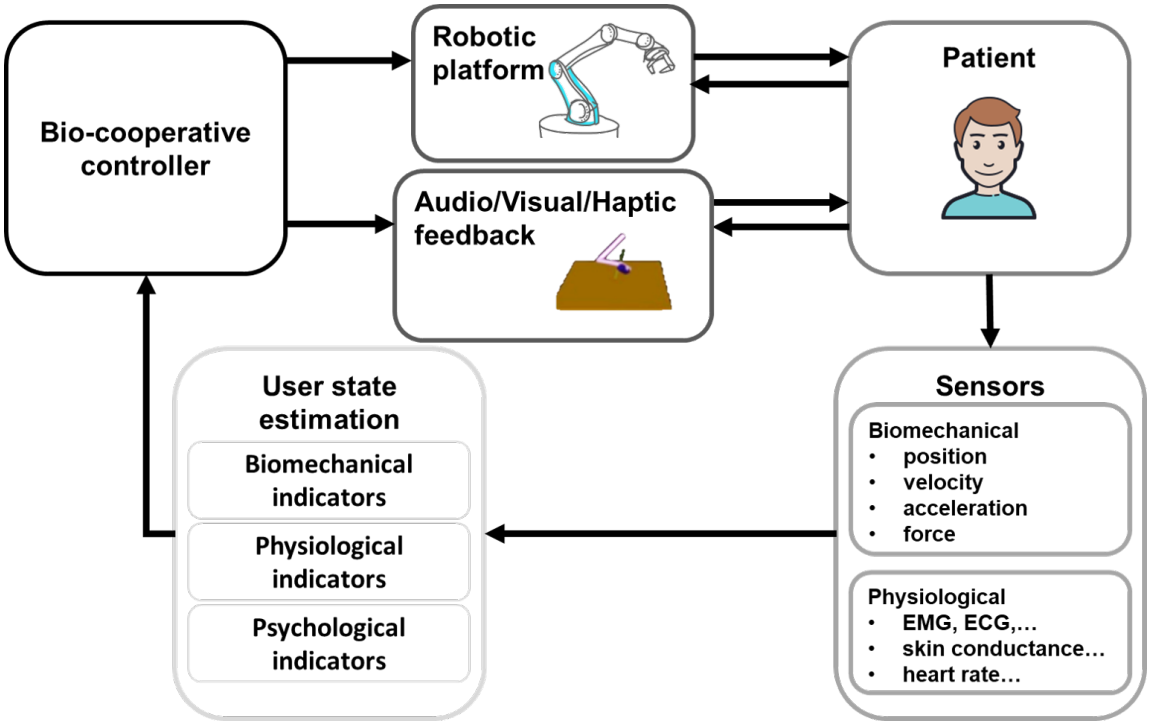

Fig. 1.1 A general overview of a bio-cooperative robotic platform.

aspect is of fundamental importance, because it allows describing the state of the user and defining the exact level of assistance necessary for the patient. Furthermore, although muscle fatigue has already been extensively analyzed, both for isometric and dynamic contractions also during human-robot collaboration tasks, the use of this indicator during robot-mediated rehabilitation to assess muscle fatigue during therapy has not still been investigated.

For these reasons, the first contribution of this thesis is to propose a novel multimodal interface able to record simultaneously patient data from different sensors, such as position/force, M-IMU and EMG data, and develop a sensor fusion algorithm in order to extract performance indicators and describe biomechanical and physiological patient status both during and after the interaction with the robot, as sensors and user state estimation modules presented in Fig. 1.1. The proposed solution includes the patient in the control loop by continuously monitoring his/her state, extracting objective biomechanical and electromyographic indicators and consequently adapting the level of assistance provided by the robotic platform. In particular, subjects performance and muscular fatigue are taken into account to shape the level of assistance on the patient's specific characteristics guaranteeing a patient-tailored therapy with an assistance-as-needed approach. Moreover, an analysis of hand muscular synergies of stroke patients have been performed, in order to investigate hand

Francesco Scotto di Luzio

muscular patterns of the subjects affected by stroke and perform a detailed evaluation of stroke patients treated with robot-aided rehabilitation.

Patient-centered approaches are expected to drastically increase patients' engagement in robotic therapy resulting in better motor and functional recovery, compared to the previous studies reported in the field. Nevertheless, the majority of end-effector robots for rehabilitation [57] are normally equipped with *simple* position controllers that constrain subject's upper extremities to follow predefined trajectories [61, 76] without having a complete picture of the patient state. Furthermore, the gravity effect due to the weight of the upper limb are often not considered. Supporting the weight of the subject limb during rehabilitation appears to be a key point in post-stroke rehabilitation limiting the unhealthy effects of abnormal synergies thus permitting a greater range of motion [40, 75]. In [4] it has been demonstrated that a gravity compensation strategy based on sling suspension led to an improvement of arm function of stroke patients after 9 weeks of training. Therefore, the sole application of gravity compensation might be a valuable strategy to foster functional improvement in post stroke subjects. Exoskeleton robots can provide compensation of the arm weight and apply forces to several segments of the arm to help the subject in performning the desired task [52]. The main drawbacks of these systems are the reduced adaptability to subject's different anthropometry, the passive gravity compensation, the significant amount of time needed to setting-up the device for a particular patient and therefore the complexity of the control algorithms [59]. End-effector devices can overcome the limitations of exoskeleton robots related to anthropometry adaptability, facility in setting-up and control algorithm complexity. The main drawback of these systems is that the arm support is provided depending only on spatial limbs configuration since gravity torque of upper limb is highly coupled with its dynamics. Therefore, subjects' voluntary participation and their muscular activation patterns might be affected.

Hence, the second contribution of this thesis is to design and develop a bio-cooperative control algorithm able to: i) perform different tasks for robot-aided rehabilitation safely for the user; ii) support the affected arm of the patient in order to prevent excessive biomechanical stress and muscle fatigue; iii) adapt to patient condition thanks to performance indicators computed by multimodal interface, as bio-cooperative controller and robotic platform modules presented in Fig. 1.1. The proposed bio-cooperative control algorithm is purposely developed for upper limb robot-aided 3D rehabilitation platform composed of an end-effector robot and an arm-gravity support able to overcome literature limitations. It integrates patient status evaluated by the multimodal interface and controls robot and arm-gravity support in order to provide the correct level of assistance to the patient.

Moreover, several systems have been proposed in literature to objectively evaluate the patient's behaviour during a rehabilitation session and provide them with a feedback related to the correctness of the exercise. Sensory feedback has an important role in rehabilitation; it promotes a higher level of user participation in the task accomplishment than traditional therapy, thanks to the stimuli the user is provided with. In fact, the feedback on the results and/or performance achieved during the robotic training simplifies the execution of the target movement and promotes subject involvement in the rehabilitation exercise [104]. During robot-aided rehabilitation, it is always necessary to provide a visual feedback to the subject during the execution of the task, in order to maximize his/her involvement during the task with an engaging task, making the most of all the potential offered by robotic devices. Additionally, it is important to make sure that the patient does not assume incorrect positions during the interaction with the robot and possibly provide integrated feedback to the patient in order to promote autonomous correction of incorrect posture. In this case, the user should be stimulate for a better posture control and improve the exercise performance. Methods proposed for postural assessment can be based on wearable and non wearable devices and can be evaluated on the basis of the level of intrusion caused by the devices themselves [107]. Non-wearable devices, such as marker-based motion capture systems, are cumbersome and constraint the motion. Non marker-based systems, such as RGB-D cameras [14], require an environment with good illumination conditions, where the occlusion between the worker's body and the tools used for working are limited. Furthermore, their accuracy does not consent high precision in angle reconstruction. Wearable sensors such as magnetoinertial and electromyographic sensors [53], smart textile [87] or Hall effect sensors [16] can represent a valuable alternative to provide a quantitative measure of patient posture. The main limitations of the proposed solutions are the difficulty of daily usage, due to bulky sensors and wires, or to the limited number of monitored degrees of freedom [31].

The third contribution of this thesis is to propose a novel feedback module able to show the execution of robot-aided task to the user and provide visual and/or vibrotactile feedback stimulation when incorrect postures are assumed, as audio/visual/haptic feedback module presented in Fig. 1.1. The proposed solution is based on a modular virtual reality module, integrated in the architecture introduced in the Fig. 1.1, able to show to the user the rehabilitation task to be performed in both 2D and 3D environments. It also adopts three inertial sensors to evaluate head and trunk posture. One M-IMU is positioned on a fixed part such as the chair using for the treatment and acts as reference. The other two M-IMU sensors are located on the head and trunk of subject and are used to measure trunk and neck flexion/extension (F/E), respectively. Information about user incorrect posture is provided by specifically designed indicators in the virtual environment and/or two lightweight

vibrating actuators located on the user's arms.

Thesis organization

Some of the contents included in this thesis are taken from conference and journal papers previously published by the author of this work. To summarize, the thesis is structured as follows:

- In Chapter 2 an overview of the patient assessment tool used in clinical setting are presented and the main performance indicators presented in the state-of-the-art for quantitative evaluation of patient status are shown. Moreover, an analysis of muscular synergies of the hand in combination with robot-aided rehabilitation is presented. Subsequently, the experimental setup and protocol is reported and experimental results are discussed.
- In Chapter 3 a novel bio-cooperative platform for robot-aided 3D upper limb rehabilitation composed of an end-effector robot and an arm-gravity support and its control algorithms are presented. Hence, the experimental setup and protocol used to validate the proposed approach is reported and experimental results are discussed. Part of the contents included in this chapter are already published in [91] and [20].
- In Chapter 4 a visual and vibrotactile feedback module for the proposed bio-cooperative platform is presented. Therefore, a comparison of the two feedback modalities is performed in order to evaluate their effectiveness to improve patients posture in robot-aided rehabilitation treatments and their acceptability. The experimental setup and protocol used to validate the proposed approach is reported and experimental results are discussed. Part of the contents included in this chapter are already published in [19] and [90].
- In Chapter 5 conclusions and final considerations are reported.

Chapter 2

Quantitative assessment and muscle synergies in chronic stroke

Abstract

Patient evaluation plays a crucial role in the rehabilitation context. In the clinical setting, the evaluation is carried out with validated clinical scales, however this type of evaluation is not free from errors and requires highly specialized personnel. The recent development of new technologies has allowed the use of new systems for the quantitative evaluation of the subject's performance. The data recorded by the sensors can be used to derive performance indicators. Among these, muscle synergies can represent a valid indicator of muscle patterns during robot-mediated therapy.

2.1 Assessment of patient status

2.1.1 Introduction

The clinical evaluation of the patient plays a fundamental role in the rehabilitation treatment for both traditional and robot-aided therapies. Clinical assessment can be defined as a complete evaluation of the clinical condition of the subject carried out by a medical staff also through validated clinical scales, which are mainly subjective evaluation's tools, thus suffering from a series of hindrances. In the literature there are many validated clinical scales normally used in clinical practice. A clinical evaluation tool should be sensitive, validated and reliable in order to obtain high-quality measures. Furthermore, the selected clinical scale is appropriate for the patient if it is able to assess any differences in case of improvement or worsening of the patient's clinical conditions. Clinical scales are widely recommended as evaluation tools being integral part of the rehabilitation treatments. However, the use of such clinical scales has a series of hindrances that have to be considered. Scales are

subjective, i.e. operator-dependent, with discrete scores and limited to specific movement characteristics; in addition, they often have low sensitivity and require time-consuming administration procedures.

In this scenario, robotic systems can be useful tools not only to carry out therapy, but also to allow a quantitative assessment of the subject to be associated with clinical scales and medical evaluation. In this way it is possible to have an objective and repeatable measure in a simple and fast way of the clinical parameters, relieving the medical staff of an excessive workload and of measures often affected by errors.

During the rehabilitation treatment, the robot is able to apply forces to the patient's limb, favoring its mobilization. The robotic platforms can be used in different modalities, in order to maximize the active contribution of the patient and providing the minimum necessary assistance. To reach this goal, the machines available on the market have different training methods for the subject, based on the residual abilities of the subject and selected at the beginning of the treatment by the medical staff. It is possible to choose between four training modes:

- passive training: the subject is completely passive and the robot allows the subject to perform the task;
- active-assisted: the robot provides the assistance for the completion of the task only if the subject is not able to actively perform it.
- active training: the subject is completely active and independently moves the robot in order to perform the task
- resistance-training: the subject performs the task against an external force which is opposed to the subject movement

In order to provide a patient-tailored rehabilitation, assist-as-needed approach has been investigated in different studies. It is based on providing the minimum level of assistance to the patient to complete the movement. The challenge is to select the correct amount of assistance and the difficulty of the task. To do this, the patient is constantly monitored during the execution of the task and the assistance provided by the robot is evaluated on the basis of patient performance. Therefore, as reported in Fig. 1.1, patient status monitoring plays a crucial role for this approach during the rehabilitation treatment. The monitoring module is composed of all the sensors of the robotic platform that return data useful for defining the status of the patient during therapy. As shown in Fig. 2.1, the data acquired during the treatment can be of different nature and can be classified into two macro-categories:

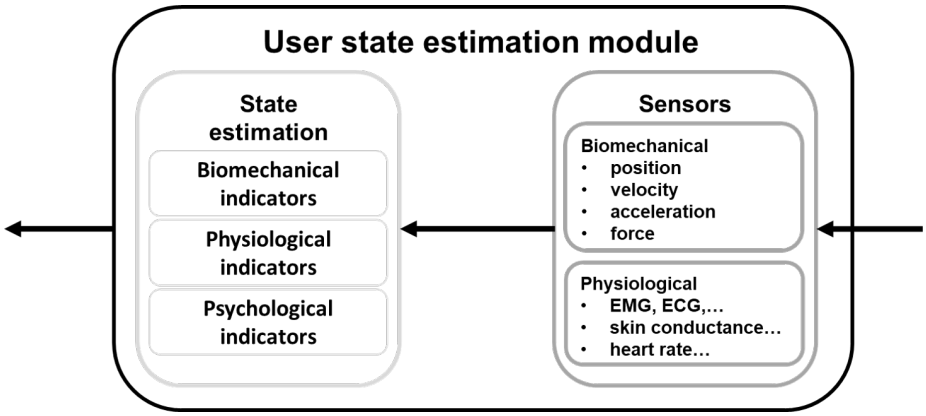

Fig. 2.1 Block scheme of the user state estimation module included in the patient-in-the-loop approach.

Biomechanical measurements such as position, velocity, acceleration and forces obtained through position/force sensors embedded into the robot or wearable sensors or positioned in the environment such as RGB cameras and optoelectronic system

Physiological measurements obtained from biological signals such as EMG, EEG, EOG, heart and respiration rate, skin conductance, temperature and blood pressure.

These data are recorded and used to compute the correct level of assistance to the patient, in order to build an assistance tailored on the current state of the user and his/her residual abilities. Starting from biomechanical and the physiological data, the definition of the correct level of assistance is not so trivial. Indeed, different indicators have been presented in the literature, in order to establish an estimator of the user state for the bio-cooperative controller and improve the interaction between the patient and the robotic system.

Robot-assisted performance indicators are mainly divided into kinematics, kinetics and neuromechanics indicators. Kinematics indicators evaluate subject's movement in spatial and temporal domains and can be defined either in Cartesian space or in the arm joint space; kinetic indicators measure the force, work, power and energy consumption exerted by the patient during the movement. Finally, neuromechanical indicators allow to estimate viscoelastic characteristics or mechanical impedance of upper limb at rest. However, performance indicators are strictly related to the motor task they are conceived for, , although there are some of them that can be used for all motor tasks; they can be calculated both online and offline during task execution, on the basis of their different computational costs. Furthermore, traditional robotic therapy does not actively include the patient in the control loop and the level of assistance provided by the robot is not adjusted on the level of performance of each patient. Obviously this aspect reduces the role of the platform to a basic movement along predefined trajectories. The inclusion of the data acquired during the therapy and the

computed indicators allow to tailor the therapy on the specific needs of each patient and considerably increase the patient's involvement during the therapy.

Some preliminary results of the inclusion of the patient's status in the platform control loop have already been presented in the literature. In [67] Novak et al. introduced psychophysiological measurements in the feedback loop for upper extremity rehabilitation. In this work, the robotic platform for upper limb post stroke rehabilitation is able to adapt the level of the assigned task on the basis of data extracted from physiological measurements. Guerrero et al. in [32] included data from three physiological channels to update and maintain therapy level as intensive as possible. Experimental tests on eight healthy subjects showed that the use of a bio-cooperative control system may increase the engagement of the user by modulating motor effort. The findings in the state-of-the-art about the inclusion of physiological measurements in performance metrics show that they only induce a few improvements in estimating user needs [45]. From this analysis it is clear that the use of such approaches is still limited and the obtained results are preliminary. Moreover, the lack of a standardized protocol for the choice of performance indicators is evident, fundamental for obtaining satisfactory outcomes at the end of the rehabilitation protocol and in order to select the correct level of assistance [95].
For these reasons, the aim of the first part of the Chapter is to give a complete overview of the patient assessment tool used in clinical setting and show the main performance indicators presented in the state-of-the-art for quantitative evaluation of patient status.

2.1.2 Traditional assessment of patient status

The traditional clinical evaluation of the patient status is carried out by medical staff using validated clinical scales. There are different types of clinical scales that are used to obtain an assessment of the patient. The reasons for the administration of the clinical scale can be multiple: to program rehabilitation intervention, to evaluate rehabilitation results, to do a cost-effectiveness analysis of the rehabilitation program or for research scope (Fig. 2.2).

However, for an effective administration of this assessment tool, trained and experienced personnel are required to highlight and signal the patient's difficulties. The scales differ from each other since they may address several rehabilitation assessment aspects, distinguishing among body function/structure, activity and participation in life/society. Figure 2.3 reports an overview of the main features of clinical assessment tools. A clinical scale should be appropriate for the pathology of function to be evaluated, reliable to avoid errors and allow the repeatability of the measurement. Important aspects are also the validity and sensibility in order to be able to measure what we want and to identify the variations in the clinical picture of the patient.

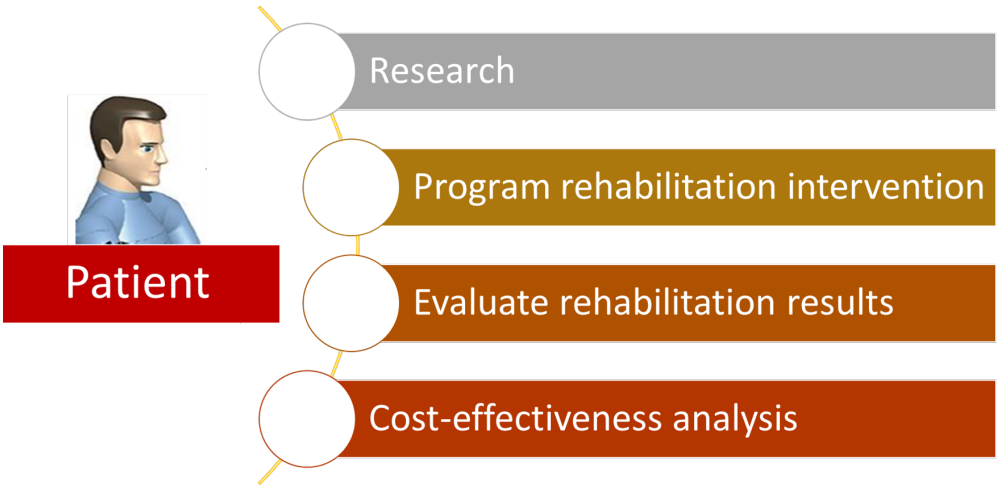

Fig. 2.2 Some of the main reasons for using a clinical scale.

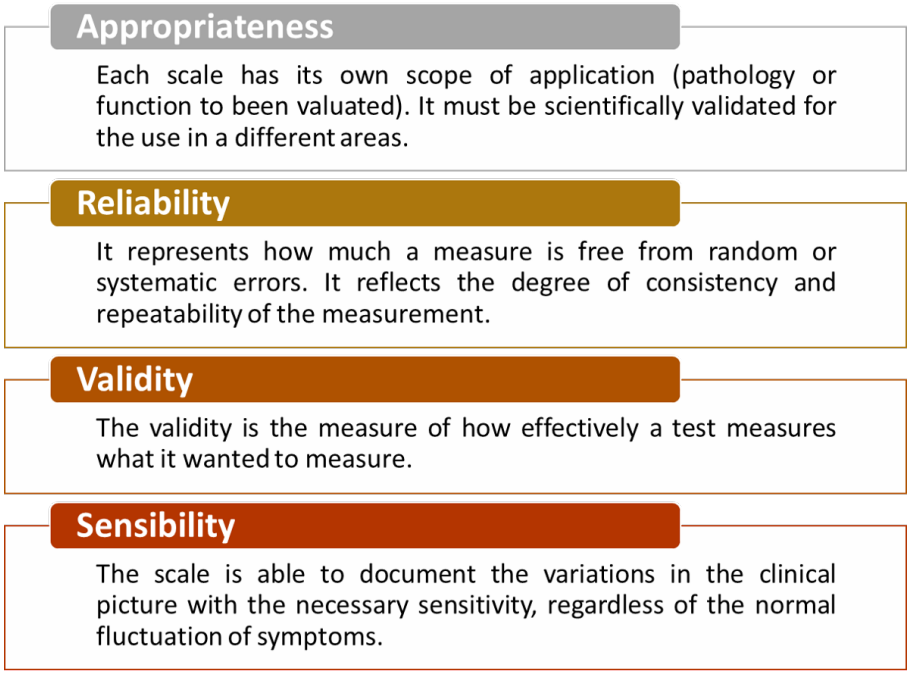

Fig. 2.3 An overview of the main features for clinical assessment tools.

As suggested in [51], in order to have a complete overview of the clinical evaluation tools, they can be divided into three groups:

- Time-Based (TB) assessments: the subject is evaluated based on the time taken to perform an assigned task. An example of TB assessment is the Nine Hole Peg Test [63]. This assessment consists in measuring hand manipulation dexterity moving nine pegs from a small box to a corresponding hole as fast as possible;
- Performance-Based (PB) assessments: the subject is evaluated in terms of ability to perform a standardized task. An example of PB assessment is the Fugl-Meyer Assessment [27], in which the subject is asked to perform some basic actions involving both upper and lower limbs and measure data about range of motion, balance, sensation and pain;
- Impairment-Based (IB) assessments: the subject is evaluated in terms of his/her pathology/its aspects that cause a disability condition. An example of IB assessment is Modified Ashworth Scale [11], in which the patient is asked to keep passive and evaluate the perceived resistance on a numerical scale.

2.1.3 Quantitative assessment of patient performance

The rise in the incidence of neurological pathologies and the high percentage of orthopedic pathologies involving the upper limb have pushed research to develop innovative solutions to improve patient rehabilitation, guaranteeing a careful and detailed performance analysis. It has been shown that some factors such as high-intensive, repetitive and active training, play a fundamental role in the success of rehabilitation therapy.

Robotic devices have also a key role for evaluation purposes. Indeed, robotic platforms are equipped with different types of sensors that allow to obtain a quantitative measure of the task performed by the subject, guaranteeing a continuous monitoring of the patient. Rehabilitation robots are equipped with high-resolution sensors that allow accurate measurements of movement kinematics (i.e. upper limb trajectories) and kinetics (i.e. interaction forces), sometimes they also integrate additional sensors such as Inertial Measurement Unit (M-IMU) and surface Electromyographic sensors (sEMG). Patient's motion can be accurately monitored and evaluated by means of opportune performance indicators to be used together with the traditional clinical scales; such approach may lead to a more exhaustive and complete evaluation of patient's recovery. In the following Sect. 2.1.3.1 and 2.1.3.2, kinematic, kinetic and muscular parameters have been investigated in more details.

2.1.3.1 Kinematic and kinetic parameters

During robot-aided rehabilitation therapy, it is very useful to record data deriving from sensors embedded in the robot in order to obtain useful kinetic and kinematic information such as interaction force, active range of motion, movement smoothness, movement accuracy, movement velocity, motor coordination, and amount of robotic assistance. The challenge of modern robotic platforms is to make this data suitable for clinical purposes and for the patient himself, in order to increase the psychological involvement of the user who should be motivated to improve his/her residual capabilities in order to obtain better results. Several studies have been carried out with the purpose of monitoring kinematic parameters during robot-aided rehabilitation with stroke patients and their correlation with traditional clinical assessment tools. For example, significant results have been obtained in [13] with stroke patients about quantifing sensorimotor impairments. They found that the aiming angle is suitable to evaluate capability of users to perform point-to-point movements. Furthermore, in [38] a significant decrease in time to reach the peak speed suggests that this parameter is able to measure planning changes in different direction and gravitational influence. In [85], the use of peak speed and percentage time with respect to peak speed is proposed in order to manage movement planning in symmetrical bi-manual movement, they tested this approach on chronic stroke patients and obtained a decreasing in assistive force level. Finally, based on the classification reported in [66], a complete overview of kinematic and kinetic parameters is reported in Fig. 2.4, divided on the basis of the aspects to be monitored during the robot-patient interaction. Different kinematic parameters have been presented in the literature, in order to monitor patient performance and tailor the level of the assistance on the basis of his/her performance.

2.1.3.2 Muscular parameters

Robot-aided rehabilitation systems often integrate electromyographic (sEMG) sensors. Such a signal is produced by the contraction of the muscle and is detected by a non-invasive surface electrode positioned on the subject's skin: sensors are usually located in correspondence of the selected muscle. In recent years, sEMG signals have been used for evaluating the level of muscle contraction for various purposes, such as movement recognition, hand rehabilitation and gesture classification. This kind of data can be analyzed to detect muscle activity level and medical abnormalities in human biomechanics. This type of data represents the most simple and intuitive way to trigger the support provided by the robot. EMG-based robot adaptation is adopted if the subject is able to contract the muscles, but is not able to perform a complete movement [95]. In this case, sEMG signals can be used to trigger the movement

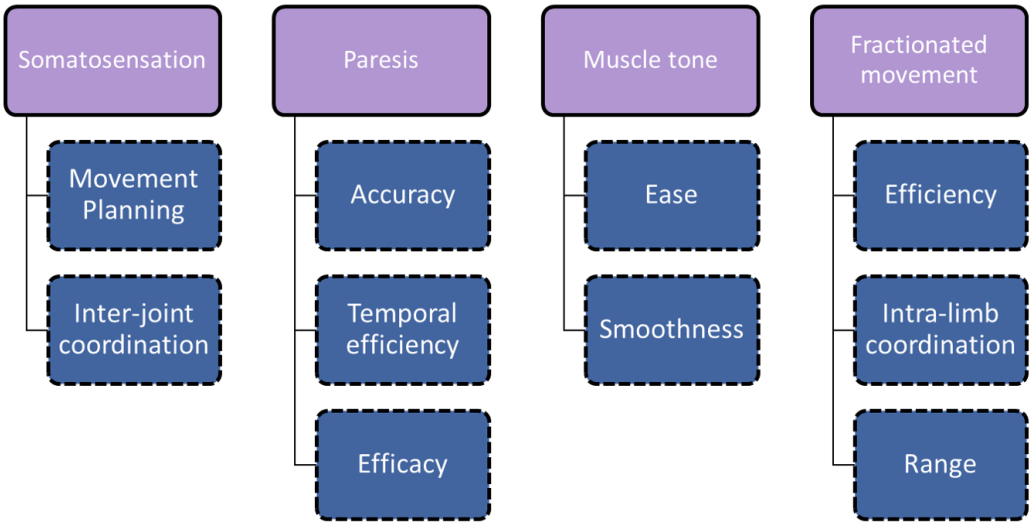

Fig. 2.4 An overview of kinematic and kinetic parameters adopted for patient assessment in robot-aided rehabilitation.

performed by the robot, to control robot movements through muscles contraction, or to vary the value of the assistance provided by the robot, as in [97]. Other online approaches vary the level of assistance based on the obtained performance [61] or the application scenario [25]. Furthermore, some researchers study surface electromyography of the upper part of the human arm to verify variability in different muscular position and different age group [1]. They analyzed the average, standard deviation and coefficient of variations to study the muscular activities that are useful for rehabilitation concerns. Different analysis have been performed in the state-of-the-art to monitor and evaluate muscular signals.

The EMG signals can be used to assess the muscular synergies of subjects subjected to robotic rehabilitation treatment. This approach makes it possible to highlight muscle patterns in both the upper and lower limbs on subjects who are healthy or have pathologies that limit the patient's movements such as stroke. For these reason, in the following section a detailed muscular synergies analysis during robot-aided rehabilitation in chronic stroke patients has been conducted.

Furthermore, sEMG signals can be used to evaluate muscular fatigue during the execution of a robot-aided rehabilitation task, as proposed in Chapter 3. To do this several indices have been presented in the state-of-the-art, such as Root Mean Square (RMS) and Median Frequency (MF) of EMG signals [30]. However, in the proposed approach the Dimitrov

Index (DI) was chosen because it guarantees a more accurate identification of the level of fatigue. The reason for this is evident by observing the Eq. 3.4 and taking into account that EMG signal in the presence of muscle fatigue increases in amplitude and moves towards the low frequencies. The definition of DI in fact allows to highlight these characteristics of the EMG signal, although it has the disadvantage of being defined in the frequency domain. DI was proposed for the first time by Dimitrov in [30], to monitor muscular fatigue. This is not the only method to estimate muscular fatigue, indeed different complex models have been proposed with this aim [58], but they often need an offline calibration and muscle force measurements. Although such models can provide a very accurate estimate of human muscle fatigue, their use in robotic applications is very limited, because of their computational costs. Peternel [73] proposed an approximate method for assessing fatigue level during human-robot collaboration tasks based on an RC circuit because the dynamic behavior of muscle fatigue reflects this simple behavior. In this case, the normalized capacitor voltage is equivalent to fatigue, the conductance of the resistor is equivalent to the current effort of the muscle and the muscle capacity is expressed in terms of resistance.

2.2 Muscle synergies in chronic stroke patients

2.2.1 Introduction

Motor coordination represents one of the most fascinating aspects of human nature. Central Nervous System (CNS) is able to control a very high number of degrees of freedom to perform complex movements of both upper and lower limbs [86]. However, what are the strategies that the CNS puts in place to perform complex tasks are not yet completely clear and are still being studied [2]. Many studies have highlighted the existence of motor primitives, which would allow the CNS to manage the complex architecture of the human body, guaranteeing complex movements starting from simple movements [96]. Among these, many researchers have investigated Muscular Synergies, a term from the Greek that means "working together", presented for the first time in a work of Bernestein as: "*...solution to the problem of selecting one movement among the infinite possibilities of motor solutions to perform a specific task...*". It has been suggested that complex movements are constructed through smaller blocks (i.e. muscular synergies), in order to overcome the difficulties related to the coordination of a high number of degrees of freedom [8, 96, 86]. As shown in Fig. 2.5, a muscle synergy can be considered as a small group of muscles whose activation patterns are predetermined. Each muscle can be part of different synergies and the combination of these simple patterns allows

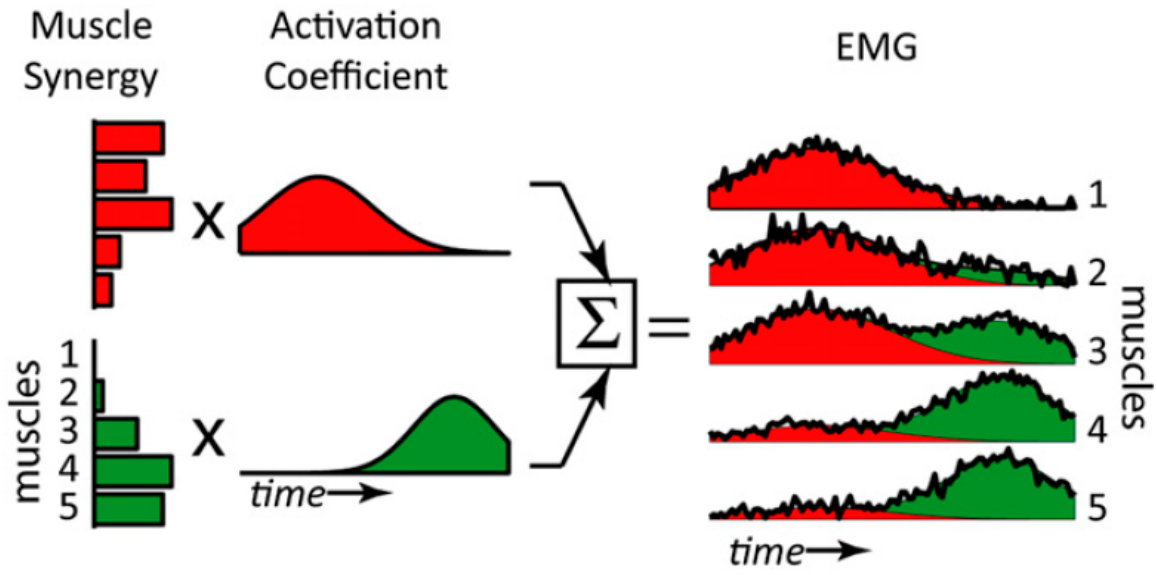

Fig. 2.5 A schematic illustration of the basic principle of muscle synergies (taken from [12]). Muscle synergies (i.e. the group of muscles contributions) are modulated by an activation coefficient. Their composition returns the EMG signal recorded during the execution of the movement.

generating complex movements through an activation coefficient that allows you to modulate the contributions of individual muscles [12].

In particular, the upper limb and the hand are very complex districts of our body that are able to perform very precise movements, such as grasping small objects [2]. A detailed understanding of the mechanisms governing such complex movements would have enormous implications in the rehabilitation and prosthetic fields. Muscle synergies are extracted from electromyographic (EMG) signals acquired from muscles involved in the movement. Surely, the monitoring of these muscle patterns would allow to have a quantitative picture of patients suffering from movement pattern disorders such as stroke and musculoskeletal pathologies in general. The synergies, together with the biomechanical, physiological data and the corresponding indices described in Sect. 2.1.3, could give a complete picture of the patient status. Furthermore, an advantage of this analysis is the non-invasiveness of the adopted sensors and the reduced computational cost, since the analysis and extraction of muscle synergies can be performed offline. Unfortunately there is not a defined protocol on how many and which muscles should be selected to analyze a certain movement or a certain synergy. This choice is left to the experience of the researcher who selects the muscles on the basis of the task to be performed.

Moreover, there are several algorithms to extract muscle synergies from EMG signals, such as Non-Negative Matrix Factorization (NNMF), Principal Component Analysis (PCA), Factory Analysis (FA) [102]. The first studies concerning muscle synergies aimed to demonstrate that motor control could be described by a set of muscle synergies. Several studies have been conducted on the number of synergies to be extracted and the stability of this method. From this point of view the results have been very promising and have pushed researchers to investigate in different fields of application ranging from sport, to clinic and robotics [100]. In several papers, muscle synergies in the lower limbs have been investigated for both walking and balance, in order to highlight elementary muscle patterns.
Several studies have been conducted on the alteration of the muscular synergies in subjects affected by stroke. In particular, the anomalies of the synergies of the upper limb in subjects with strong and moderate impairment were analyzed. The results showed a similarity between the synergies of the healthy and the affected limb. From the literature analysis, it is evident the presence of a particularly strong coupling of elbow flexion and shoulder movements in stroke patients which affect reaching movements.

Few studies have been devoted to explore the impact of stroke in motor control, to analyze how and how much robot-aided rehabilitation allows improving hand control and manipulation [12, 82, 81]. Furthermore, there are no studies analyzing the motor patterns of the hand of subjects affected by stroke, although it represents a tool of fundamental importance for the development of ADL and stroke can significantly alter the mobilization of this part of the body. Thanks to the approach adopted to extract them, muscle synergies are useful for the recognition of alterations during the execution of motor tasks, since they allow to highlight the contribution of the single components that constitute complex movements [96].

Progress beyond the SoA For these reasons, the aim of the second part of the Chapter is to investigate muscular synergies of the hand in combination with robot-aided rehabilitation. The progress compared to the state-of-the-art is twofold:

(i). to investigate the muscular synergies of the hand in subjects affected by stroke;

(ii). to highlight some possible benefits in the robot-mediated rehabilitation treatment of the hand in these subjects.

2.2.2 Non-invasive muscle synergies analysis in combination with hand robot-aided rehabilitation

Seven chronic stroke patients (mean age: 59.6 ± 12.8) with mild and moderate impairment (Fugl-Meyer: 35.4 ± 6.0 and Motor Power: 9.9 ± 5.1) have been involved in this study. Subjects had to perform treatment with Gloreha Sinfonia (IDROGENET, Brescia, Italy), a robotic glove for hand rehabilitation. At the beginning and the end of the course of treatment the subjects' electromyographic (EMG) signals were recorded to show any significant differences in the hand muscular synergies.

2.2.2.1 Gloreha Sinfonia

Gloreha Sinfonia ® is a robotic exoskeleton for robot-aided neuro-rehabilitation of the hand. It is composed of three independent modules:

- A motorized glove for hand mobilization driven by five permanent magnetic actuators (LA12 Actuator, TECHLINE). Each actuator commands the tension of a cable connected to the corresponding finger. This glove is controlled by a motor unit placed distant from patient, to maximize patient safety and ergonomics of the glove. Motor unit is connected to the computer by means of USB protocol.

- A sensorized glove in which five Bend-Sensors (Flexpoint Inc.) are positioned. The sensors are inserted in the glove (i.e. on the corresponding finger) in the correct position. Sensors are connected to an electronic board, that decodes signals and sends them to the computer by means of USB protocol.

- A software for acquiring sensors data and controlling motors, installed on a touchscreen computer. It integrates virtual reality environments to replicate activities of daily living (ADLs) in a simulated scenario. This software implements different kind of tasks, as grasping and moving objects. The motorized glove can be used as an independent module for passive mobilization of the hand or in combination with the sensorized glove in order to perform one-handed or bimanual tasks. Gloreha Sinfonia is equipped with two passive arm-weight supports fixed to an ergonomic table, in order to provide relief of limb weight force during the execution of the tasks.

Moreover, the software of the Gloreha Sinfonia is able to record success rate of different tasks to allow monitoring patient improvements.

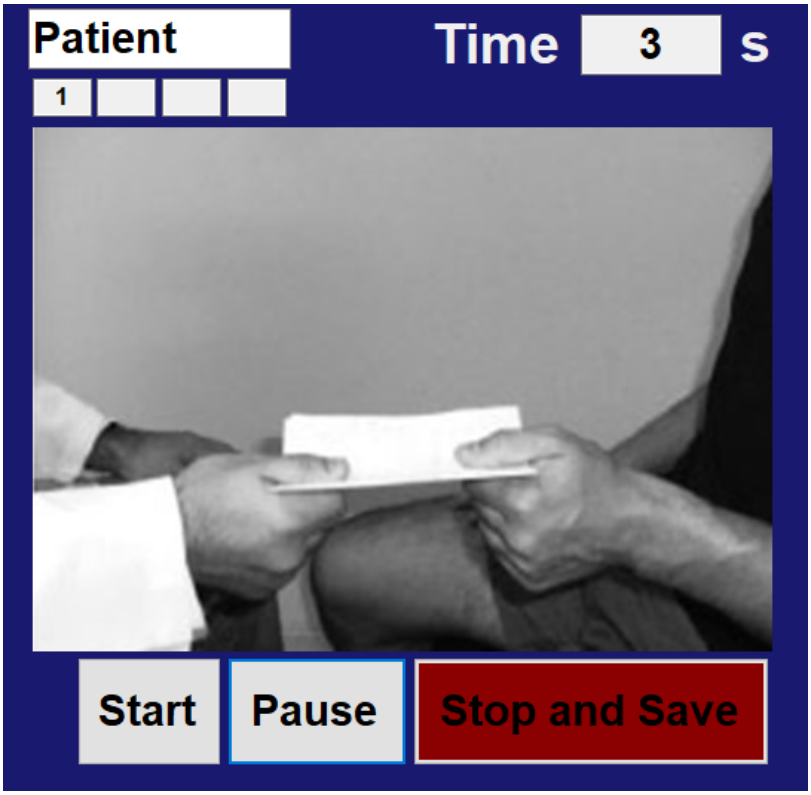

Fig. 2.6 The tasks performed by the patient.

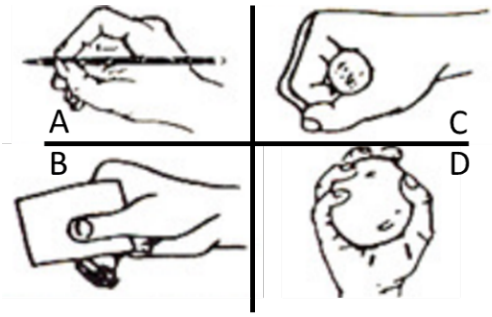

Fig. 2.7 The tasks performed by the patient: grasp a pencil (A), grasp a sheet (B), grasp a small can (C) and a tennis ball (D).

Francesco Scotto di Luzio

2.2.2.2 EMG acquisition and muscle synergies extraction

sEMG signals have been acquired from 6 muscles of the hand: Flexor Digitorum Superficialis (FDS), Exstensor Digitorum Superficialis (EDS), Flexor Pollicis Brevis (FPB), Abductor Pollicis Brevis (APB), Abductor Digiti Minimi (ADM), Exstensor Digiti Minimi (EDM). Before placing the electrodes, the hairs were removed from the skin surface and cleaned thoroughly with alcohol. sEMG data were collected at 1 kHz and stored for offline analysis. A visual inspection was performed to avoid the presence of artifacts that contaminated the signal. They were filtered with a sixth-order Butterworth filter with cutoff frequencies of (30,450) Hz and a second-order Butterworth notch filter (50 Hz) and then rectified to extract muscle synergies. Muscle synergies have been extracted from EMG signals by using the Non-Negative Matrix Factorization (NNMF) Algorithm. It was introduced for the first time by Lee and Seung and commonly adopted in the literature in order to identify muscle synergies and the corresponding weights as

$$E(t) = \sum_{i=1}^{n} (W_i * H_i(t)) + e \tag{2.1}$$

where $E(t)$ is a N x M EMG signals matrix (N muscles and M number of the samples), W is the N x S synergy matrix (S number of synergies) and H is the R x M coefficient matrix. Each column of W contains the weights of each muscle for the corresponding synergy and each row of H represents how much the corresponding synergy was activated or used to generate force.

For muscle synergies extraction, NMF algorithm was initialized with random matrices with elements belonging to a uniform distribution with values between 0 and 1, then updated until convergence, so that $R^2 < 0.01\%$. The synergy extraction were iterated 50 times for each limb of each subject and selected the synergies with the highest R^2 for further comparisons, because the obtained solutions for the synergies and their coefficients found by the algorithm may represent a local extremum on the R^2 surface. As in [12], the number of extracted synergies was chosen on the basis of r^2. The number of synergies N extracted from the EMG signal is the minimum value that returns r^2 at least equal to 80%.

2.2.3 Experimental validation

2.2.3.1 Experimental setup and protocol

Seven chronic stroke patients (mean age: 59.6 ± 12.8) have been involved in this study. As reported in Fig. 2.8, each of them carried out a robot-aided rehabilitation treatment with

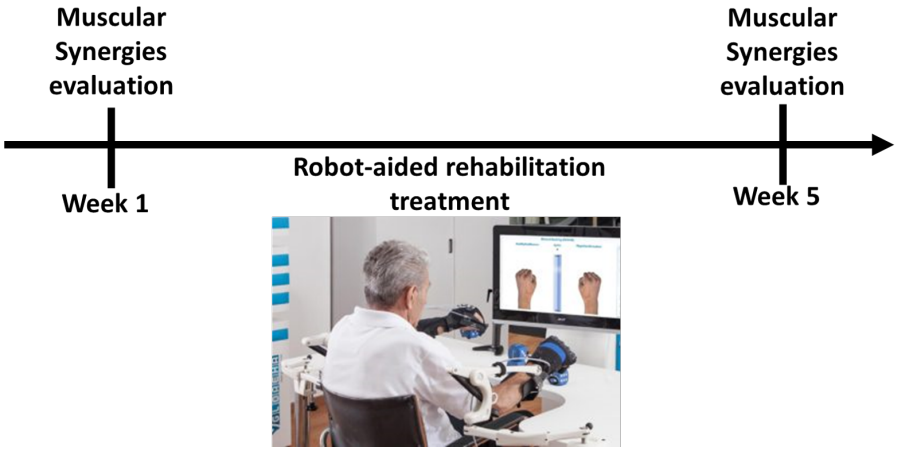

Fig. 2.8 The experimental protocol.

Gloreha Sinfonia composed of 5 sessions per week for 4 weeks. At the beginning and at the end of the course of treatment with robot (i.e. Before Rehabilitation and After Rehabilitation, BR and AR, respectively), sEMG signals were recorded from injured and healthy hand in order to extract muscular synergies of each subject and compare them to evaluate patient rehabilitation outcome.

For this assessment the patient was sitting in a comfortable position, in front of a screen that showed him/her the grip to perform. The subject performed 4 different grasps selected randomly. He/she had to grab and keep the following objects: a can, a pencil, a sheet and a tennis ball (see Fig. 2.7). It was required to perform the grasp and keep the object for ten seconds, at the end of this interval a pause of at least ten seconds followed. sEMG data were recorded during the ten seconds of grasp execution. The subject was asked to perform the same task with the injured limb and subsequently with the healthy limb in order to have the Healthy muscle patterns (H) a comparison term for the same subject. Furthermore, at the beginning and end of the treatment, the subject was assessed by means of the Fugl-Meyer (FM) and Motor-Power (MP) scales to evaluate the performance through literature validated tools.

Data of the patients involved in the study have been reported in Tab. 2.1. He/she performed the four assigned tasks showed randomly on the screen in front of the patient.

Data about clinical scales before and after robot-aided rehabilitation have been reported in Tab. 2.2. All the patients showed an increase in the FM and MP scores between before and after the robot-mediated rehabilitation with Gloreha. The average increase was 7.3 ± 3.7 for the FM and 3.1 ± 2.1 for the MP. This underlines the improvement in the mobilization of the injured limb in the selected population ($p=0.02$ for FM and $p=0.03$ for MP with Wilcoxon paired-sample test).

Table 2.1 Summary table of patients involved in this study. A=Age, S=Sex, T=Stroke Type, TSE=Time from Stroke Event.

	A	S	T	TSE [months]
1	56	M	ischemic	68
2	53	F	hemorrhagic	96
3	40	M	ischemic	75
4	79	F	ischemic	18
5	61	M	hemorrhagic	49
6	56	M	hemorrhagic	30
7	72	M	ischemic	33
	59.6 ± 12.8			52.7 ± 28.1

Table 2.2 Summary table of patients involved in this study.

	FM BR	FM AR	MP BR	MP AR
1	39	45	5	10
2	37	48	9	12
3	36	48	6	12
4	45	51	15	18
5	34	37	4	8
6	31	34	16	16
7	26	36	14	15
	35.4 ± 6.0	42.7 ± 6.9	9.9 ± 5.1	13.0 ± 3.5

2.2.3.2 Performance indices

The muscular synergies extracted during the assigned tasks in the three conditions (i.e. H, BR and AR) were compared for the same patient using three similarity indices:

- Cosine Similarity (CS): it is described by Eq. 2.2 and varies between -1 and 1. Values close to 1 indicate equal synergies, values close to -1 indicate vectors of equal but opposite synergies

$$CS = cos(\theta) = \frac{W_i * W_j}{\|W_i\| \|W_j\|} \tag{2.2}$$

  where θ is the angle between the two synergy vectors W_i and W_j, $\|W_i\|$ is the norm of the synergy vector, $*$ denotes the scalar product

- Similarity Index (SI): it is described by Eq. 2.3 and is a similarity index between two synergy vectors

$$SI = 1 - \frac{1}{S}\sum_{i=1}^{n} |W_i - W_j| \tag{2.3}$$

where S is the number of muscular synergies, W_i and W_j are the two synergy vectors.

2.2.3.3 Statistical analysis

A statistical analysis based on Wilcoxon paired-sample test was conducted in order to analyze the results obtained by the FM and MP scales (in this case the significance was achieved for $p < 0.05$) and to evaluate the statistical significance between the muscular synergy sets extracted in the three considered conditions (i.e H, BR and AR) and for the two performance indices calculated (CS and SI). In this case the significance was achieved for $p < 0.02$ (with Bonferroni correction).

2.2.3.4 Results and discussions

Seven stroke patients (mean age: 59.6 ± 12.8) have been involved in this study. Fig. 2.9 shows the trend of r^2 for the selected tasks as the number of synergies increases. In particular, the comparisons between the r^2 of the EMG signals and the reconstructed one ($W * H$) of the healthy limb with the injured limb data before and after treatment with the Gloreha robot are shown. It is evident that for $N = 3$ the $r^2 > 80\%$, therefore 3 synergies have been extracted from the EMG signal in order to allow the comparisons between the different conditions examined (i.e. H, BR and AR).

For the sake of brevity, in the Figs. 2.10, 2.11, 2.12 and 2.13 results about contributions of each muscles synergy have been reported for a representative subject. Similar results were obtained for the other involved subjects. In particular, the first bar is the rate of the corresponding muscle in the healthy limb (H), the second and the third bars are the rate of each muscle before and after rehabilitation (BR and AR).
A similarity among the synergistic patterns extracted from the EMG signals is already evident from a visual inspection of the results reported for the representative subject. This similarity is also confirmed by the comparisons made with the similarity indices introduced in Sect. 2.2.3.2. The results are summarized in Tab. 2.3 for each subject.

The monitored patients show CS values very close to 1, highlighting a very high degree of similarity of the involved synergies (mean CS values: H-BR: 0.74 ± 0.09, H-AR: 0.91 ± 0.06, BR-AR: 0.82 ± 0.09). This manifests in the comparison between the healthy limb and the injured limb before and after the rehabilitation treatment. These results confirm what has been achieved in the state-of-the-art with regard to muscle synergies of the upper limb on

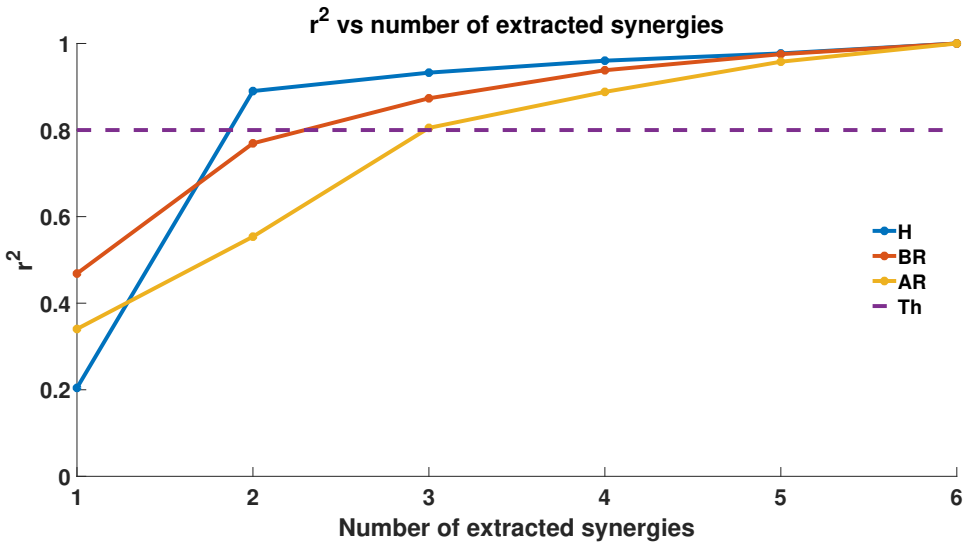

Fig. 2.9 r^2 between mean EMG data and reconstructed EMG data of healthy limb and affected one before and after robot-aided rehabilitation with Gloreha. H=Healthy limb, BR=Before Rehabilitation, AR= After Rehabilitation.

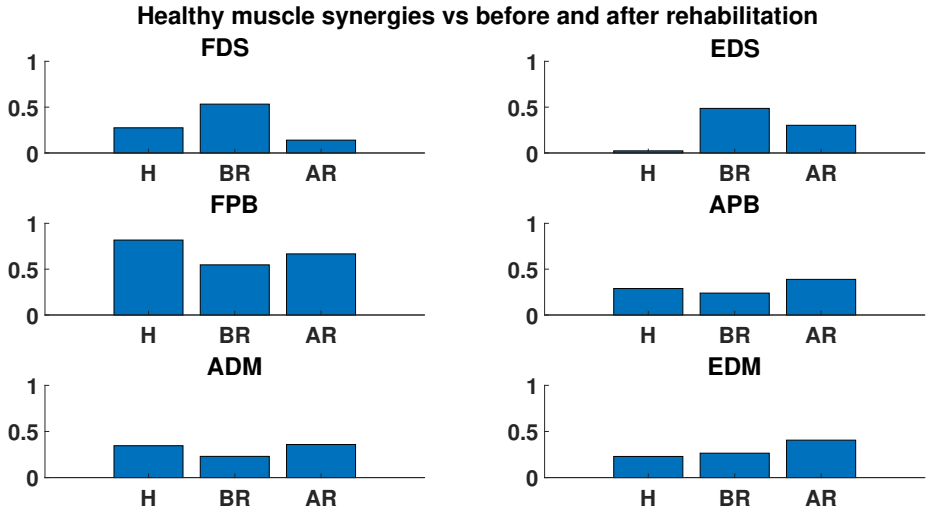

Fig. 2.10 Muscle synergies of healthy hand in comparison with the affected one before and after robot-aided rehabilitation with Gloreha for pencil grasping. H=Healthy limb, BR=Before Rehabilitation, AR= After Rehabilitation.

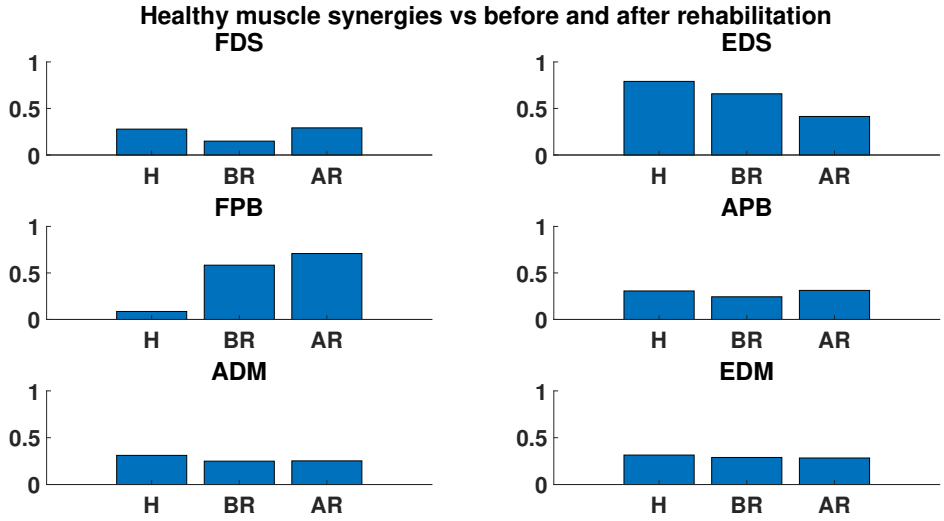

Fig. 2.11 Muscle synergies of healty hand in comparison with the affected one before and after robot-aided rehabilitation with Gloreha for sheet grasping. H=Healthy limb, BR=Before Rehabilitation, AR= After Rehabilitation.

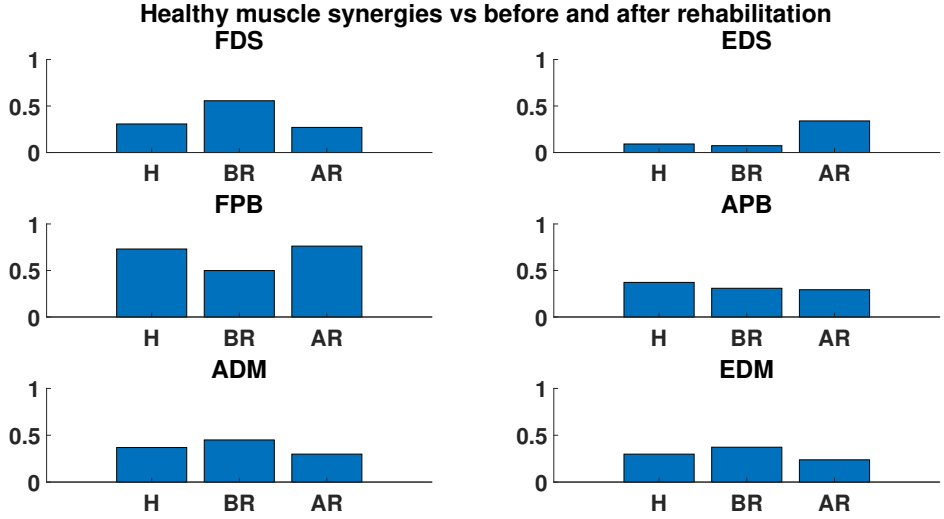

Fig. 2.12 Muscle synergies of healty hand in comparison with the affected one before and after robot-aided rehabilitation with Gloreha for small can grasping. H=Healthy limb, BR=Before Rehabilitation, AR= After Rehabilitation.

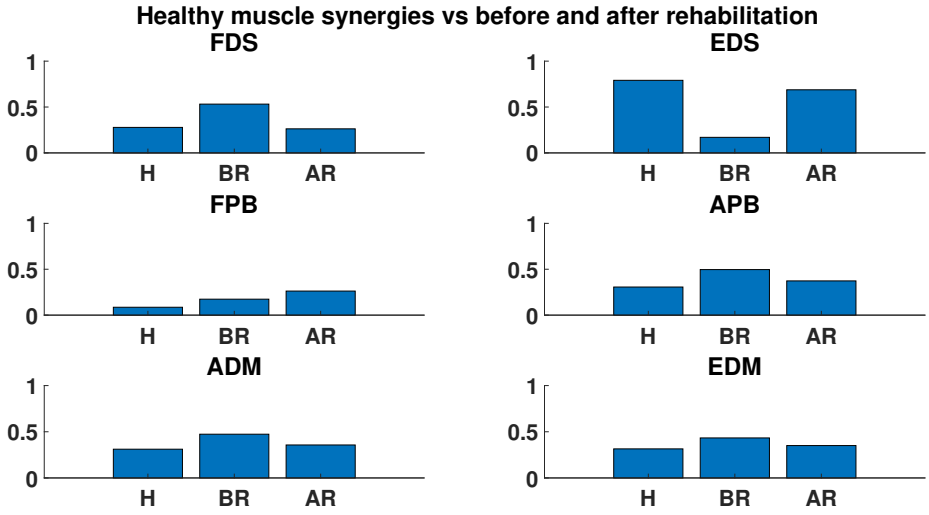

Fig. 2.13 Muscle synergies of healty hand in comparison with the affected one before and after robot-aided rehabilitation with Gloreha for tennis ball grasping. H=Healthy limb, BR=Before Rehabilitation, AR= After Rehabilitation.

	CS			SI		
	H-BR	H-AR	BR-AR	H-BR	H-AR	BR-AR
P	0.87 ± 0.08	0.94 ± 0.03	0.92 ± 0.06	0.91 ± 0.04	0.95 ± 0.05	0.92 ± 0.04
S	0.75 ± 0.13	0.85 ± 0.05	0.87 ± 0.10	0.86 ± 0.03	0.94 ± 0.03	0.84 ± 0.02
C	0.70 ± 0.22	0.98 ± 0.01	0.72 ± 0.19	0.85 ± 0.04	0.90 ± 0.02	0.85 ± 0.03
B	0.65 ± 0.14	0.87 ± 0.09	0.76 ± 0.20	0.89 ± 0.05	0.96 ± 0.04	0.93 ± 0.04
	$\mathbf{0.74 \pm 0.09}$	$\mathbf{0.91 \pm 0.06}$	$\mathbf{0.82 \pm 0.09}$	$\mathbf{0.88 \pm 0.03}$	$\mathbf{0.94 \pm 0.03}$	$\mathbf{0.89 \pm 0.05}$

Table 2.3 Summary table of comparisons among muscular synergy vectors divided by exercise. P=Pencil, S=Sheet, C=Cylinder, B=Ball, H=Healthy limb, BR=Before Rehabilitation, AR= After Rehabilitation

chronic stroke patients [12], but it broadens the results to the hand district and to the robot-mediated rehabilitation treatment. The increase in CS following rehabilitation treatment can be synonymous with its effectiveness, even if a larger population would be needed. This aspect has also been confirmed by statistical analysis, in fact the increase in CS is statistically significant in H-BR, H-AR and BR-AR comparisons (p=0.018, 0.012, 0.015 with Wilcoxon paired-sample test, respectively). Furthermore, the results of the comparisons made with SI for each patients were reported in Tab. 2.3. The similarity between the vectors of synergies is very high also in this case both for the comparisons with the healthy limb and with the injured limb before and after the robot-mediated rehabilitation (mean SI values: H-BR: 0.88 ± 0.03, H-AR: 0.94 ± 0.03, BR-AR: 0.89 ± 0.05). The high average SI level, also confirmed by

the statistical analysis on the analyzed population (p=0.016, 0.015, 0.012 with Wilcoxon paired-sample test, respectively), suggests a high degree of similarity of the muscle pattern both before and after rehabilitation and in comparison with the contralateral limb. This testifies that, despite very similar synergistic patterns between the injured and the healthy limb, the modulation function described by the matrix H determines in the injured limb a net reduction of its mobility. This analysis on muscle of stroke subjects points out the possibility of using them as a marker to identify anomalies in muscle activation patterns, not only on the shoulder-elbow district, as in [12], but also for the hand. Moreover, it demonstrates the initial hypothesis of using muscle synergies as an objective assessment tool of the patient motor improvements, in order to i) tailor the therapy also on the basis of the patient's muscular ability, ii) strengthen the muscular districts and/or the most affected movements with targeted exercises. This allows describing a complete picture of the subject affected by stroke, comparing the data of the injured limb and the motor pattern extracted on the contralateral side of the same subject, making the evaluation extremely accurate and custom-built on each patient. Muscle synergies can therefore be used as an indicator for regulating the level of assistance provided by the platform to improve motor tasks and enhance muscle synergies in which the subject manifests abnormalities.

2.3 Conclusions

The assessment of the patient's status is commonly performed in the clinical setting through the use of validated tools, such as clinical scales. From the analysis carried out in this Chapter, it emerges that these tools allow carrying out a qualitative evaluation and have some disadvantages: they require qualified personnel and are often difficult to administer. The sensors in the platforms for robotic rehabilitation are an alternative for obtaining a quantitative assessment of the subject's performance, ensuring ease of use and non-invasiveness. The data obtained from these sensors, such as force/position sensors, M-IMU and EMG, are used to define performance indices to get a complete picture of the patient's status. Taking this into account, the use of muscle synergies as an index for the evaluation of muscle patterns in stroke patients has been investigated. The preliminary analysis on 7 patients revealed that it is possible to highlight differences between the healthy limb and the injured limb before and after robot-mediated rehabilitation. This indicator can be used to estimate the patient status, although it cannot be used online due to the computational costs and the need to carry out an offline analysis of the EMG signals for the extraction of synergies.

Chapter 3

Patient-tailored control of an end-effector rehabilitation robot

Abstract

The bio-cooperative approach represents a new frontier in robot-mediated rehabilitation treatment. In this approach, it is necessary to take into account the patient's status during therapy, in order to constantly adjust the level of assistance that the robot provides to the patient. The proposed approach involves the use of an end-effector robot and a purposely developed arm-weight support for the patient limb. Biomechanical and physiological indicators are estimated to regulate the robot assistance level and the level of muscle fatigue is used to support the patient limb, in order to avoid stress conditions and excessive muscle fatigue.

3.1 Introduction

Robot-aided rehabilitation has been globally accepted as an effective therapeutic approach for motor recovery [49] [105]. In the last 20 years, the development of novel platforms for robot-aided rehabilitation provided fundamental tools for recovering limb functionality. Furthermore, robots can provide objective data of patient performance during rehabilitation sessions. In fact, sensorial data provided by biomechanical, physiological and psychological measurements, as well as intentions and environmental factors, may contribute to provide a continuous feedback on patients global conditions [78]. Control algorithms for robotic platform play a crucial role in robot-aided rehabilitation. They have the task of adapting the robot's behavior based on different input parameters. Although control algorithms have been extensively studied in the state-of-the-art and successfully applied in industrial automation, the controls of robotic platforms for rehabilitation, that interact with humans, are not so trivial. The first condition to be guaranteed is certainly patient safety, taking into account that the

subject who interacts with the machine is a patient, who has a motor deficit. For this reason, since the first clinical studies with MIT-MANUS [47], the concept of back-driveability has been explored, in other words try to develop robots that were able to move in the event that forces are applied from the outside. This allows the patient to move the machine easily and avoid dangerous situations. The design and development of these algorithms becomes even more complex in the bio-cooperative approach, because it is necessary to adapt the robot's behavior based on the subject's performance. The bio-cooperative approach is based on the inclusion of the patient in the control loop of the platform, in order to allow a continuous adaptation during the execution of the task, closing the loop on the patient, avoiding a completely passive movement of the user and promoting continuous monitoring of the patient status during human-robot interaction. The bio-cooperative platforms are equipped with different sensors, able to provide biomechanical, physiological and psychological measurements, as well as intentions and environmental factors. It allows getting a continuous feedback on global conditions of the patient [78]. The assistance provided by robotic platform can be changed on the basis of his/her state monitored by embedded sensors [65]. Strategies based on this approach provide the so called assistance-as-needed to the patients. Different approaches have been tested in the stae-of-the-art to customize therapy on patient needs [77, 32].

As shown in the Figs. 1.1 and 3.1, the control algorithm should receive the indicators of patient status as input and return a suitable physical quantity to facilitate the movement of the robot, that constantly interacts with the patient's limb, as output. The limit of the platforms presented in the state of the art is the lack of integrated systems that allow regulating the assistance to be provided to the patient on the basis of his/her performance and able to monitor and compensate the muscle fatigue perceived by the subject, as described in the Chapter 2.

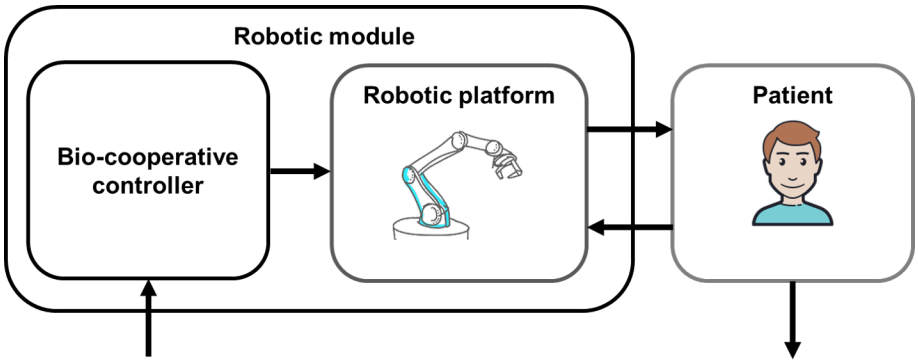

Fig. 3.1 Block scheme of robotic module included in the in the patient-in-the-loop approach.

These platforms showed the ability to manage the gravitational force component during the execution of task although patient limb movements are not completely free and sometimes hampered [62]. In this context, supporting the weight of the subject hemiplegic arm appears to be a key point in rehabilitation, limiting the unhealthy effects of abnormal synergies and permitting a greater arm range of motion [41].
Several strategies have been investigated to support hemiplegic limb, but their real contribution is still undetermined [74]. In both healthy and stroke subjects, weight support strategies demonstrated to facilitate arm reaching movements in horizontal [74] and frontal plane [18] by decreasing the activation of upper limb muscles that are mainly involved in gravity support. These findings suggested that subjects could focus more on the direction of the movement thus resulting in a larger range of motion and an increased number of repetitions per movement. Furthermore, in stroke survivors affected by severe motor impairments, arm-weight support has shown the capability to reduce the abnormal coupling occurring between shoulder abductors and elbow flexors [84]. Generally, arm gravity compensation can be achieved by means of either passive [55] or active devices [44]. As regards the passive methods, the Armeo Boom consists of an overhead sling-suspension system allowing gravity compensation at different levels thanks to several springs. It is the commercial version of the Freebal system which demonstrated its capability to facilitate upper limb movement tracking in a 3D workspace without altering muscular activation patterns [98].
Active gravity compensation with fixed or manually adjusted systems has been widely used in robotic exoskeletons for the upper limb [36] [42]. However, these strategies did not consider the strict relationship that occurs between gravity torque of upper limb, its dynamics and its dependence on the postures and positions of moving limbs. To this purpose, the development of position-varying compensation strategies based on human physical characteristics has guaranteed useful solutions to face this issue [37] [56]. Usually, such a a systems are integrated in exoskeletons or, if used with end-effector machines, do not adapt their behaviour to patient motion. Therefore, it is evident the need of a system that i) can be easily integrated with different platforms for robot-aided rehabilitation and ii) can adapt its behaviour to patient motion.

Progress beyond the SoA For these reasons, the aim of this Chapter is twofold:

- introduce a novel bio-cooperative platform for robot-aided 3D upper limb rehabilitation composed of an end-effector robot and an arm-gravity support able to overcome literature limitations. The patient is included in the control loop by continuously monitoring his/her state, extracting objective biomechanical and electromyographic indicators and consequently adapting the level of assistance provided by the robotic platform.

In particular, subjects performance and muscular fatigue are taken into account to shape the level of assistance on the patient's specific characteristics guaranteeing a patient-tailored therapy with an assistance-as-needed approach

- introduce a novel mechatronic system and its control algorithm for online adaptation of arm-weight support during robot-aided rehabilitation in the 3D space. Such a system has been conceived to be used as a gravity compensation device which can be easily integrated with end-effector robotic platforms for upper limb rehabilitation. Moreover, the adopted control algorithm based on the bio-cooperative approach for an end-effector robot has been described

Therefore, a detailed analysis of the proposed system and its control algorithms are presented. To this purpose, 8 healthy subjects were asked to perform 3D point-to-point movements with the aid of the end-effector machine in two different conditions, i.e. with and without the proposed arm-gravity support system. In order to evaluate the proposed arm-weight support and its control architecture, the robotic arm did not provide assistance to the user motion. During the task execution, the subject's hand motion in 3D space has been recorded throughout the position sensors embedded into a 7 DoF robotic arm that was opportunely fixed to the subject's wrist by means of an electromagnetic flange.
Moreover, a preliminary evaluation of the effects of the proposed platform on healthy subjects is performed in order to give a complete picture of the subject state ensuring his/her complete integration inside the control loop. Muscular activity of the anti-gravity muscles and biomechanical indicators was recorded from 10 healthy subjects during the execution of state-of-the-art 3D point-to-point movements in two different conditions, i.e. with or without assistance provided by the end-effector robot and by the arm-gravity support. A comparative analysis between the two different conditions has been performed by means of biomechanical and electromyographic indicators to evaluate effects on movement kinematics and muscular activation patterns. The same indicators have been also used to develop a bio-cooperative control strategy able to adjust robotic assistance on the basis of subject's state. Furthermore, the kinematics of the arm movement is preserved in all arm-weight support conditions while, as suggested by previous studies [74], weight compensation strategy may affect the muscular activation patterns of the upper-limb muscles used for 3D arm reaching movements.

3.2 The proposed human-in-the-loop approach for robot-aided rehabilitation

The proposed robotic platform is composed of a 7-DoFs anthropomorphic robot arm (i.e. the Kuka Light Weight Robot 4+ [7]), a purposely developed motorized arm-weight support system and a multimodal interface. It includes an adaptive interaction control for the on-line evaluation of patient performance, and adaptively and dynamically change the level of assistance by changing stiffness and arm-gravity support [91].

The overall system, presented in Fig.3.2, is devised as an end-effector machine that, interacting with the patient at the end-effector, offers assistance in point-to-point movements in 2D and 3D space, as well as in activities of daily living (ADLs). Moreover, an additional mechatronic arm-weight support system has been developed; the objective of this system is to overcome patients' difficulty to self-sustaining their own arm during the motor exercises. To this purpose, an adaptive level of support is provided by compensating the gravity force acting on the arm depending on both the subject's performance and the arm configuration in the space.

The overall robotic platform is based on an adaptive strategy that allows personalizing the therapy including the human-in-the-loop, and assisting the patient as needed in performing rehabilitation treatment. For further promoting patient motivation and engagement, a virtual reality (VR) is developed in Matlab, in which the selected task is reproduced and updated according to the patient biomechanical data. VR is composed of a virtual limb that is able to move along selected 3D directions, in order to reach the assigned targets, based on robot end-effector (i.e. subject hand) position.

During the exercise execution, the subject's wrist is attached to the robot arm end-effector that provides the subject with assistance-when-needed during the execution of a predefined trajectory. The encoders at the joint and the robot forward kinematics provide hand 3D trajectory. The robotic platform is composed of two independent modules (i.e.end-effector robot and arm-weight support) that communicate through USB and UDP protocol (Fig.3.3).

The multimodal interface is characterized by the following sources of information, opportunely fused together to provide a picture of the patient's condition:

i. robot sensors for determining hand pose

ii. a magneto-inertial units (M-IMU) for reconstructing the user's upper-extremity joint motion

iii. electromyographic (EMG) electrodes for recording muscular activity and selecting the correct amount of arm-gravity compensation.

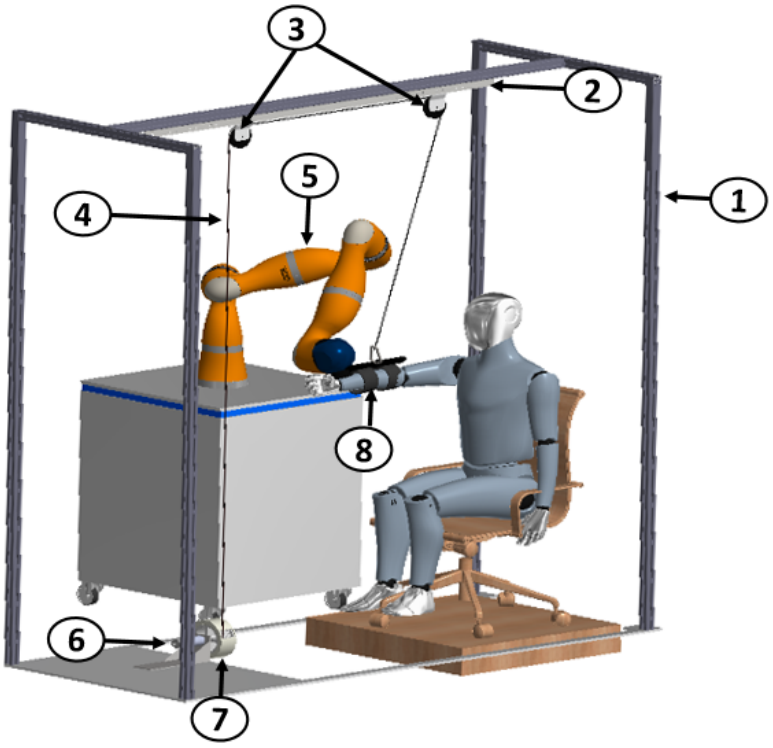

Fig. 3.2 A. Mechanical structure of the adaptive arm-gravity support system: 1 Frame, 2 Support bar, 3 Pulleys, 4 Cable, 5 7-DoF robot arm Kuka LWR4+, 6 Maxon EC-max 40 motor, 7 Encoder, 8 Ergonomic backing for the arm.

M-IMU is positioned on subject upper arm, instead EMG signals are recorded from the upper trapezius (UT, shoulder elevator), the posterior deltoid (PD, shoulder extensor), the lateral deltoid (LA, shoulder abduction), the anterior deltoid (AD, shoulder flexor), the pectoralis major (PM, arm adduction), the biceps brachii (BB, elbow flexor) and the lateral triceps (LT, elbow extensor). These muscles are chosen because they are surface muscles and their activation describes most of the upper-limb activity for desired task. Electrodes for each muscle are placed according to SENIAM guidelines [35].

The proposed platform is able to provide the correct level of assistance thanks to the close interaction between end-effector robot and arm-weight support, as shown in Fig. 3.3. More in detail, the correct level of assistance is assured through:

- the arm-weight support, by increasing or decreasing the weight of the arm felt by the subject. The level of the arm-weight support is evaluated through the level of muscular fatigue, measured by sEMG, as described in the Sect. 3.3

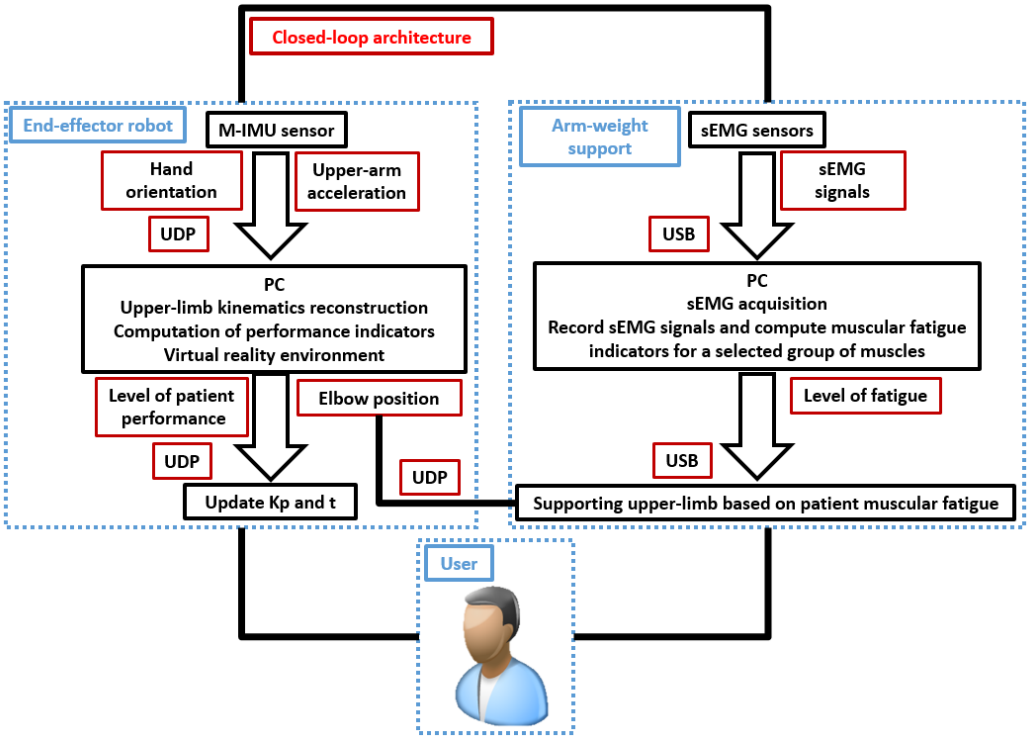

Fig. 3.3 Block scheme of the proposed closed-loop architecture

- the robotic arm, by helping the subject to complete the required task. This level of assistance depends on biomechanical indicators, as described in the Sect. 3.3

The level of assistance (K_p) provided by the robotic arm and the time (t) given to the subject for executing the task are computed in the end-effector robot block shown in Fig.3.3). On the other hand, the amount of support to be provided to the subject elbow is computed in the arm-weight support block (Fig.3.3).
The patient biomechanical data acquired through the M-IMU, i.e. the orientation of the hand and the upper-limb acceleration, provided by robot, and the muscular signals, recorded by means of the sEMG sensors are used for i) reconstructing the kinematics of the subject upper-limb, by means of the Augmented Inverse Kinematics (AIK) [68], ii) computing performance indicators, iii) evaluating the level of muscular fatigue. The obtained parameters are then used to update robot control parameters (i.e. robot stiffness and the execution time) and the amount of arm support (computed on the basis of the muscular fatigue) for shaping accordingly the level of assistance and task complexity in the 3D workspace. Moreover, the elbow Cartesian position provided by the AIK is adopted in the control of the arm-weight support to track the subject's limb during task execution, without interfering with its motion.

3.3 Closed-loop control of the bio-cooperative robotic platform

The subjects are constantly monitored during the execution of the task and their status is evaluated through the multimodal interface described in the Chapter 2. In particular, sEMG, M-IMU and robot position/force data are acquired to constantly describe the subject's state and to guarantee a strong and safe human-robot interaction.
sEMG data are collected at 1kHz, digitalized and then filtered by using a sixth-order Butterworth bandpass filter with cutoff frequencies (30,450)Hz and a second-order Butterworth notch filter (50Hz) to remove noise from power lines. The filtered sEMG signal is normalized with respect to the Maximum Voluntary Contraction (MVC).
M-IMU and position/force data are acquired at 100Hz and use to reconstruct the subject's arm movement and evaluate biomechanical indicators in order to adapt robot stiffness.
The proposed architecture allows dynamically supporting subjects in order to provide the correct amount of assistance with an assistance-as-needed approach. Furthermore, the proposed platform is designed to guarantee the correct ergonomic posture during the execution of the task, as demonstrated in [19].

3.3.1 The indicators integrated in the bio-cooperative platform

The analysis of the state-of-the-art made highlighted a set of useful parameters to be monitored for the bio-cooperative approach introduced in the Chapter 2. Some parameters have been selected to fully describe the movement performed by the patient with the help of the robotic platform, such as inter-joint coordination and smoothness (Fig. 2.4), and monitor the level of muscle fatigue in order to ensure patient safety and prevent excessive fatigue conditions for him/her. The subjects are constantly monitored during the execution of the task and their status is evaluated through the multimodal interface described in the Chapter 2. In particular, sEMG, M-IMU and robot position/force data are acquired to constantly describe the subject's state and to guarantee a strong and safe human-robot interaction.
M-IMU and position/force data are acquired at 100Hz and used to reconstruct the subject's arm movement and evaluate biomechanical indicators in order to adapt robot stiffness. Different biomechanical and physiological indicators have been adopted to evaluate subject performance during therapy in the proposed bio-cooperative platform for robot-aided rehabilitation. More in detail, biomechanical indicators, used to describe subject limb movements are ([70]):

- *Aiming angle* (α) : angle between the desired direction $\vec{tg_{dir}}$ and the real direction of the task from the starting point up to peak speed point $\vec{m_{dir}}$

$$\alpha = \frac{acos(\vec{tg_{dir}} * \vec{m_{dir}})}{(\|\vec{tg_{dir}}\| * \|\vec{m_{dir}}\|)} \tag{3.1}$$

- $Mean - Arrest - Period - Ratio$ $(MAPR)$: it represents the ratio between the number of samples (t_{perc}) in which the joint velocity is more than 10% of the peak velocity and the whole task duration (t_{tot})

$$MAPR = \frac{t_{perc}}{t_{tot}} \tag{3.2}$$

- $Inter - joint\ coordination$ $(q_{corri,j})$: it represents a coordination index beetween two upper-limb joint angles q_i and q_j

$$q_{corri,j} = \frac{R(q_i, q_j)}{\sqrt{R_{qi}(q_i) * R_{qj}(q_j)}}, \tag{3.3}$$

  where $R(q_i, q_j), R_{qi}(q_i)$ and $R_{qj}(q_j)$ are covariance and autocovariance matrices

- $Useful - Mean - Force\ UMF$: it is the mean force along the desired direction $\vec{tg_{dir}}$

- $Useful - Peak - Force\ UPF$: it is the peak force along the desired direction.

sEMG data are collected at 1kHz, digitalized and then filtered by using a sixth-order Butterworth bandpass filter with cutoff frequencies (30,450)Hz and a second-order Butterworth notch filter (50Hz) to remove noise from power lines. The filtered sEMG signal is normalized with respect to the Maximum Voluntary Contraction (MVC) and used to compute Dimitrov's Spectral Fatigue Index (DI), defined as

$$DI = \frac{\int_{f_1}^{f_2} f^{-1} * PS(f) * df}{\int_{f_1}^{f_2} f^{5} * PS(f) * df} \tag{3.4}$$

where $PS(f)$ is the signal power spectrum and f_1 and f_2 are the lowest and the highest frequency of the bandwidth. The DI index is computed only during the contraction phase of each muscle. The DI index has been chosen since the literature shows that it is an effective indicator of muscular fatigue and increases with the muscular fatigue [21, 29]. This parameter, normalized with respect to its maximum value, is estimated for each muscle and then weighted as follows

$$C_m = \frac{1}{7}(\frac{1}{2}DI_{BB} + \frac{1}{4}DI_{LT} + \frac{3}{4}DI_{AD} + \frac{3}{4}DI_{LA} + \frac{1}{4}DI_{PD} + \frac{1}{2}DI_{PM} + \frac{1}{2}DI_{UT}) \tag{3.5}$$

The weights were selected through a 'trial and error' approach, depending on contributes of each muscle for the chosen 3D movement. The C_m parameter continuously varies in the range [0,1]; a threshold strategy is used to evaluate the fatigue level and correspondingly adapt the arm-gravity support level (L_s) as

$$L_s = \begin{cases} 0 & \text{if } C_m < 0.20, \\ 1 & \text{if } 0.20 \leq C_m < 0.40, \\ 2 & \text{if } 0.40 \leq C_m < 0.60, \\ 3 & \text{if } 0.60 \leq C_m < 0.80, \\ 4 & \text{if } 0.80 \leq C_m < 1. \end{cases} \tag{3.6}$$

The so-obtained L_s values correspond to the following values of K: $0, 0.25, 0.50, 0.75, 1$.

3.3.2 Mechanical design of the arm-weight support

The entire mechanical framework has been envisioned and designed to be modular, lightweight, stable and compact in order to sustain subject's arm (both right and left arm) during 3D task execution. Moreover, the structure has been equipped with four moving wheels (each with a brake) in order to be easily moved and fixed in the desired position (Fig. 3.2). It is an optimized version of the preliminary design reported in [94].
Arm weight (i.e. the load), arm moment of inertia, approximate task velocity and required range of motion (ROM) have been selected as the main parameters for a correct dimensioning of the motorized mechanical system. In particular, the following values have been chosen: load equal to $5kg$ [108], arm moment of inertia is taken equal to $0.0245kgm^2$ [108], arm velocity is set at $0.5\frac{m}{s}$ [70], arm ROM along z-axis is $0.5m$ [70]; a safety factor 2 is used for overestimating these values.
The transmission system includes a cable-pulley system (3 pulleys and 1 cable) that is driven by a DC brushless geared motor (gear ratio of 74:1), secured at the bottom of the mechanical structure. The motor is also connected to one extremity of the cable by means of a driven pulley, while the other cable extremity is fixed to a specific brace for arm/forearm support. Once dimensioned, the structure has been fabricated in aluminum and assembled into a laboratory setting.
The selected actuation group is able to provide the maximum continuous torque (load acceleration torque plus continuous torque) for sustaining the upper limb, which has been estimated as 4.1 Nm. Moreover, the actuation group and the cable-pulley system can be adjusted according to the patient anthropomorphic characteristics and sitting position.

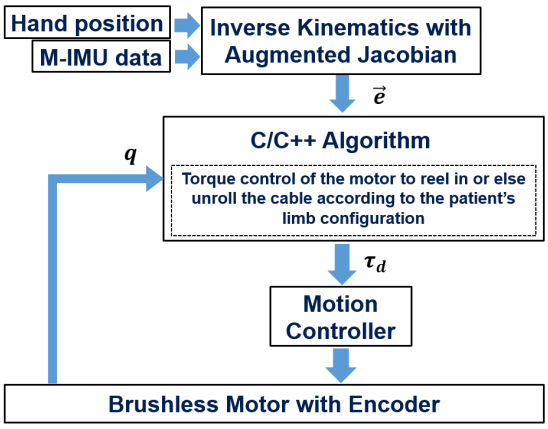

Fig. 3.4 Communication diagram between robot and arm-weight support

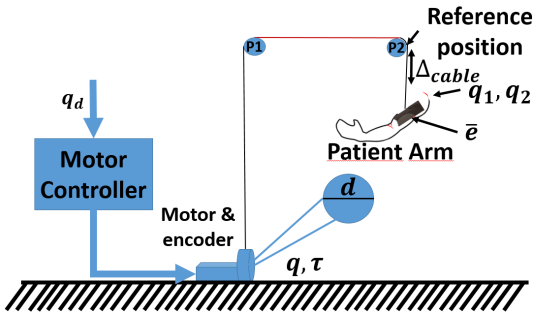

Fig. 3.5 Lateral view of arm-weight support

3.3.3 Control strategy for the arm-weight support

The control strategy has been conceived to adjust the cable driven by the motor on the basis of patient arm motion, in order to continuously support the subject's movement by compensating his/her arm weight.

During the exercise execution, the subject's wrist is attached to an antropomorphic 7 Dof robot end-effector (Kuka Light Weight Robot 4+). The robot is controlled with a near zero passive impedance to allow transparency while interacting with the user. In addition, a Magneto Inertial Unit (M-IMU), i.e. a 9-DoF Xsens MTw positioned on the subject upper arm, is adopted to reconstruct the subject's upper limb joint angles.

In particular, the hand position (i.e. the robot end-effector position) and M-IMU data are given in input to an Augmented Inverse Kinematics (AIK) algorithm [69] implemented in C++ language under Microsoft Visual Studio Community 2017®. The AIK uses hand position and M-IMU data to solve human arm redundancy and allows computing upper limb joint angles (Fig. 3.4).

The inverse kinematics algorithm relies on the augmented task space thanks to the swivel

angle, which represents the angle between the plane containing shoulder, elbow and wrist joints and a reference plane. This approach has been validated in the state-of-the-art and the performances have been compared with the stereophotogrammetric system obtaining good results [69].
The obtained joint angles are used to compute the elbow joint Cartesian coordinates (in the shoulder frame) as

$$\bar{e} = \begin{bmatrix} l_u \sin q_1 \cos q_2 \\ -l_u \cos q_1 \cos q_2 \\ -l_u \sin q_2 \end{bmatrix} \tag{3.7}$$

where l_u is upper arm length, q_1 and q_2 are the abduction-adduction and flexion-extension joint angles of the subject's shoulder, respectively.
The elbow coordinates, computed as in Eq. (3.7), are used to determine the desired position of the crankshaft of the motor as follows

$$\bar{q_d} = \frac{gear_{ratio} * \Delta_{cable}}{\pi * \delta * d} \tag{3.8}$$

where $gear_{ratio}$ is the gear ratio of the gearhead, Δ_{cable} is the difference between the new cable length and the reference position (i.e. initial position of the task), δ is the dimensionless encoder resolution and d is the diameter of the driven pulley, built-in with motor crankshaft (Fig.3.5). In our case, $gear_{ratio} = 74$, $\delta = 5^{-4}$ and $d = 0.14m$.
The new cable length is computed as the difference between the desired elbow coordinates and the position of the pulley placed above the subject's head. The desired crankshaft position is used to evaluate the position error with the real crankshaft position, obtained from the motor encoder, that needs to be compensated at each iteration. To this purpose, a torque control with gravity compensation is developed. The torque τ supplied to the motor is computed as

$$\tau = \tau_{PD} + \tau_{g(q)} \tag{3.9}$$

where τ_{PD} and $\tau_{g(q)}$ are the output torque of a proportional-derivative (PD) control and the gravitational torque. They are calculated as

$$\tau_{PD} = K_p(q_d - q) + K_d \frac{d(q_d - q)}{dt} = K_p err + K_d \dot{err} \tag{3.10}$$

$$\tau_{g(q)} = L_s \tau_{max} \cos(q_d - q) = L_s \tau_{max} \cos(err) \tag{3.11}$$

in which K_p and K_d are the proportional and derivative gains, q_d and q are the desired and effective crankshaft position, L_s is the percentage of support (range in between 0 and 1, in this case set to 1), τ_{max} is the maximum torque to be compensated, evaluated at the beginning

of the session when the subject arm is completely relaxed and placed in the arm brace, and *err* is the normalized position error remapped in the $[0,\pi/2]$ interval. In particular, $\tau_{g(q)}$ has to fulfill the following conditions:

$$\text{a. } 0 \leq \tau_{g(q)} \leq \tau_{max} \; \forall \; q \in \mathbb{R}$$

$$\text{b. } \tau_{g(q)} = \tau_{max} \; if \; err = 0$$

$$\text{c. } \tau_{g(q)} < \tau_{max} \; if \; err \neq 0.$$

In this manner, the subject arm is completely compensated when $q = q_d$.

3.3.4 Control strategy for the robot end-effector

The role of the robot controller is to assist the user connected to the end-effector of the robot during the execution of the task with an assistance level based on the subject performance. As presented in Sec. 3.2, the subject wrist is attached to the robot arm end-effector that provides the user with assistance-as-needed during the execution of a predefined task. The end-effector robot performs a minimum-jerk trajectory with different task durations t (i.e. $5, 7.5, 10s$), described as follows

$$s = \left\| p_f - p_i \right\| [10(\frac{t_j}{t})^3 - 15(\frac{t_j}{t})^4 + 6((\frac{t_j}{t})^5] \tag{3.12}$$

where p_i is the initial position, p_f is the final position, t_j is the current time value and t is the task duration evaluated as described in Eqs. 3.14, 3.15 and 3.16. The user is connected to the end-effector of the robot. The robot is controlled with an impedance control with a variable stiffness K_r in order to provide three levels of assistance, that correspond to three values of stiffness K_r (i.e. $0.1, 300, 1000N/m$), and it is able to change task duration as in [70].
Robot control can be described as

$$\overrightarrow{\tau_{cmd}} = J^T(\overrightarrow{q})[K(\overrightarrow{x_p} - \overrightarrow{x}) + \overrightarrow{FT} + D(d) + \overrightarrow{f_{dyn}}(\overrightarrow{q}, \dot{\overrightarrow{q}}, \ddot{\overrightarrow{q}})] \tag{3.13}$$

where J^T is the transposed Jacobian matrix, K is the Cartesian stiffness matrix, $\overrightarrow{x_p}$ and $\overrightarrow{x}$ are the desired and actual Cartesian position vectors, $D(d)$ is the damping term, FT is an additional superposed Cartesian force, $\overrightarrow{q}$ is the joint vector, $\overrightarrow{f_{dyn}}$ is the dynamic model. Furthermore, in order to promote patient involvement and enhancing voluntary efforts, a dead band around the reference trajectory is created [8, 98] where no assistance is provided. The indicators were evaluated using the data acquired by the position and force sensors integrated in the robot and by the M-IMU sensor positioned on the subject's arm during

therapy. Furthermore, thanks to this M-IMU sensor, the approach proposed in [71] was used for the kinematic reconstruction of the joint angles of the subject. More in detail, the robot stiffness K_r and the task duration t are modified according to a threshold strategy based on two parameters, C_{kr} and C_t, evaluated on the basis of the previously described biomechanical indicators as

$$C_{k_r} = \frac{1}{2}\alpha + \frac{1}{8}q_{corr1,4} + \frac{1}{8}q_{corr2,4} + \frac{1}{8}UMF + \frac{1}{8}UPF \tag{3.14}$$

$$C_t = \frac{1}{2}MAPR + \frac{1}{8}q_{corr1,4} + \frac{1}{8}q_{corr2,4} + \frac{1}{8}UMF + \frac{1}{8}UPF \tag{3.15}$$

where α, $MAPR$, $q_{corri,j}$, UMF and UPF are the aiming angle, Mean Arrest Period Ratio, inter-joint coordination, Useful Mean Force and Useful Peak Force, respectively. The correct level of assistance provided by the robot is estimated as

$$L_i = \begin{cases} 1, & \text{if } 0 \leq C_i < 0.5 \\ 2, & \text{if } 0.5 \leq C_i < 0.75 \\ 3, & \text{if } 0.75 \leq C_i < 1 \end{cases} \tag{3.16}$$

where $i = K_r, t$.

3.4 Experimental validation 1

3.4.1 Experimental Setup

The entire arm-weight support system, depicted in Fig. 3.6, is composed of: (1) mechanical structure in aluminum, (2) steel bar equipped with holes to choose pulley's location, fastened on the upper longitudinal axis of the mechanical structure; (3) two pulleys (BNL acetal 25 mm pulley, 18 mm pitch diameter, 102 mm external diameter, 9 mm bore) with ball bearings and bore reduction bush; (4) 4 mm steel wire rope black nylon coated to 5 mm, with winding radius equal to 70 mm; (5) an actuation system composed of: EC-max 40 brushless Maxon Motor, planetary gearhead Maxon GP 42-C 74:1, Maxon HEDL-5540 encoder and Maxon EPOS2 50/5 control unit; (6) aluminum pulley, for enveloping the steel rope, (diameter $d = 0.014m$) that is built-in with motor shaft; (7) ergonomic brace for arm support, which enables to set correct fitting depending on patient's requirements.
Furthermore, the anthropomorphic robotic arm Kuka Light Weight Robot 4+ (with 7 active Degrees of Freedom, DoFs) is integrated in the system to record the subject's hand Cartesian position and for the purpose of developing an assistance-as-needed approach while perform-

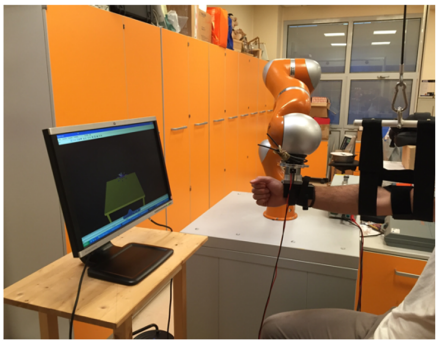

Fig. 3.6 Experimental setup

ing the required tasks. In this phase, the robot is impedance controlled with low stiffness value to make it transparent during the interaction with the user in order to not interfere in the evaluation of the arm-weight support. It is therefore evident that the proposed arm-weight support can be easily used with different systems for upper-limb rehabilitation by integrating in the platform a device for reconstructing the subject wrist position, such as RGB-D cameras. The robot exploits information coming from position and torque sensors at each joint and communicates with a PC on which the Fast Research Interface (FRI) Library runs.

3.4.2 Experimental Protocol

To test this architecture, 8 healthy subjects (27.3 ± 3.2 years old) were asked to perform 16 point-to-point 3D movements, in two different conditions, i.e. with and without gravity support. During the task with the gravity support the subject was seated on a chair, in a comfortable position, with the arm positioned in the ergonomic brace and the wrist connected to the robot end-effector.
The robot was in a transparent mode (K = 0.1 N/m) and recorded the subject's hand trajectory during the planned 3D point-to-point movements. Moreover, the recorded hand trajectories were online sent to the arm-weight control system and to the AIK algorithm, by means of UDP communication.
Subjects performed the exercises in front of a screen where a Matlab Virtual Reality (The MathWorks, Inc.) environment was reproduced (Fig. 3.6). The virtual reality enabled the subjects to online visualize the reference trajectory to be followed (Fig.3.7).
The same protocol has been replicated for the second condition, i.e. without gravity compensation strategy. The order of execution of the two experimental conditions was randomized among subjects. Finally, at the end of the assigned task, subjects answered a questionnaire about acceptability and ease of use of the proposed platform, based on the 9 point-Likert

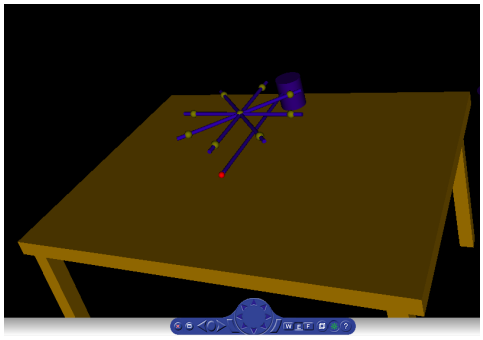

Fig. 3.7 Matlab Virtual Reality for point-to-point movement

rating scale. The questionnaire was composed of the following four questions

Q_1 Is the system easy to use?

Q_2 Is the elbow support useful for robot-aided neuro-rehabilitation?

Q_3 Do you feel your arm not completely supported and not free to move in any direction of the space?

Q_4 Do you think that patients could appreciate it?

It is important to outline that the participatns were physioterapists and physiatrists and therefore qualified for answering questions as Q_2 and Q_4.

3.4.3 Results and Discussions

The robot Cartesian end-effector position and the position error of the arm-weight support have been monitored during the task execution.

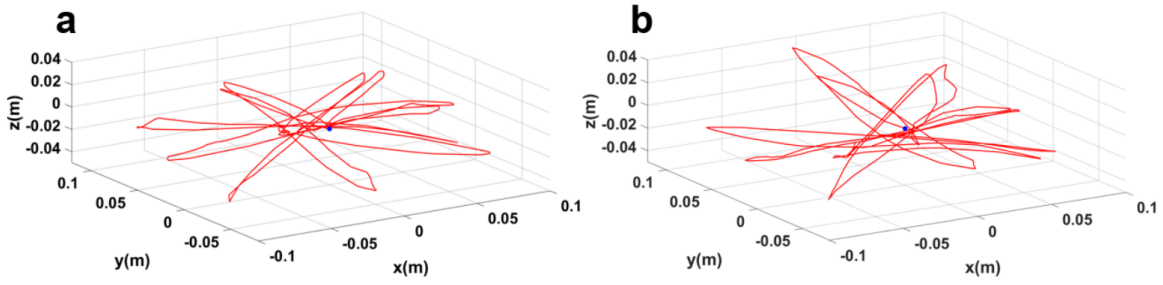

Fig. 3.8 Robot end-effector position during the task execution by a representative subject with (a) and without (b) the arm-gravity support system

In Fig.3.8, the Cartesian coordinates of the robot end-effector during the task execution with (a) and without (b) the arm-gravity support are shown, respectively. For the sake of brevity, only the results obtained from one representative subject are displayed (subject 4). It is evident that hand trajectories (i.e. robot end-effector trajectories) are smooth and present a similar profile each other. The AIK algorithm exploited the robot end-effector position and the acceleration obtained by the M-IMU to compute the subject's elbow Cartesian position (in the robot frame).
In Fig. 3.9, the normalized desired and effective crankshaft positions (with respect to their maximum) of the arm-weight support are shown in red and blue for a representative subject, respectively. The mean value and standard deviation of the position error of the arm-weight support, computed for each subject during the whole task, are reported in Tab.3.1.
The time employed by the subjects to perform the whole task has been also computed since it is an important indicator adopted for quantifying user motor performance. In particular, the time employed by each subject to perform the assigned task in both experimental conditions (i.e. with and without arm-weight support) is reported in Tab.3.4, together with the mean time and the standard deviation.

Table 3.1 Position error of arm-weight support control algorithm

Patient ID	err [rad]
1	0.000±0.007
2	0.002±0.009
3	0.001±0.005
4	0.004±0.015
5	0.001±0.014
6	0.003±0.016
7	0.003±0.010
8	0.001±0.019
Mean±std	0.002±0.001

Finally, the results of the questionnaire are reported in Tab.3.3. A score equal to 9 corresponds to strongly agree and a score equal to 0 corresponds to completely disagree. The results obtained from the test are highly cheering in term of adequate easiness of system use and to sustain patient limb during robot-aided rehabilitation. Patients confirmed that their arm was completely supported and free to move and demonstrated appreciation in system performance.

Table 3.2 Execution Time

Patient ID	Time without support [s]	Time with support [s]
1	67	72
2	78	67
3	80	94
4	56	49
5	72	63
6	95	78
7	62	70
8	80	87
Mean ± std	74±12	73±14

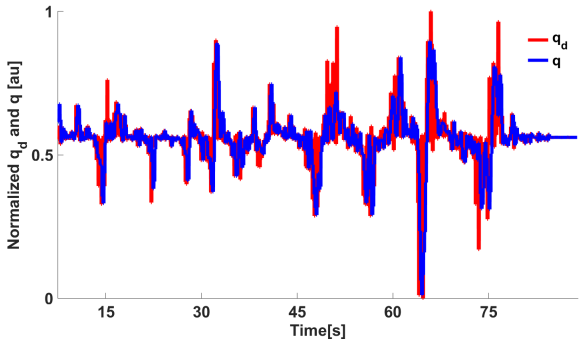

Fig. 3.9 Arm-weight support position error during the execution of task

Table 3.3 Usability results (9-point Likert scale)

Patient ID	val ± std
$Q1$	6.63±1.19
$Q2$	7.25±0.89
$Q3$	7.25±1.04
$Q4$	7.09±1.18
Comments	
The proposed platform could be more effective with a rigid brace for the arm	
It could be exploit for other 3D tasks	

The 3D hand trajectory in the Cartesian space with (Figure 3.8a) and without arm-gravity support system (Figure 3.8b) has shown that the proposed system has the capability to successfully follow the subject's movement without interfering with the natural motion

pattern. This aspect is also proved by the smoothness of the trajectories (Fig. 3.8a and 3.8b) and it is crucial for choosing the best control strategy for the motorized arm-gravity support system. In fact, an ideal gravity compensation system should be able to compensate for the weight while not restricting the subject freedom of movement in any of the motion axes.
The score of the Likert Scale for Q_3 clearly reported that the users had a good perception of the arm-gravity support system (7.25 ± 1.04). Therefore, they did not experience any significant movement constraint during the execution of the required tasks, although they suggested to use an orthosis that is tightly coupled with the arm instead of the actual soft sling. Also, the time employed by the subjects to perform the whole task has been taken into account during the evaluation of the system.
In particular, the task execution time for both conditions has been compared to investigate the possible motion hindrance caused by the proposed gravity compensation strategy.
Computed time reported in Table 3.4 confirmed that the introduction of the arm-weight support system does not create any effects regarding the quality of the performed movement (mean time with support 73 ± 14s, mean time without support 74 ± 12s, $p = 0.76$ with paired t-test).
Summarizing, the proposed solution provides an arm-weight compensation system that fulfill the design specifications illustrated in Sect.3.3.2. The arm movement is not constrained by the ergonomic brace and subjects can freely move their arm in the 3D space thanks to the implemented control strategy based on the estimation of arm's gravity torque. Compared with the platforms described in the literature, the proposed system and control approach have the capacity fo follow the position of the limb, which is reconstructed thanks to AIK.
Such an estimation might be affected by the different positioning of the arm inside the ergonomic brace, thus resulting in a non-appropriate quantification of the torque to be compensated. A possible solution to overcome this issue might be the introduction of a force sensor, placed between the end of the cable and subject's arm, that will enable to estimate the arm torque with high resolution, compared to the present solution. However, the control method appears to be intuitive, generic and the overall compensation system might be used also in several rehabilitation contexts with different robots.
Finally, the method has been successfully evaluated on 8 healthy subjects and it is expected to achieve similar results when tested with patients.

3.5 Experimental validation 2

3.5.1 Experimental setup

The proposed robotic platform, shown in Fig.3.10, is composed of the anthropomorphic robotic arm and the actuated arm-weight support. The robotic arm is the Kuka Light Weight Robot 4+. It is characterized by 7 active Degrees of Freedom (DoFs) and embeds position and torque sensors at joints. The communication between the robot and a remote PC is guaranteed by the Fast Research Interface (FRI) Library. The arm-weight support actuation system is composed of: EC-max 40 brushless Maxon Motor, planetary gearhead Maxon GP 42-C 74:1, Maxon HEDL-5540 encoder and Maxon EPOS2 50/5 control unit. An aluminum pulley, for enveloping the steel rope, (diameter d = 0,14m) is built-in with motor shaft. Finally, an ergonomic brace for arm support enables to set correct fitting depending on patients requirements.

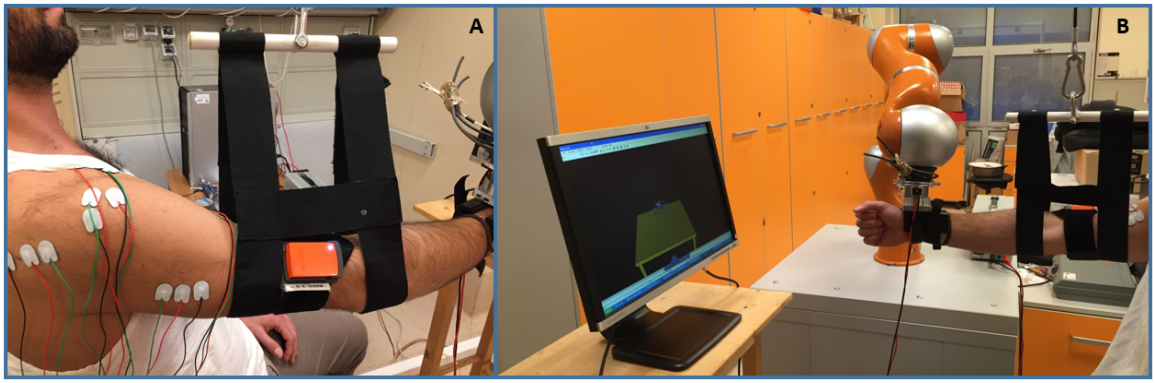

Fig. 3.10 A photo of the proposed 3D bio-cooperative robotic platform. A: Detail of M-IMU and sEMG sensors used with arm-weight support; B: Arm-weight support together with the whole platform: subject interacts with robotic arm and arm-gravity support.

Subject upper limb kinematics is reconstructed by means of a Xsens MTw M-IMU sensor.The M-IMU and robot sensors data are acquired at 100Hz and sent to the AIK algorithm via UDP communication.

sEMG data are collected at 1kHz (Grass Acquisition System, Natus Medical Incorporated, Pleasanton, CA with 15x20mm disposable electrodes) and digitalized with a National Instruments DAQ (NI DAQ USB 6218). sEMG recordings are filtered using a sixth-order Butterworth bandpass filter with cutoff frequencies (30,450)Hz and a second-order Butterworth notch filter to remove noise and artifacts. The filtered sEMG signal is normalized with respect to the Maximum Voluntary Contraction (MVC).

3.5.2 Experimental protocol

Ten right-handed healthy subjects (mean age: 27.9 ± 2.0) have been recruited to participate in this study. All the subjects were able to lift their right arm against gravity, and presented no musculoskeletal or neurological disorders. They provided written informed consent prior to participating in this study. Each subject seated on a chair in front of the virtual reality, as shown in Fig.3.10. The sensors embedded in the robot arm reconstructs the subject hand position which is used to move the subject hand avatar reproduced in the virtual reality. The virtual reality reproduces the task to be performed and gives the user a continuous feedback on him/her motion performance (in terms of error between the avatar position and the target).

The proposed bio-cooperative system for 3D upper limb rehabilitation allows performing adaptive upper-limb robot-aided therapy in two separate conditions: 1) without assistance provided by the end-effector robot and by the arm-gravity support and 2) with assistance. In condition 2), the level of assistance is tuned on the subject's muscular fatigue and on the biomechanical indicators computed during the trials executed without the assistance.

The subjects were asked to perform 2 consecutive sessions in the two conditions. Condition 1 was always executed before condition 2 in order to evaluate all the indicators introduced in Chapter 2 and correspondingly adapt the robot arm and the arm-weight support behaviour. Before each rehabilitation session, an evaluation session is envisaged. A physioterapist supervised each session and, in case of patients with severe disabilities, he/she could set the starting parameters adequately at the state of the patient.
Each session was composed of two phases of 56 point-to-point movements. Each movement consisted in reaching a target on the screen and then return to the starting point. Targets were spaced in 8 different positions, spaced $\pi/4$ *rad* apart from North to North-West direction. The transition from one target to another is performed either when the maximum value of the execution time t (established by Eq. 3.15) is reached or when position error between the target and the end-effector position is less than a predefined threshold.

During the whole task execution, data from M-IMU, robot sensors and sEMG activities of 7 shoulder and upper-arm muscles were collected.

3.5.3 Statistical Analysis

A statistical analysis based on the Wilcoxon paired-sample test was performed for the comparative analysis between two conditions (i.e. with and without the assistance-as-needed), after verifying that the data did not belong to a Gaussian distribution. In particular, the statistical analysis was performed for comparing i) the time taken by the subjects for

accomplishing the task, ii) the biomechanical indicators and iii) the muscular fatigue in the two conditions. The significance was achieved for $p-value < 0.05$.

3.5.4 Results and discussions

Ten healthy subjects have been involved in this study. Each of them performed the assigned task in two different conditions, described in Sect. 3.5.2. For the sake of brevity, only the results obtained from one subject are shown.

Furthermore, time taken by the subjects for accomplishing the task is reported in Tab.3.4 for both conditions 1 and 2. The subjects performed the assigned task without assistance-as-needed in $(283 \pm 28)s$ and with assistance-as-needed in $(290 \pm 40)s$. It was verified that the use of the support does not significantly alter the execution time of the assigned task (Wilcoxon test, $p-value > 0.05$).

Patient ID	Time without assistance-as-needed [s]	Time with assistance-as-needed [s]
1	261	320
2	308	202
3	264	274
4	289	279
5	270	269
6	302	287
7	260	349
8	253	301
9	343	322
10	276	297
Mean $\pm$ std	283$\pm$28	290$\pm$40

Table 3.4 Task duration without and with assistance-as-needed.

Robot sensors provided position and force data to customize exercise on the basis of subject motor performance. As expected, the computation of the biomechanical indicators for the involved healthy subjects did not show a significant change between the first and the second condition in robot stiffnessK_r and task duration t, since they were able to perform the task without any assistance. Indeed, it was demonstrated that, with the proposed system, the biomechanical indicators do not show significant variations due to the introduction of the support ($p-value > 0.05$ with Wilcoxon test for all the biomechanical indicators evaluated with and without arm-weight support).

In Fig.3.11 and 3.12, the mean EMG activity and its standard deviation is reported in both conditions, i.e. with and without assistance-as-needed. The 7 sEMG values range between [0,1] since each of them is normalized with respect to the corresponding MVC.

Note that it seems there are not appreciable changes for BB and LT signals, but this is due to normalization with respect to their MVC, so they were activated but their variations are not perceivable. In Tab.3.5 muscular fatigue indices and level of needed assistance are reported. These parameters are useful to establish the level of physical fatigue of the subjects.

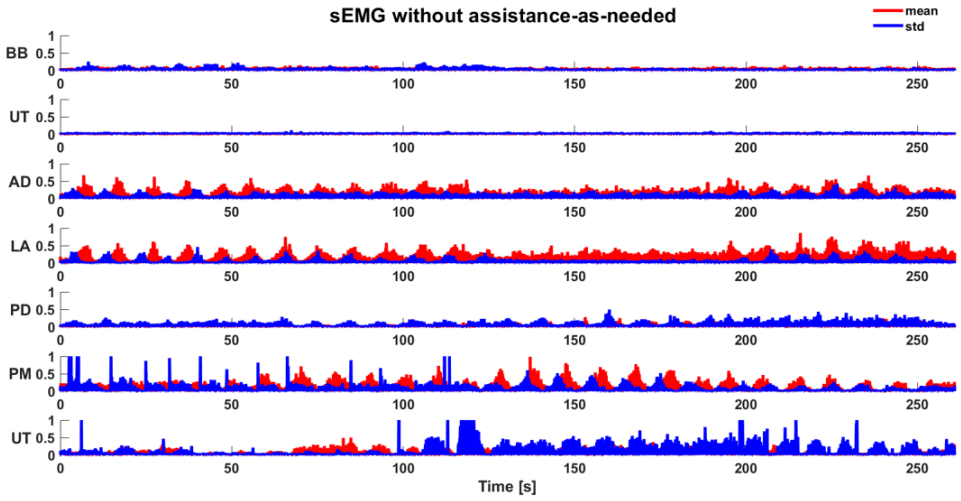

Fig. 3.11 Mean sEMG activity (normalized) and standard deviation during the execution of task without assistance-as-needed.

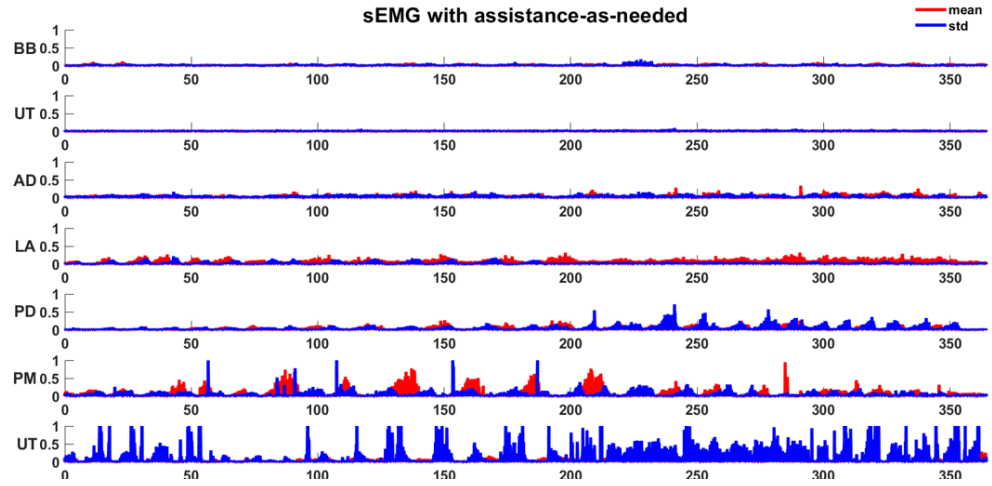

Fig. 3.12 Mean sEMG activity (normalized) and standard deviation during the execution of task with assistance-as-needed.

Furthermore, an increase in muscular fatigue emerged during the first part of the test for all the subjects. In fact, there is a statistical correlation between the decrease of fatigue after the use of arm-weight support in the second condition of the assigned task ($p - value < 0.05$

Muscle	Without assistance-as-needed [ ]	With assistance-as-needed [ ]
BB	1.00	0.65
LT	0.72	0.66
AD	0.71	0.60
LA	0.84	0.12
PD	0.79	0.51
PM	0.85	0.58
UT	0.72	0.00
L_s	2	1
K	0.50	0.25

Table 3.5 Normalized DIs of the example subject without and with assistance-as-needed for each muscle and the level of necessary support.

with Wilcoxon test). The level of support to be applied in Condition 2 is selected on the basis

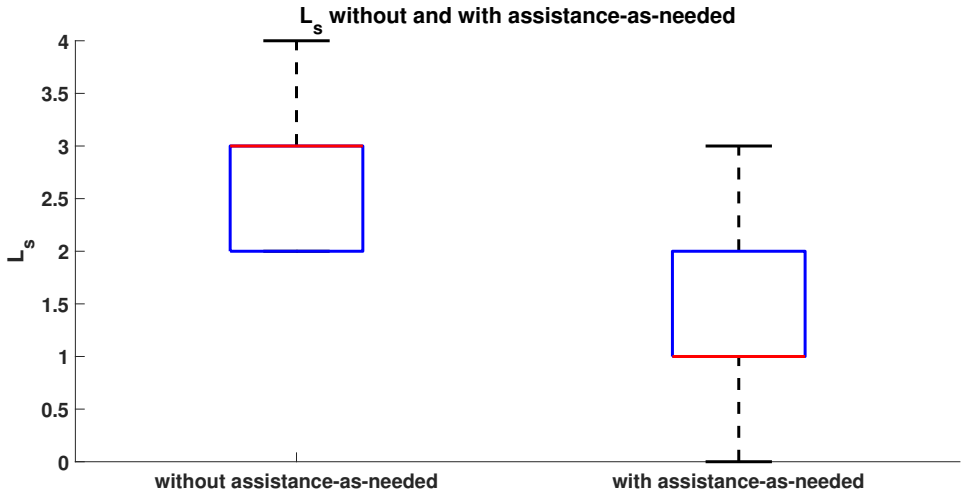

Fig. 3.13 Mean sEMG activity (normalized) and standard deviation during the execution of task without assistance-as-needed.

of the fatigue level evaluated during Condition 1. In this way, the support assistance level can be adapted to patient fatigue performance allowing to follow subject arm movements. Results about desired crankshaft position (q_d) and desired torque (τ_d) are reported in Fig.3.14 for an example subject. During the task execution in Condition 1, the level of assistance to be given to the arm support for this subject has been estimated to be equal to the 50% of the necessary τ_d to support subject arm completely (i.e. $\tau_{max} = 35mNm$, evaluated at the beginning of the experimental session).

The movements of the robot end-effector (i.e. subject hand) and elbow position, reconstructed by AIK algorithm, demonstrate that the proposed approach allows executing 3D task

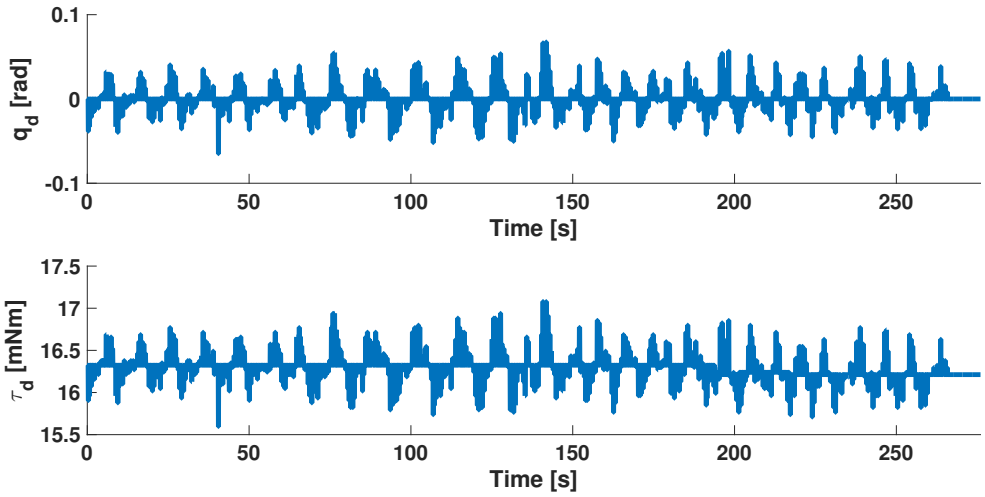

Fig. 3.14 Desired crankshaft position q_d and desired torque τ_d of the arm-gravity support for an example subject with a compensation of 50% of the necessary τ^{max} to support subject arm completely.

without interfering with the natural motion pattern and therefore not negatively affecting the motion execution. It is demonstrated by the results of the statistical analysis performed on the biomechanical indicators: their values do not change in a statistically significant manner between the two conditions ($p-value > 0.05$). It is due to the fact that the subject did not present musculoskeletal or neurological disorders and therefore they were able to perform the assigned task without any assistance. For the same reason, the mean values of task duration confirmed that there is not statistically significant difference between the time obtained without the assistance-as-needed (mean time = $283 \pm 28s$) and with assistance-as-needed (mean time = $290 \pm 40s$). In fact, the $p-value > 0.05$ obtained with the Wilcoxon test applied on these values.

As shown in Sec.3.5.4, the use of the arm-weight support reduces muscular activity, as evident from Figures 3.11 and 3.12, also confirmed through Wilcoxon test applied for each muscle ($p-value > 0.05$). It is demonstrated also by the statistical analysis performed with the Wilcoxon test, which outlined the statistically significant difference between the fatigue evaluated with and without arm-weight support ($p-value > 0.05$). The subjects referred to perceive a reduced muscular fatigue after the introduction of the arm-weight support. This finding could certainly have a huge impact on neuro-rehabilitation. In fact, a reduced muscular fatigue could lead to an increase in therapy session duration and a decrease in wrong arm configurations that may result for compensating for the fatigue of some muscles.

As shown in Fig.3.14, the control algorithm for arm-weight support allows following subject arm movements and produces a desired torque τ_d, with a profile similar to q_d, that is able to both compensate gravity component of the arm and move his/her limb in the 3D space.

The support level applied on the subject's arm by the arm-weight support was varied in accordance to the fatigue level estimated for each subject on the basis of Eq. 3.6.

From these results, it is clear that the proposed bio-cooperative robotic platform is based on a closed-loop control that includes the subject in it. The goal is to execute 3D point-to-point movements adapting to the state of the subject from both biomechanical and muscular fatigue point of views.

3.6 Conclusions

In this Chapter a novel bio-cooperative platform for upper-limb robot-aided rehabilitation, composed of a robotic arm, an arm-weight support for patient arm and a multimodal interface for monitoring human-interaction has been introduced. The proposed approach includes the patient in the control loop by providing him/her the correct amount of assistance on the basis of biomechanical performance and muscular fatigue indicators. Human-robot interaction was constantly monitored to extract biomechanical and muscular indicators and consequently modify the level of assistance and the difficulty of the exercise. Two experimental sessions have been carried out. The first showed that the proposed torque control depicts a simple and robust way to allow subjects performing the required task and assist both right and left-handed of subjects. The complete platform was tested on 10 healthy subjects performing a 3D point-to-point movements with and without assistance-as-needed. The experimental sessions, carried out on healthy subjects, had the aim of testing the preliminary behavior of the developed platform at the borders of its desired operational range in order to verify the goodness of the proposed approach. The obtained results demonstrated that the proposed system reduces the muscular fatigue without negatively influencing correct motor patterns.

Chapter 4

Non-invasive feedback for posture assessment during upper-limb robot-aided rehabilitation

Abstract

The feedback module allows returning visual, sound or haptic feedback to the patient during the robot-aided rehabilitation with a bio-cooperative platform. This ensures that the patient performs the task correctly. A module for visual and vibrotactile feedback has been integrated into the bio-cooperative platform presented in the Chapter 3. The proposed bio-cooperative robotic platform avoids negative effect on subject posture during robot-aided rehabilitation. Moreover, the feedback module has been tested on healthy subjects in order to evaluate the effectiveness to improve patients posture in robot-aided rehabilitation treatments and its acceptability.

4.1 Introduction

The adoption of robotic technologies in rehabilitation is widely increased in the recent years, since they have the ability to deliver highly intensive, repeatable and accurate motion therapy and contemporary to measure the clinical outcome [6, 66]. Various approaches for robot-aided rehabilitation have been presented in the literature to allow varying the level of assistance based on patient state and his/her performance [111, 25]. In the bio-cooperative approaches described in the Chapters 2 and 3, the feedback module is used to provide useful information to the patient during the execution of the rehabilitation task. Typically these feedbacks can be audio/visual and/or haptic. The feeback can be provided during the execution of the task with the aim of improving movement and allowing to obtain the best efficacy from the rehabilitation treatment. Fig. 4.1 shows a block diagram of the module

for returning feedback to the subject managed by the bio-cooperative controller. Repetitive and intensive exercises during robot-aided rehabilitation treatments may expose patients to inappropriate and unsafe spine postures that could cause neck and back pain as well as some other negative effects, both physically and mentally. Improper posture conditions have in fact a long-term negative influence on internal functioning of the body like breathing, blood flow and digestion and also result in higher stress levels [79].

Patients who perform exercises under the supervision of a physiotherapist assume less dangerous configurations and experience less pain during the treatment compared to the unsupervised ones [26]. Although there is a great evidence supporting the benefits of patient supervision during the treatment, an objective posture evaluation and a constant monitoring of the patient behavior is difficult to achieve since physiotherapists are usually required to control multiple aspects of a rehabilitation session (e.g. correctness of motion, patient involvement, feeling and progresses).

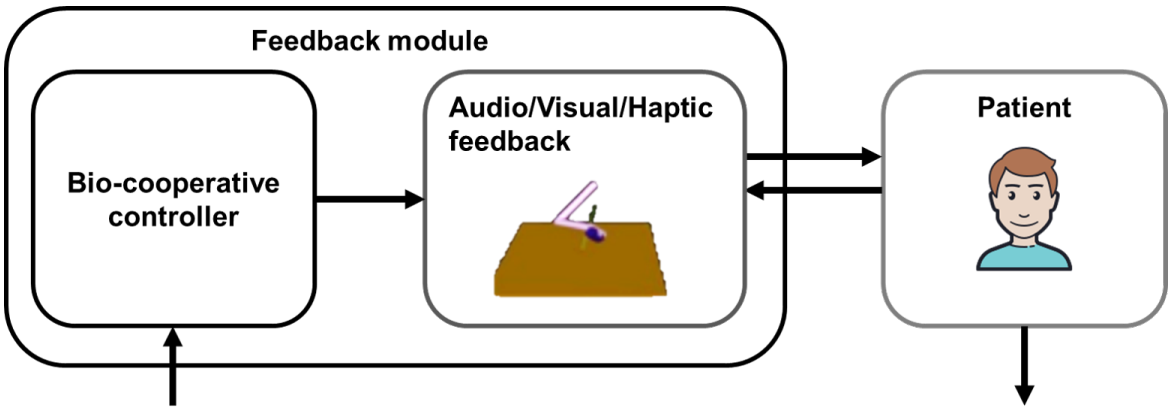

Fig. 4.1 Block scheme of audio/visual/haptic feedback module included in the patient-in-the-loop approach.

Several systems have been proposed in literature to objectively evaluate the patient's behaviour during a rehabilitation session and provide them with a feedback related to the correctness of the exercise. Sensory feedback has an important role in rehabilitation; it promotes a higher level of user participation in the task accomplishment than traditional therapy, thanks to the stimuli the user is provided with. In fact, the feedback on the results and/or performance achieved during the robotic training simplifies the execution of the target movement and promotes subject involvement in the rehabilitation exercise [104].

Patient body motion can be monitored by means of motion capture systems, such as optoelectronic systems, cameras [15], or wearable sensors such as magneto-inertial and electromyographic sensors [53], Hall effect sensors [17] or smart textile [88]. They are valuable solutions to provide a quantitative measure of the patient posture during a rehabilitation

treatment as well as to assess the correctness of the exercise execution, differently from the simple qualitative visual observation used in clinical practice by therapists.

Once an incorrect position is detected or the exercise is assessed as improperly performed during the rehabilitation treatment, the patient can be provided with a feedback in order to stimulate a better posture control and improve the exercise performance.

In [5], bend sensors are adopted to detect the flexion/extension angle of the knee during a rehabilitation treatment. The acquired information is used to give a visual notification of the bend progression as the patient performs knee extensions. In [50], a system providing the user with continuous visual feedback and guidance to improve quality of motion performance during the rehabilitation treatment is proposed. Vision is assessed to be the most important sensory modality during the interaction with the environment. For perceiving information with high resolution, vision dominates other senses [22]. However, visual feedback uses an important sensory channel that is essential for a successful accomplishment of the task. Hence, when the patient is focused on a complex task, visual feedback may be perceived as cumbersome or confusing since visual perceptual channel becomes overloaded[93].

To overcome this drawback, auditory feedback was introduced in the rehabilitation treatment in order to convey important information to the patient related to the performed task. In [72] and [101], it was demonstrated that auditory feedback is a valuable mean to provide information about spine posture of post-stroke patients during the execution of reaching tasks. However, there could be a delay between the time when the incorrect spine posture is detected and the time when the warning feedback is transmitted to the patients by means of words.

Haptic feedback could be a valid solution to face this issue. Haptic refers to the sense of touch, and haptic interfaces are meant to provide force or tactile feedback by applying pressure, vibrations, forces. Although a great number of haptic feedback devices could be employed during the rehabilitation session to correct the patient's posture, there are some drawbacks that cannot be neglected. For instance, electrotactile systems can cause pain on the skin and fatigue [43]. Force feedback systems can be cumbersome and have limited spatial resolution on the patient skin [23].

Vibrotactile feedback (VtF) systems can be considered to be safe and have an acceptable spatial resolution [54] in comparison to the other tactile solutions. In [39], VtF was used to train post stroke patients suffering from hemiplegia to perform lower-limb rehabilitative tasks. In [83], VtF was delivered to the palm and the fingers of post stroke patients while training to hold and manipulate objects. In [34], VtF was proposed to teach post stroke patients how to perform Activities of Daily living (ADLs).

Despite the wide use of VtF in many fields, this kind of feedback seems not to be suitable for applications that require long term usages [28]. Indeed, it is well known in the literature that an extended vibrotactile stimulation of the fast adapting sensory receptors on the user skin induces sensory adaptation effects in the patient. However, this does not apply to rehabilitation sessions that may expose patients only to short and infrequent stimuli.

From an in-depth analysis of the literature emerged that VtF feedback can enhance motor learning and performance and is preferred by users over visual or auditory feedback [3] [46] [99]. However, there is poor attention to the type of feedback preferred by the users, in terms of acceptability and comfort, for correcting spine posture while performing activities in sitting positions [110]. Moreover, to the best of our knowledge, there are no previous studies in literature that investigate which type of feedback could be effectively and efficiently employed during robot-aided rehabilitation treatments to improve patient spine postures.

Progress beyond the SoA For these reasons, a preliminary test on healthy subjects had been carried out on a bio-cooperative robotic platform to avoid negative effect on subject posture during robot-aided rehabilitation. Eight healthy subjects have been involved in this first study. Each subject performed 16 point-to-point reaching movements in the 3D space in two different conditions: 1) with full assistance provided by the platform (i.e. 100% of arm weight support and high gain for the robotic arm); 2) without assistance provided by the platform (i.e. 0% of arm weight support and low gain for the robotic arm). Subject's upper limb kinematics and their posture are reconstructed by means of the M-IMU sensors.

The literature confirms that both VF and VtF could be suitable tools to correct patient postures in robot-aided rehabilitation treatments. Therefore, this Chapter aims at in-depth investigating the two feedback modalities in experimental conditions by comparing their i) effectiveness to improve patients posture in robot-aided rehabilitation treatments, ii) acceptability and iii) comfort.
To reach these objectives, ten healthy subjects were asked to perform 3D reaching tasks with the aid of the robotic platform. Quantitative indicators, such as reaction time and trunk and neck angles, are extracted and a questionnaire was submitted to the subjects to understand the utility of the feedback and subject preference between VF and VtF.

4.2 The proposed non-invasive posture assessment during robot-aided rehabilitation

In this work, a variation of the robotic platform for upper limb rehabilitation proposed in the Chapter 3 is adopted. The original platform was composed of three modules:

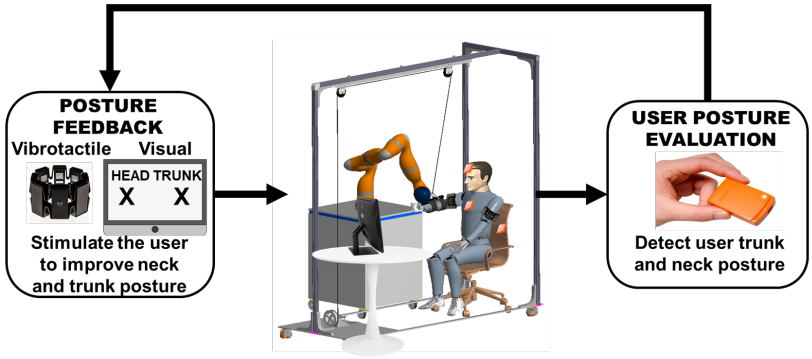

Fig. 4.2 Block diagram of the proposed robotic rehabilitation platform.

I. An anthropomorphic 7-DoFs (Degrees of Freedom) robotic arm, i.e. the Kuka Light Weight Robot 4+, connected to the user wrist by means of a purposely developed flange.

II. A motorized arm-weight support for the patient impaired limb. It provides a variable support level of the patient limb on the basis of muscular fatigue. To assess user muscular fatigue, the Dimitrov Index [21] is computed on electromyographic (EMG) data acquired at 1 kHz with surface EMG electrodes (i.e. Delsys Trigno wireless sensors) positioned on the following muscles: upper trapezius, posterior deltoid, lateral deltoid, anterior deltoid, pectoralis major, biceps brachii and lateral triceps.

III. A virtual reality environment (VR), ad-hoc developed in Unity 3D, to show the patient the task to be performed.

In addition to these modules, the modules shown in Fig. 4.2 were developed for i) monitoring the patient posture and ii) conveying to the user warning stimuli when an incorrect position is detected, during the robot-aided rehabilitation treatment. In the following, some theoretical details about the modules of posture evaluation and stimulation feedback are given, based on [90].

4.2.1 Posture Evaluation

Three magneto-inertial measurement units (M-IMUs, XSens MTw) were used to assess subject posture during the rehabilitation treatment. As shown in Fig. 4.3, the M-IMU sensor S1 was positioned on the chair where the subjects were seated during the treatment; the sensor S2 was located on the subject's trunk and S3 was fixed on the subject's head. The sensor placed on the chair acted as reference for the sensors positioned on the subject's trunk

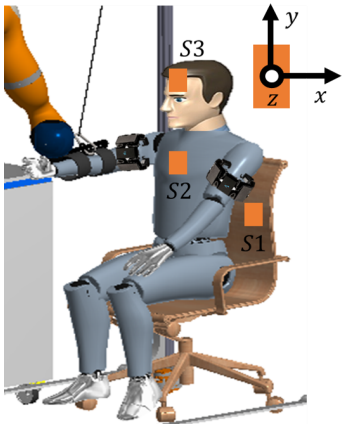

Fig. 4.3 Positioning of the M-IMU sensors on the subject body.

and head, while the other two sensors were used to measure trunk and head flexion/extension (F/E) (Fig. 4.4), respectively.

Let R^G_{chair}, R^G_{trunk}, and R^G_{head} be the rotation matrices that express the orientation of the three M-IMUs with respect to the earth-fixed reference coordinate system G. In order to evaluate trunk F/E (α_{trunk}) and head F/E (β_{head}), the inverse problem of the RPY Euler angles was solved, starting from the rotation matrices R^{chair}_{trunk} and R^{trunk}_{head} calculated as follows

$$R^{chair}_{trunk} = (R^G_{chair})^{-1} R^G_{trunk} \tag{4.1}$$

$$R^{trunk}_{head} = (R^G_{trunk})^{-1} R^G_{head} \tag{4.2}$$

The M-IMUs are synchronised through an Awinda Station that checks the reception of wireless data from the M-IMUs at 100 Hz.

The Rapid Upper Limb Assessment (RULA) scale [64] was adopted to establish appropriate thresholds for trunk and head F/E angles. The RULA is a tool to assess the exposure to ergonomic risk factors during working tasks. Briefly, it allows to detect any ergonomically incorrect postures through a score from 1 to 7. In our case, in which head and trunk F/E angles (α_{head} and β_{trunk}) are monitored, the upper and lower thresholds for both angles were conventionally set at 0.17 and 0 rad, respectively. These values correspond to the first thresholds that determine a score increase for the head district in the RULA test. As regards the trunk, according to the RULA test, the upper threshold should be 0.34 rad. However, it has been decided to consider a lower threshold (i.e. 0.17 rad) also for the trunk in order to recreate a situation similar to the one that could occur with patients during robot-aided rehabilitation, where trunk compensatory movements should tend to be larger and more frequent with respect to those of healthy subjects [103]. To set the trunk threshold at 0.17

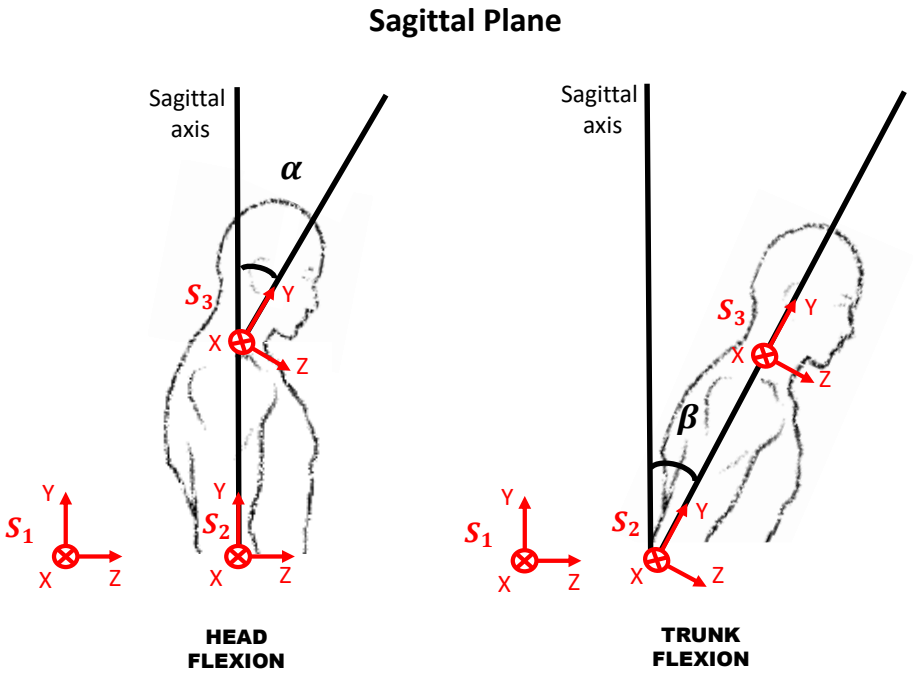

Fig. 4.4 Head and Trunk F/E angles considered to provide feedback.

rad increases the difficulty of the task performed by healthy subjects, and let us understand if the feedback modalities are valid also in conditions where trunk compensatory movements are frequent, as in case of patients during robot-aided rehabilitation.

4.2.2 Feedback for posture improvement

The VR module, introduced in Sect. 4.2, has been developed in order to allow the user to perform pick and place tasks in nine predefined positions in the 3D virtual reality space. The subject hand position, monitored by the sensors embedded in the robotic arm, was reconstructed in the Virtual Environment. The subjects were asked to reach 9 positions with their hand. These positions are shown in Fig. 4. They are located at three different heights from the subject's shoulder position (i.e. 0 m, 0.19 m and 0.38 m). Left, middle and right positions for each height are placed in order to make the subject abduct his/her shoulder of, -0:21 rad, 0 rad, and +0:21 rad, respectively. In Fig. 4.5, the virtual environment seen by the subjects during the whole rehabilitation session by means of a video screen positioned in front of them is shown. The object to be picked and placed is a brown box initially located in the starting position (circled in red). Once picked, the object should be moved with point to point movements up to the 9 white balls (i.e. the target positions) passing through the starting position each time the target position is changed.

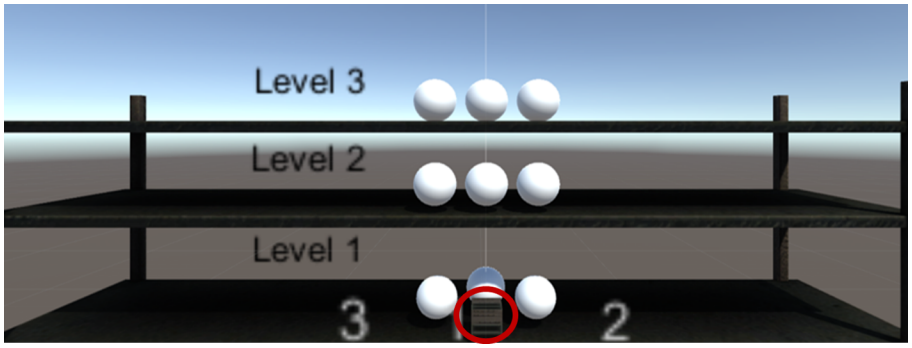

Fig. 4.5 The proposed VR module with target positions (in white) and the starting position (in red).

The user is provided with two types of feedback, namely the visual (VF) and the vibrotactile (VtF) feedback, to allow him/her to maintain a correct posture during the rehabilitation session. A posture is considered correct as long as the trunk and head angles are within the thresholds defined in Sect. 4.2.1.

1. The Visual feedback (VF) is integrated in the VR module and consists of showing to the user some warning visual stimuli when the user trunk and neck are considered to be in unsafe positions. In particular, two warning indicators are shown on the screen for each of the considered Degrees of Freedom, i.e. the trunk and head F/E. When the user is considered to be in a correct position, the indicators are black. Otherwise, when the user overcomes the preset Range of Motion (RoM) limits with the trunk and/or the neck, the indicator related to the specific DoF become red accordingly. The red indicator visualized by the subjects is continuous if $\alpha_{head} > 0.17$ rad or $\beta_{trunk} > 0.17$ rad, whereas it is blinking if $\alpha_{head} < 0$ rad or $\beta_{trunk} < 0$ rad.

2. The Vibrotactile feedback (VtF) is provided by two light-weighted vibrating actuators integrated in two Myo Armbands (Thalmic Labs, CDN) positioned on the arms of the subject. The vibration of the Myo Armband on the right/left arm of the subject is activated when the subject head/trunk exceeds the correct posture range defined in Sect. 4.2.1. The vibration supplied to the subjects is continuous if $\alpha_{head} > 0.17$ rad or $\beta_{trunk} > 0.17$ rad, whereas the vibration is intermittent if $\alpha_{head} < 0$ rad or $\beta_{trunk} < 0$ rad.

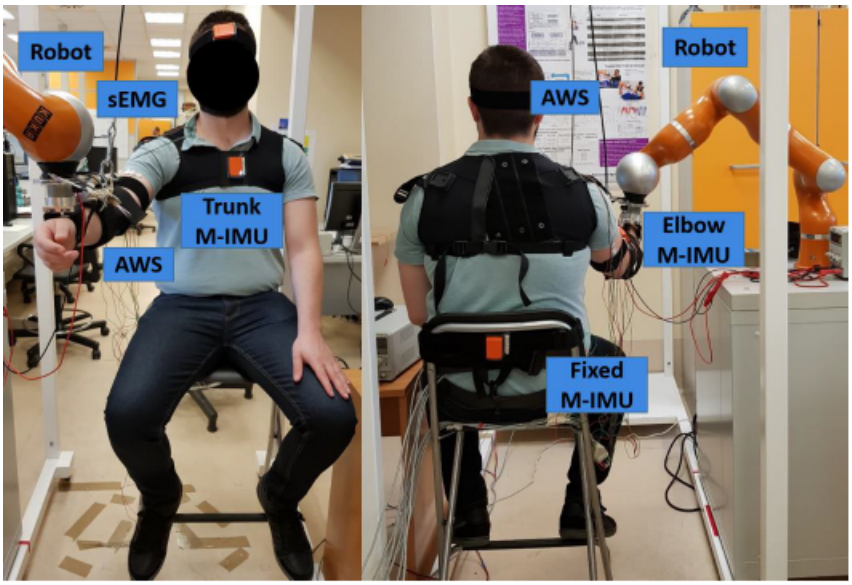

Fig. 4.6 A frontal and posterior view of the experimental setup.

4.3 Experimental validation 1

4.3.1 Experimental setup

The proposed bio-cooperative platform, shown in Fig. 4.8, is composed of the anthropomorphic robotic arm, the actuated arm-weight support and a multimodal interface. The robotic arm is the Kuka Light Weight Robot 4+, which is characterized by 7 Degrees of Freedom (DoFs) and embeds position and torque sensors at joints. The arm-weight module actuation system is based on an EC-max 40 brushless Maxon Motor. Finally, an ergonomic brace for arm support enables to set correct fitting depending on patients requirements. The multimodal interface is composed of sEMG sensors, to monitor sub-ject muscular activity and extract information about muscular fatigue, and M-IMUs (i.e. XSens MTw), which are integrated in the system with the twofold aim of reconstructing the upper-limb kinematics to control the AWS and of monitoring the behavior of sub-ject trunk, neck and shoulder during therapy. The M-IMU and robot sensors data are acquired at 100Hz. A virtual reality is included in the platform to help subjects to know the action to be performed and to monitor his/her performance during task execution.

4.3.2 Experimental protocol

Eight healthy subjects have been involved in this study. Each subject performed the task sitting on a chair, in front of a virtual reality, with his/her right arm positioned in an ergonomic

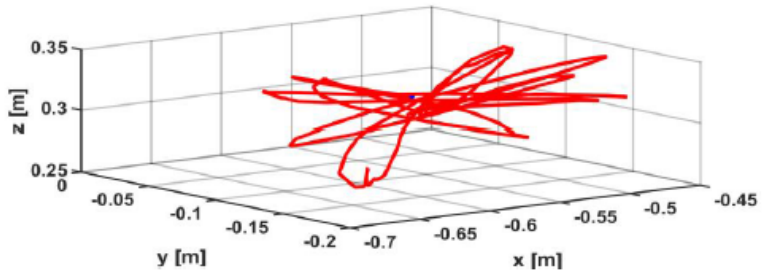

Fig. 4.7 Robot end-effector position with full assistance for a representative subject during point-to-point reaching movements.

backing for the arm and with the wrist connected to the end-effector of the robot. Each subject performed 16 point-to-point reaching movements in the 3D space. In order to understand if the proposed platform influences the subjects posture, subjects performed the assigned task in two different conditions: 1) with full assistance provided by the platform (i.e. 100% of arm weight support and high gain for the robotic arm); 2) without assistance provided by the platform (i.e. 0% of arm weight support and low gain for the robotic arm). Subject's upper limb kinematics and their posture are reconstructed by means of the M-IMU sensors.

4.3.3 Results and discussions

The results of one representative subject are reported, but similar results have been obtained for the other subjects. The robot end-effector position during task execution with full assistance is shown in Figure 4.7. The 3D Cartesian coordinates of the elbow in the two conditions are shown in Figure 4.8. As evident the difference between the two work-ing conditions is small (i.e. the maximum error is along the X-axis and is less than 0.05m). The same behavior was obtained for the other joints. It means that the level of assistance provided by the platform does not influence the subject's posture. During the two conditions, the muscular fatigue was evaluated. In particular, the mean value and standard deviation, computed on the 8 subjects, of the muscular fatigue indicator C_m of the corresponding level of AWS L_s are $C_m = 3 \pm 0.15$ and L_s =2 or 3, with full assistance, and $C_m = 0.220.13$ and L_s ==0 or 1, without assistance.

The subject's trunk, head, shoulder, elbow and wrist angles were evaluated during the trials. In order to assess if the platform negatively influences the posture, the RULA score was computed on these values. For all the subjects, the shoulder F/E angle is comprised between 0° and 20° the shoulder I/E is comprised between 15° and 15°, the elbow F/E is comprised between 5° and 35°, the wrist is fixed with a null angle, the neck pitch is comprised between 0° and 10°, the neck roll and yaw are less than 5°, the trunk F/E is comprised between 0° and

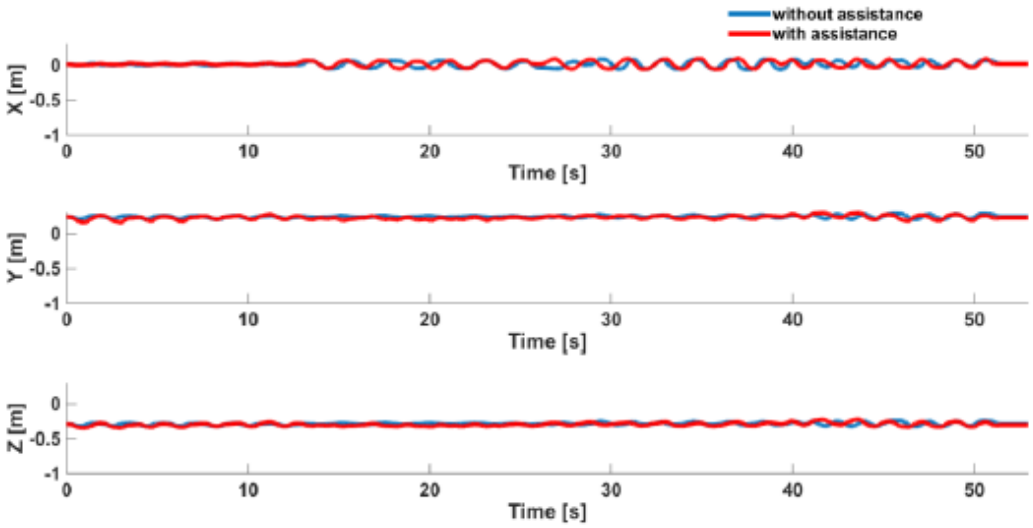

Fig. 4.8 Elbow position with and without assistance for a representative subject point-to-point reaching movements.

20° the trunk lateral F/E and left/right rotation are less than 5°. Legs and feet are supported and the load to be held by the subjects is null. Therefore, the RULA score is equal to 2, which correspond to an acceptable posture.

4.4 Experimental validation 2

4.4.1 Experimental setup

Ten healthy subjects were recruited for participating in the study (28.7 ± 4.7 years old) after providing written informed consent. They were asked to test the overall platform (Fig. 4.9) by performing two consecutive repetitions of the nine 3D reaching movements with the aid of the robotic platform and the feedback modules. The subjects seated on a chair in front of a screen projecting the VR and had the right wrist attached to the robot arm end-effector by means of the connection flange and the right arm supported by the arm-weight support. In order to determine the level of support to be provided by the robotic arm and the arm-weight support, an initial evaluation session was performed. During it, the subjects were asked to reach the 9 target positions with the robotic arm and the arm-weight support modules passive (i.e. the two modules did not provide assistance to the subjects) and without any feedback about posture. After the evaluation session, biomechanical indicators and muscular fatigue were computed. As expected, being the subjects healthy, it was confirmed that no assistance is needed and therefore, a low value of robot arm stiffness (i.e. $K = 0.1 N/m$)

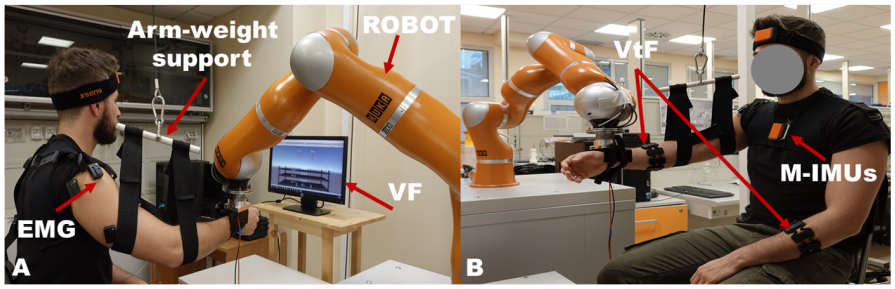

Fig. 4.9 The proposed rehabilitative robotic platform. The subject is receiving information about his posture by means of A) Visual Feedback, B) Vibrotactile Feedback.

and a level equal to 0 of arm gravity support were obtained. A null arm gravity support level is also due to the very short duration of the trial, which not generates muscular fatigue on healthy subjects. As demonstrated in [92], a long duration of the trial could generate muscular fatigue, therefore requiring a level of arm gravity support different from 0 even on healthy subjects.

Robot end-effector position was represented in the VR by a hand avatar holding a virtual box; hence, the users were able to move the virtual box in the VR by using the robot end-effector as input device. The users were asked to move the virtual box to reach the nine virtual balls positioned at different distances and heights into a virtual shelf and to push them outside the shelf as shown in Fig.4.5.

4.4.2 Experimental protocol

The experimental session was divided into 3 phases, where the subjects were required to perform the tasks without feedback, with VtF and with VF. The enrolled subjects were randomized into two groups, called Group 1 and Group 2, composed of five people each. Both groups performed the 9 movements twice without getting any feedback about the correctness of their trunk and neck posture (No FB phase). Subsequently, Group 1 executed the 9 movements twice: with the visual feedback first (VF phase) and later with vibrotactile feedback (VtF phase) to improve their trunk and neck posture. Group 2 performed the same movements of Group 1 but with the feedback modalities inverted. A washout period among the different phases was considered for all the subjects.

4.4.2.1 Performance indices

Data from the sensors integrated in the whole platform were collected for each trial, phase and subject in order to extract quantitative indices to evaluate the task performance. They are:

- Normalized Incorrect Posture Time ($NIPT$), defined as

$$NIPT = \frac{IPT}{T_{tot}} \tag{4.3}$$

  where IPT is the time in which the users trunk and neck are outside the RoM limits defined in Sect. 4.2.1 and T_{tot} is the completion time of the trial.

- Mean Reaction Time (MRT). It represents the mean time, computed on the whole trial, needed by the subject to return in a correct posture after receiving the feedback, and is defined as

$$MRT = \frac{1}{N}\sum_{i=0}^{N} |T^i_{thr} - T^i_{peak}| \tag{4.4}$$

  where N is the number of times the user exceeds the trunk and head RoM limits defined in Sect. 4.2.1, T^i_{thr} is the i_{th} time instant the user exceeds the limits and T^i_{peak} is the i_{th} time instant when the derivative over time of trunk and head F/E changes sign.

Moreover, one questionnaire was administered to the recruited subjects after testing the whole platform during the VF and VtF phase. The questionnaire was aimed to assess the users' preferences about the two types of feedback. The questionnaire is shown in Table 4.1. The users could express their satisfaction in a Likert scale from 1 to 5 where: Strongly agree = 5, Agree= 4, Neither agree nor disagree=3, Disagree = 2, and Strongly disagree = 1. Hence, a synthetic indicator of the user answers, i.e. the Mean Rate (MR), was computed, on average, for each statement and subject.

4.4.3 Statistical Analysis

Mean value and standard deviation (SD) of the aforementioned performance indices were computed on the ten subjects and each phase, i.e. No FB, VF and VtF phase. A statistical analysis based on a Wilcoxon paired-sample test was performed for the following three comparisons: No feedback vs. VF, No feedback vs. VtF and VF vs. VtF.

Table 4.1 The administered questionnaire to evaluate the platform.

Questions about Visual Feedback
I did not notice the Visual Feedback
The Visual Feedback was pleasant
The Visual Feedback motivated me to maintain a correct posture
The Visual Feedback was difficult to follow
I found useful the information provided by the Visual Feedback
Questions about Vibrotactile Feedback
I did not notice the Vibrotactile Feedback
The Vibrotactile Feedback was pleasant
The Vibrotactile Feedback motivated me to maintain a correct posture
The Vibrotactile Feedback was difficult to follow
I found useful the information provided by the Vibrotactile Feedback

4.4.4 Results and Discussions

Figures 4.10 and 4.12 show the behaviour of trunk and head F/E angles reached by a representative subject belonging to Group 2 during the No feedback, VF and VtF phases.

In Fig. 4.12 it can be noted that when the defined trunk and neck thresholds are exceeded, the user corrects his/her posture thanks to the Visual or Vibrotactile feedback. Conversely, in absence of feedback (Fig. 4.10), the user overcomes very often the trunk and neck RoM limits without clear attempts of corrections. Similar results have been obtained for subjects belonging to Group 1. Therefore, it is evident that the type of feedback adopted for first does not influence the results. It is also confirmed by the results of the statistical analysis performed on the NIPT value computed for the two groups ($p-value > 0.05$).

In Figs. 4.13 A and B the NIPT for head and trunk computed on all the subjects, independently of the group they belong to, is shown for the three described conditions, i.e. No FB, VF and VtF. The statistically significant differences are outlined with an asterisc. As evident, when some kind of feedback is provided to the subjects, NIPT is reduced both for head and trunk with respect to the absence of feedback. These differences are statistically significant for No FB vs VF and for No FB vs VtF ($p-value < 0.017$, with Bonferroni correction) for both the angles. No statistically significant differences are obtained for NIPT between the two types of feedback (i.e. VF vs VtF) ($p-value > 0.017$, with Bonferroni correction). NIPT mean values and standard deviations are also listed in Tab. 4.2 with the statistical significance. These results confirm the feasibility and utility of providing feedback to the patients for correcting postures during robot-aided rehabilitation and therefore for improving the outcome of the therapy.

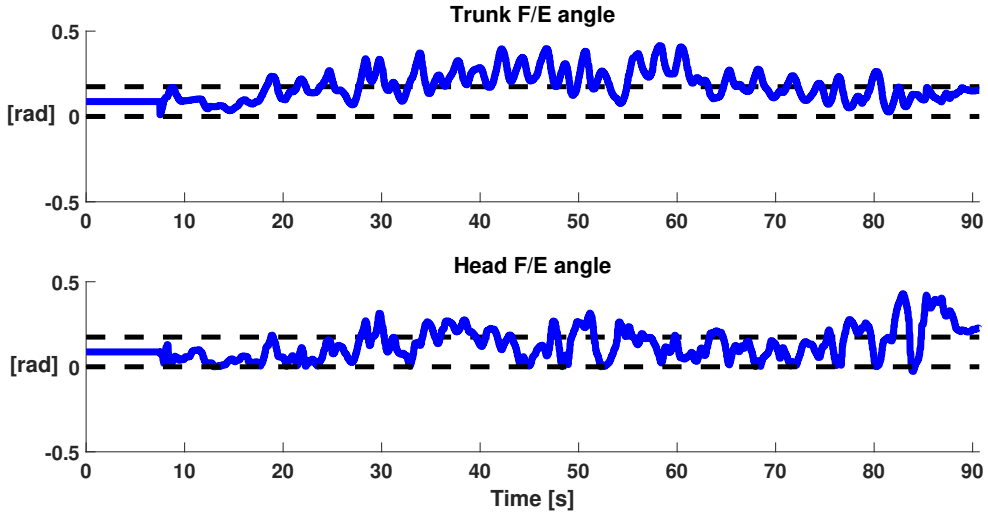

Fig. 4.10 Trend of trunk and head F/E angles during task execution without feedback. The angle behaviour is shown in blue, the angle thresholds are in black.

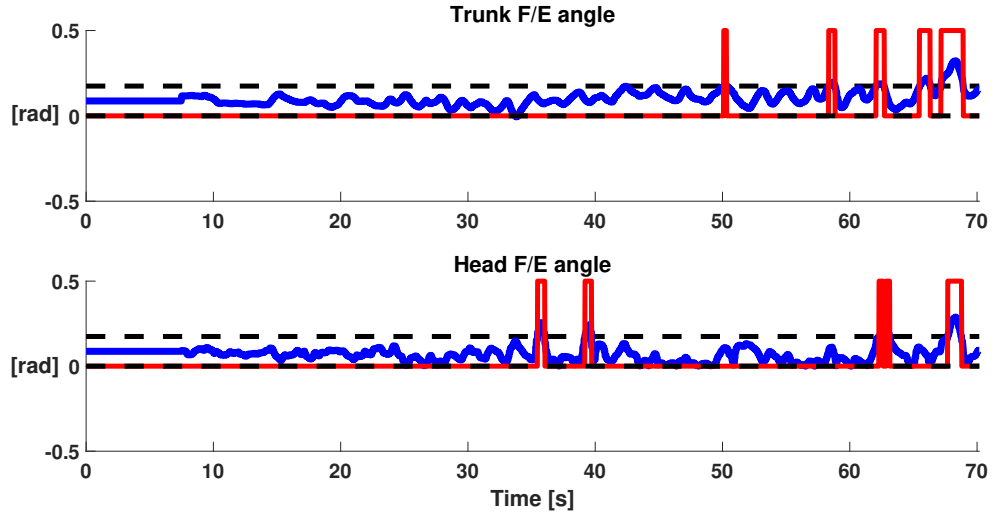

Fig. 4.11 Trend of trunk and head F/E angles (in blue) reached by one representative subject belonging to Group 2 during task execution with VF. The angle thresholds are in black and the VF is outlined in red.

	No FB [au]	VF [au]	VtF [au]
Head	0.24 ± 0.21	$(0.03 \pm 0.03)^*$	$(0.13 \pm 0.19)^*$
Trunk	0.41 ± 0.32	$(0.1 \pm 0.08)^*$	$(0.14 \pm 0.13)^*$

Table 4.2 Mean and std of NIPT for head in trunk in the three described conditions.

In Fig. 4.13 C the Mean Reaction Time is reported for each type of feedback provided to the users. More in detail, the Mean Reaction Time for VF computed on all the subjects,

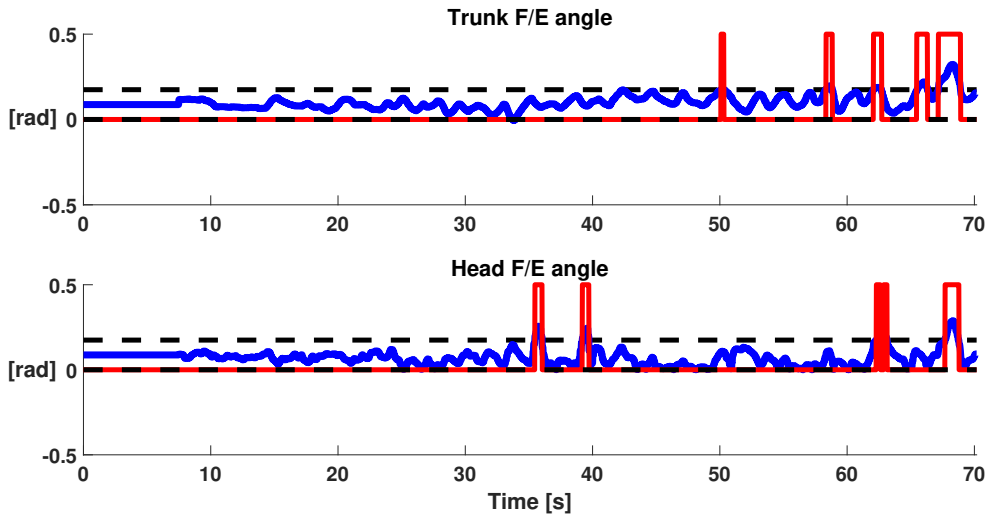

Fig. 4.12 Trend of trunk and head F/E angles (in blue) reached by one representative subject belonging to Group 2 during task execution with VF (A) and VtF (B). The angle thresholds are in black and the VF is outlined in red.

independently of the group they belong to, is 1.48 ± 1.06 s for the head and 1.02 ± 0.60 s for the trunk. In the case of VtF, the Mean Reaction Time is 1.77 ± 0.84 s for the head and 1.52 ± 1.26 s for the trunk. Statistical analysis revealed that the difference in the MRT obtained with VF and VtF for both the head and trunk is statistically significant ($p - value < 0.05$). It means that the subjects require less time to react to the VF with respect to the VtF.

In Fig. 4.14 the robot end-effector position (i.e. hand position of the user) without and with feedback is shown. It is evident that the subject is able to reach the target points assigned in both conditions. The execution of the task is not affected by postural feedback and the visual inspection does not show cross-talk phenomena between the two feedback provided (virtual reality and VF/VtF). Table 4.3 reports the users' answers to the questionnaire in terms of how much the subjects strongly disagreed, disagreed, neither agreed nor disagreed, agreed and strongly agreed with the statements about the VF and the VtF reported in Tab 4.1. Their evaluation can range from 1 (strongly disagree) to 5 (strongly agree). The first 5 columns contain the percentage of subjects who answered in a certain manner with respect to the total number of subjects. In the last column, the mean and standard deviation computed on all the subjects who answered to one question is shown. A statistical analysis was performed to understand if the subjects preferred one feedback modality to another. The results revealed that there are not statistically significant differences between the subjective evaluation of the two feedback modalities ($p - value > 0.05$ for the five statements). In summary, the statistical analysis revealed a significant difference in the MRT between the two types of

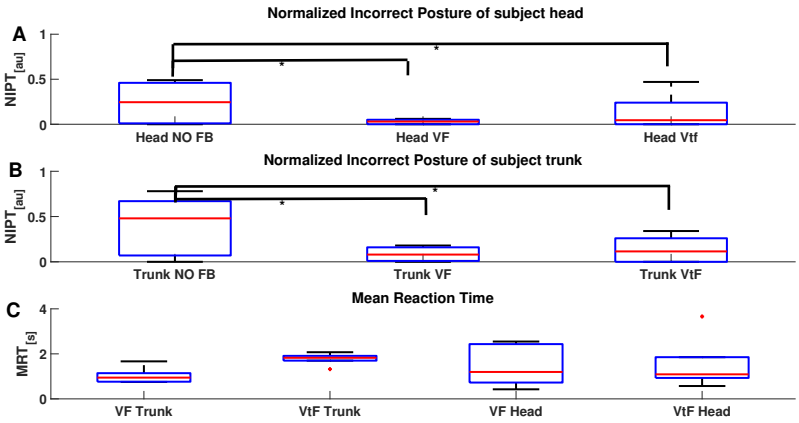

Fig. 4.13 Normalized Incorrect Posture Time (NIPT) of subject head (A) and trunk (B) and Mean Reaction Time for VF and VtF (C).

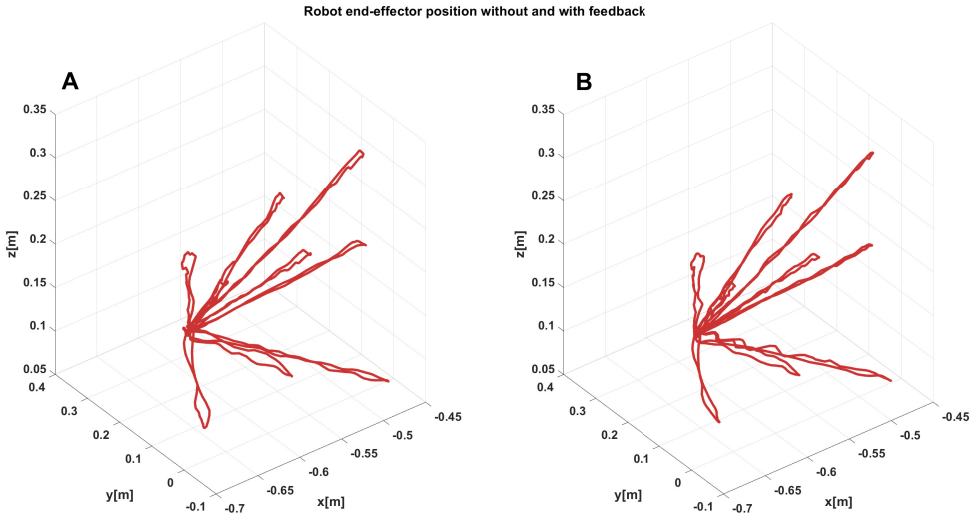

Fig. 4.14 Robot end-effector position (i.e. hand position of the subject) without (A) and with feedback (B) provided to the user during the execution of the task.

Table 4.3 Users' answers to the questionnaires, Strongly Disagree (SD) = 1 , Disagree (D) = 2, Neither agree nor disagree (N) = 3, Agree (A) = 4, Strongly Agree (SA) = 5. Results are reported as a percentage of the total subjects.

	SD	D	N	A	SA	Mean rate±std
Results about Visual Feedback						
I did not notice the Visual Feedback	20	50	30	0	0	2.1±0.2
The Visual Feedback was pleasant	0	0	40	60	0	3.6±0.3
The Visual Feedback motivated me to maintain a correct posture	0	0	0	60	40	4.4±0.3
The Visual Feedback was difficult to follow	0	60	40	0	0	2.3±0.3
I found useful the information provided by the Visual Feedback	0	0	20	70	10	3.9±0.3
Results about Vibrotactile Feedback						
I did not notice the Vibrotactile Feedback	20	40	10	30	0	2.5±0.2
The Vibrotactile Feedback was pleasant	0	20	20	50	10	3.5±0.2
The Vibrotactile Feedback motivated me to maintain a correct posture	0	0	30	70	0	3.7±0.3
The Vibrotactile Feedback was difficult to follow	30	20	20	30	0	2.5±0.1
I found useful the information provided by the Vibrotactile Feedback	0	0	20	60	20	4±0.3

feedback ($p_{MRT} < 0.05$). Conversely, the difference between the two tested feedback in terms of NIPT and of subjective evaluation (obtained by means of the questionnaire) is not statistically significant ($p - value > 0.05$). From these results, it is evident that both the VF and VtF are accepted and are considered to be useful by the subjects involved in the study.

4.5 Conclusions

In this Chapter a module for visual and/or vibrotactile feedback during robot-aided rehabilitation with the bio-cooperative platform proposed in the Chapter 3 has been introduced. The module, through continuous monitoring of the subject posture, provides feedback if the subject assumes incorrect postures with his/her trunk and/or head. The system was preliminarily tested on healthy subjects using RULA test, to ensure that the proposed platform does not lead the subject to assume an incorrect configuration. The bio-cooperative platform proposed in the Chapter 3 was then tested with the addition of visual and vibrotactile feedback module. This has shown that adding feedback allows performing the assigned task by trying to maintain a correct posture with both trunk and head.

Chapter 5

Conclusions and future work

In this work, a novel bio-cooperative robotic platform for robot-aided rehabilitation based on the human-in-the-loop control strategy was designed and developed. The proposed platform is able to provide a level of assistance based on the performance of the subject, the proposed strategy allows to include patient in the control loop by providing him/her the correct amount of assistance on the basis of biomechanical performance and physiological indicators. Personalization of the treatment is a prerogative of the proposed system; in fact, physiological and sensory-motor measurements are included into the control loop to create a rehabilitative scenario that is tailored to the specific subject needs. More in detail, the robotic platform is composed of an end-effector robot, an arm-gravity support and a purposely developed multimodal interface. The interaction between the subjects and the proposed platform were constantly monitored to extract biomechanical and physiological indicators and consequently modify the level of assistance and the difficulty of the exercise. To do this, the multimodal interface is composed of embedded force/torque sensors, M-IMU and EMG sensors in order to record data during robot-aided rehabilitation tasks and monitor patient status to adapt assistance to the user residual functional and motor capabilities.
Various biomechanical and physiological indicators have been tested and integrated into the platform, such as aiming angle, MAPR, inter-joint coordination, UMF and UPF. Furthermore, the level of muscle fatigue, based on the Dimitrov index, was calculated in order to take into account the level of muscle fatigue when defining the level of assistance to be provided to the patient.
A detailed analysis of the hand muscle synergies in chronic stroke patients during robot-aided rehabilitation was performed, in order to assess hand muscular activation patterns of the patients affected by stroke and estimate the feasibility of using muscle synergies for the assessment of the patient's status following robotic rehabilitation treatment. Seven stroke subjects were involved in this study. Each of them underwent a month of robotic therapy and

the muscle synergies of six hand muscles were evaluated before and after treatment with the robot, carrying out simple standardized tasks. The results show a high index of similarity of the muscle activation patterns between the healthy and the affected hand both before and after the rehabilitation treatment. Furthermore, it emerges from the comparison that, following the treatment with the robot, the degree of similarity between the synergies of the injured and the affected side tends to increase, synonymous with the possible benefit of the rehabilitation treatment, even if a larger population is needed to demonstrate this. However, muscle synergies can be a useful tool to evaluate the patient undergoing robotic therapy, although the high computational cost to compute them does not allow this indicator to be used online for updating the level of therapy to the specific patient needs.
Moreover, the proposed platform, composed of end-effector robot and the upper limb adaptive arm-weight support, was preliminary tested on 10 healthy subjects performing a state-of-the-art 3D point-to-point movements with and without assistance-as-needed provided by the robotic platform. The obtained results demonstrated that the proposed system reduces the muscular fatigue without negatively affect motor execution of the task and muscular activation patterns. The presented arm-gravity support, thanks to its modular structure and its control strategy, has shown its potential capability to assist both right and left-handed subjects who cannot self-sustain their upper limb against gravity. The torque control depicts a simple and robust way to allow subjects performing the required task. Furthermore subjects consider that this solution might have a crucial role during rehabilitation session. The evidence obtained in this analysis show the potential of using muscle synergies not only for the evaluation of the patient, but also as an indicator for regulating the level of assistance provided by the platform in order to improve motor tasks and enhance muscle synergies in which the subject manifests abnormalities.
A module for visual and/or vibrotactile feedback was developed, capable of showing the task and providing feedback in case the subject assumes incorrect postures during the execution of the assigned task, and have been integrated in the proposed bio-cooperative platform. M-IMU sensors were adopted to monitor the changes in the posture during the execution of the task, providing appropriate information to the feedback devices, and subsequently to the user when necessary. First of all, a preliminary analysis was conducted to ensure that the proposed bio-cooperative platform is able to avoid negative effect on subject posture. The experimental results on eight healthy subjects demonstrated that the proposed platform does not negatively influence the subject posture. The preliminary analysis investigated the effects of sensory feedback during robot-aided rehabilitation to ensure users' ergonomic postures. To this purpose two feedback modalities, i.e. visual and vibrotactile, were included in the upper-limb robotic platform presented in [89] and were compared. The system performance

was assessed in terms of effectiveness in improving subject posture, acceptability and user comfort. The whole platform was tested on 10 healthy subjects performing 3D reaching movements without feedback, with visual feedback and with vibrotactile feedback. In the first case, the subjects performed the task without any information about their posture and therefore frequently reaching incorrect configurations. In the other two cases, the subjects, aware of the presence of feedback, tended to perform the task trying to maintain a correct posture with both trunk and head. The obtained results revealed that both the feedback modalities are valid solutions to provide posture information, but it emerged that the visual feedback is more intuitive than the vibrotactile feedback.

Clinical evaluation of the proposed bio-cooperative platforms on patient

The proposed bio-cooperative platform for upper limb robot-aided rehabilitation, presented in the Chapters 2, 3 and 4, composed of:

- an end-effector robotic arm
- an arm-weight support for relieving the weight of the patient's limb
- a multimodal interface consisting of: position and force sensors of the robots, magneto-inertial sensors, electromyographic electrodes (EMG)
- a visual and vibrotactile feedback module
- a virtual environment that reproduces simulated scenarios

is currently adopted in a clinical validation on patients suffering from humerus fracture and subjects in aftermath of surgical repair of rotator cuff injury.

The primary objective of this experimentation is to verify the efficacy and validate a bio-cooperative system for the robot-mediated rehabilitation of the shoulder and for the rehabilitation of the working gesture of subjects affected by musculoskeletal pathology of the upper limb. For this study, 10 patients have been enrolled for 40 sessions of robotic therapy divided into two phases of 20 sessions each. The 1^{st} phase consists of robot-assisted reaching tasks in different directions of the working space with decreasing compensation of the weight of the arm on the basis of a modulation function associated with predefined thresholds - 25%, 50%, 75%, 100% - of the weight of the patient's limb. During the 2^{nd} phase, the patients is divided into four groups and carry out robotic therapy aimed at recovering the working gesture. The working gestures implemented are four: load handling, hammering, screwing manually, screwing with screwdriver. The Figs. 5.1 and 5.2 shows some preliminary results of this study on one example subject. In particular, a trajectory performed by the subject in

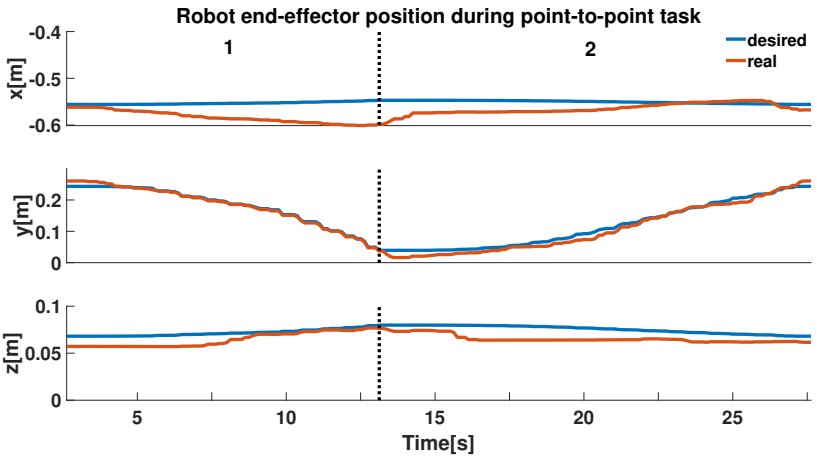

Fig. 5.1 Robot end-effector position (i.e. patient hand) during point-to-point task. 1=Forward Movement;2=Backward Movement.

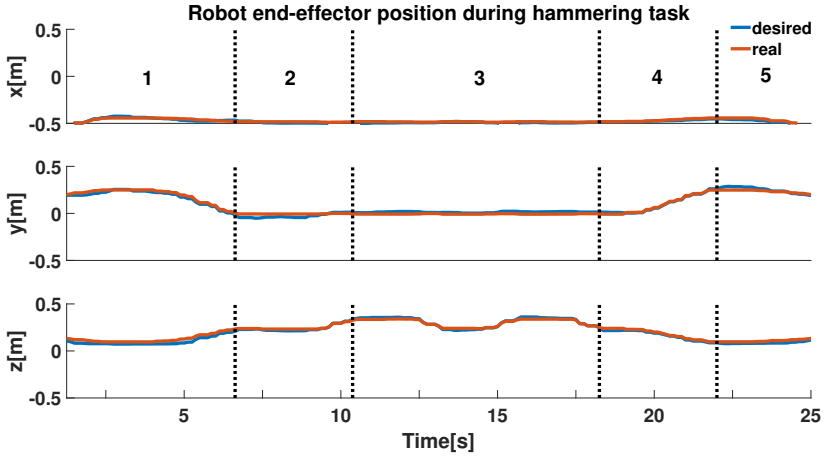

Fig. 5.2 Robot end-effector position (i.e. patient hand) during hammering task. 1=Grab the hammer, 2=Reach the object, 3=Hammer, 4=Release the hammer, 5=Return to starting point.

the first phase (point-to-point) and a trajectory performed by the same subject during the second phase for the assigned work task (hammering) is reported.

Future works will be mainly addressed to:

- implement a higher number of activities of daily living (ADL) in the proposed platform and to test them on patients;
- test the proposed bio-cooperative platform on patients affected by various disease, such as stroke and musculoskeletal disorders, with an ad hoc experimental protocol, to establish the effects of this platform on patients with motor disabilities;

- reconstruct of patient status based on different physiological data: skin conductance, heart rate, respiration rate, ...

List of Publications

Published

International peer-reviewed journals

1. **Scotto di Luzio, F.**, Simonetti, D., Cordella, F., Miccinilli, S. , Sterzi, S., Draicchio, F. , Zollo, L., (2018). Bio-cooperative approach for the human-in-the-loop control of an end-effector rehabilitation robot. Frontiers in neurorobotics, doi: 10.3389/fnbot.2018.00067

2. **Scotto di Luzio, F.**, Lauretti, C., Cordella, F., Draicchio, F., & Zollo, L., Visual vs vibrotactile feedback for posture assessment during upper-limb robot-aided rehabilitation, (2019), Applied Ergonomics, doi: 10.1016/j.apergo.2019.102950

Peer-reviewed international conference proceedings

1. **Scotto di Luzio, F.**, Cordella, F., Lauretti, C., Simonetti, D., Sterzi, S., Draicchio, F., & Zollo, L. (2018, August). A Bio-cooperative Robotic System to Ensure Ergonomic Postures During Upper Limb Rehabilitation in Occupational Contexts. In Congress of the International Ergonomics Association (pp. 327-336). Springer, Cham.

2. **Scotto di Luzio, F.**, Simonetti, D., Cordella, F., Carpino, G., Draicchio, F., & Zollo, L. (2018, August). An adaptive arm-weight support platform for 3D upper limb robot-aided neuro-rehabilitation.In Biomedical Robotics and Biomechatronics (BioRob), 2018 7th IEEE International Conference on.

3. **Scotto di Luzio, F.**, Cordella, F., Lauretti, C., Draicchio, F., & Zollo, L. (2018, October). Assessment of muscular activation patterns in 3D upper limb robot-aided rehabilitation. International Conference on Neurorehabilitation, ICNR 2018.

4. Lauretti, C., Cordella, F., **Scotto di Luzio, F.**, Saccucci, S., Davalli, A., Sacchetti, R., & Zollo, L. (2017, July). Comparative performance analysis of M-IMU/EMG and

voice user interfaces for assistive robots. In Rehabilitation Robotics (ICORR), 2017 International Conference on (pp. 1001-1006). IEEE.

5. Cordella, F., **Scotto di Luzio, F.**, Lauretti, C., Draicchio, F., Zollo, L. (2019, June). A biofeedback-based posture correction system for working environments. In 2019 II Workshop on Metrology for Industry 4.0 and IoT (MetroInd4. 0IoT) (pp. 405-409). IEEE.

6. Lauretti, C., Cordella, F., Tamantini, C., Gentile, C., **Scotto di Luzio, F.**, Zollo, L., A Surgeon-Robot Shared Control for Ergonomic Pedicle Screw Fixation. In 2020 IEEE International Conference on Robotics and Automation. IEEE.

Peer-reviewed national conference proceedings

1. **Scotto di Luzio, F.**, Simonetti, D., Zollo, L., Arm-weight support for 3D upper limb rehabilitation, Congress of the National Bioengineering Group, GNB 2018 Milan

In press

International peer-reviewed journals

1. Lauretti, C., Cordella, F., Tamantini, C., Gentile, C., **Scotto di Luzio, F.**, Zollo, L., A Surgeon-Robot Shared Control for Ergonomic Pedicle Screw Fixation. IEEE Robotics and Automation Letters.

References

[1] Ahamed, N. U., Sundaraj, K., Ahmad, R. B., Rahaman, S. M., Islam, M. A., and Ali, M. A. (2012). Variability in surface electromyography of right arm biceps brachii muscles between male adolescent, vicenarian and tricenarian with distinct electrode placement. In *2012 IEEE Conference on Sustainable Utilization and Development in Engineering and Technology (STUDENT)*, pages 24–28. IEEE.

[2] Ajiboye, A. B. and Weir, R. (2009). Muscle synergies as a predictive framework for the emg patterns of new hand postures. *Journal of neural engineering*, 6(3):036004.

[3] Akamatsu, M., MacKenzie, I. S., and Hasbroucq, T. (1995). A comparison of tactile, auditory, and visual feedback in a pointing task using a mouse-type device. *Ergonomics*, 38(4):816–827.

[4] Amirabdollahian, F., Loureiro, R., Gradwell, E., Collin, C., Harwin, W., and Johnson, G. (2007). Multivariate analysis of the fugl-meyer outcome measures assessing the effectiveness of gentle/s robot-mediated stroke therapy. *Journal of NeuroEngineering and Rehabilitation*, 4(1):4.

[5] Ananthanarayan, S., Sheh, M., Chien, A., Profita, H., and Siek, K. (2013). Pt viz: towards a wearable device for visualizing knee rehabilitation exercises. In *Proceedings of the SIGCHI Conference on Human Factors in Computing Systems*, pages 1247–1250. ACM.

[6] Babaiasl, M., Mahdioun, S. H., Jaryani, P., and Yazdani, M. (2016). A review of technological and clinical aspects of robot-aided rehabilitation of upper-extremity after stroke. *Disability and Rehabilitation: Assistive Technology*, 11(4):263–280.

[7] Bischoff, R., Kurth, J., Schreiber, G., Koeppe, R., Albu-Schäffer, A., Beyer, A., Eiberger, O., Haddadin, S., Stemmer, A., Grunwald, G., et al. (2010). The kuka-dlr lightweight robot arm-a new reference platform for robotics research and manufacturing. In *Robotics (ISR), 2010 41st international symposium on and 2010 6th German conference on robotics (ROBOTIK)*, pages 1–8. VDE.

[8] Bizzi, E. and Cheung, V. C. (2013). The neural origin of muscle synergies. *Frontiers in computational neuroscience*, 7:51.

[9] Blank, A. A., French, J. A., Pehlivan, A. U., and O'Malley, M. K. (2014). Current trends in robot-assisted upper-limb stroke rehabilitation: promoting patient engagement in therapy. *Current physical medicine and rehabilitation reports*, 2(3):184–195.

[10] Carpinella, I., Cattaneo, D., Bertoni, R., and Ferrarin, M. (2012). Robot training of upper limb in multiple sclerosis: comparing protocols with or withoutmanipulative task components. *IEEE Transactions on Neural Systems and Rehabilitation Engineering*, 20(3):351–360.

[11] Charalambous, C. P. (2014). Interrater reliability of a modified ashworth scale of muscle spasticity. In *Classic papers in orthopaedics*, pages 415–417. Springer.

[12] Cheung, V. C., Turolla, A., Agostini, M., Silvoni, S., Bennis, C., Kasi, P., Paganoni, S., Bonato, P., and Bizzi, E. (2012). Muscle synergy patterns as physiological markers of motor cortical damage. *Proceedings of the National Academy of Sciences*, 109(36):14652–14656.

[13] Coderre, A. M., Zeid, A. A., Dukelow, S. P., Demmer, M. J., Moore, K. D., Demers, M. J., Bretzke, H., Herter, T. M., Glasgow, J. I., Norman, K. E., et al. (2010). Assessment of upper-limb sensorimotor function of subacute stroke patients using visually guided reaching. *Neurorehabilitation and neural repair*, 24(6):528–541.

[14] Cordella, F., Di Corato, F., Loianno, G., Siciliano, B., and Zollo, L. (2013a). Robust pose estimation algorithm for wrist motion tracking. In *2013 IEEE/RSJ International Conference on Intelligent Robots and Systems*, pages 3746–3751. IEEE.

[15] Cordella, F., Di Corato, F., Loianno, G., Siciliano, B., and Zollo, L. (2013b). Robust pose estimation algorithm for wrist motion tracking. In *IEEE/RSJ International Conference on Intelligent Robots and Systems*, pages 3746–3751. IEEE.

[16] Cordella, F., Zollo, L., Guglielmelli, E., and Siciliano, B. (2012a). A bio-inspired grasp optimization algorithm for an anthropomorphic robotic hand. *International Journal on Interactive Design and Manufacturing (IJIDeM)*, 6(2):113–122.

[17] Cordella, F., Zollo, L., Guglielmelli, E., and Siciliano, B. (2012b). A bio-inspired grasp optimization algorithm for an anthropomorphic robotic hand. *International Journal on Interactive Design and Manufacturing*, 6(2):113–122.

[18] Coscia, M., Cheung, V. C., Tropea, P., Koenig, A., Monaco, V., Bennis, C., Micera, S., and Bonato, P. (2014). The effect of arm weight support on upper limb muscle synergies during reaching movements. *Journal of neuroengineering and rehabilitation*, 11(1):22.

[19] di Luzio, F. S., Cordella, F., Lauretti, C., Simonetti, D., Sterzi, S., Draicchio, F., and Zollo, L. (2018a). A bio-cooperative robotic system to ensure ergonomic postures during upper limb rehabilitation in occupational contexts. In *Congress of the International Ergonomics Association*, pages 327–336. Springer.

[20] di Luzio, F. S., Simonetti, D., Cordella, F., Miccinilli, S., Sterzi, S., Draicchio, F., and Zollo, L. (2018b). Bio-cooperative approach for the human-in-the-loop control of an end-effector rehabilitation robot. *Frontiers in neurorobotics*, 12.

[21] Dimitrov, G. V., Arabadzhiev, T. I., Mileva, K. N., Bowtell, J. L., Crichton, N., and Dimitrova, N. A. (2006). Muscle fatigue during dynamic contractions assessed by new spectral indices. *Medicine and science in sports and exercise*, 38(11):1971.

Francesco Scotto di Luzio

[22] Eimer, M. (2004). Multisensory integration: how visual experience shapes spatial perception. *Current biology*, 14(3):R115–R117.

[23] Fan, R. E., Culjat, M. O., King, C.-H., Franco, M. L., Boryk, R., Bisley, J. W., Dutson, E., and Grundfest, W. S. (2008). A haptic feedback system for lower-limb prostheses. *IEEE Transactions on Neural Systems and Rehabilitation Engineering*, 16(3):270–277.

[24] Formica, D., Zollo, L., and Guglielmelli, E. (2005a). Torque-dependent compliance control in the joint space of an operational robotic machine for motor therapy. In *Rehabilitation Robotics, 2005. ICORR 2005. 9th International Conference on*, pages 341–344. IEEE.

[25] Formica, D., Zollo, L., and Guglielmelli, E. (2005b). Torque-dependent compliance control in the joint space of an operational robotic machine for motor therapy. In *9th International Conference on Rehabilitation Robotics, 2005. ICORR 2005.*, pages 341–344. IEEE.

[26] Friedrich, M., Cermak, T., and Maderbacher, P. (1996). The effect of brochure use versus therapist teaching on patients performing therapeutic exercise and on changes in impairment status. *Physical Therapy*, 76(10):1082–1088.

[27] Fugl-Meyer, A. R., Jääskö, L., Leyman, I., Olsson, S., and Steglind, S. (1975). The post-stroke hemiplegic patient. 1. a method for evaluation of physical performance. *Scandinavian journal of rehabilitation medicine*, 7(1):13–31.

[28] Gescheider, G. A. and Wright, J. H. (1968). Effects of sensory adaptation on the form of the psychophysical magnitude function for cutaneous vibration. *Journal of experimental psychology*, 77(2):308.

[29] González-Izal, M., Malanda, A., Gorostiaga, E., and Izquierdo, M. (2012). Electromyographic models to assess muscle fatigue. *Journal of Electromyography and Kinesiology*, 22(4):501–512.

[30] Gonzalez-Izal, M., Malanda, A., Navarro-Amezqueta, I., Gorostiaga, E., Mallor, F., Ibanez, J., and Izquierdo, M. (2010). Emg spectral indices and muscle power fatigue during dynamic contractions. *Journal of Electromyography and Kinesiology*, 20(2):233–240.

[31] Gopalai, A. A. and Senanayake, S. A. A. (2011). A wearable real-time intelligent posture corrective system using vibrotactile feedback. *IEEE/ASME Transactions on Mechatronics*, 16(5):827–834.

[32] Guerrero, C. R., Marinero, J. F., Turiel, J. P., and Farina, P. R. (2010). Bio cooperative robotic platform for motor function recovery of the upper limb after stroke. In *2010 Annual International Conference of the IEEE Engineering in Medicine and Biology*, pages 4472–4475. IEEE.

[33] Hakim, R. M., Tunis, B. G., and Ross, M. D. (2017). Rehabilitation robotics for the upper extremity: review with new directions for orthopaedic disorders. *Disability and Rehabilitation: Assistive Technology*, 12(8):765–771.

Francesco Scotto di Luzio

[34] Held, J. P., Klaassen, B., van Beijnum, B.-J. F., Luft, A. R., and Veltink, P. H. (2017). Usability evaluation of a vibrotactile feedback system in stroke subjects. *Frontiers in bioengineering and biotechnology*, 4:98.

[35] Hermens, H. J., Freriks, B., Merletti, R., Stegeman, D., Blok, J., Rau, G., Disselhorst-Klug, C., and Hägg, G. (1999). European recommendations for surface electromyography. *Roessingh research and development*, 8(2):13–54.

[36] Housman, S. J., Scott, K. M., and Reinkensmeyer, D. J. (2009). A randomized controlled trial of gravity-supported, computer-enhanced arm exercise for individuals with severe hemiparesis. *Neurorehabilitation and neural repair*, 23(5):505–514.

[37] Hsu, L.-C., Wang, W.-W., Lee, G.-D., Liao, Y.-W., Fu, L.-C., and Lai, J.-S. (2012). A gravity compensation-based upper limb rehabilitation robot. In *American Control Conference (ACC), 2012*, pages 4819–4824. IEEE.

[38] Iwamuro, B. T., Cruz, E. G., Connelly, L. L., Fischer, H. C., and Kamper, D. G. (2008). Effect of a gravity-compensating orthosis on reaching after stroke: evaluation of the therapy assistant wrex. *Archives of physical medicine and rehabilitation*, 89(11):2121–2128.

[39] Jaffe, D. L., Brown, D. A., Pierson-Carey, C. D., Buckley, E. L., and Lew, H. L. (2004). Stepping over obstacles to improve walking in individuals with poststroke hemiplegia. *Journal of Rehabilitation Research & Development*, 41.

[40] Johnson, M. J. (2006a). Recent trends in robot-assisted therapy environments to improve real-life functional performance after stroke. *Journal of NeuroEngineering and Rehabilitation*, 3(1):29.

[41] Johnson, M. J. (2006b). Recent trends in robot-assisted therapy environments to improve real-life functional performance after stroke. *Journal of NeuroEngineering and Rehabilitation*, 3(1):29.

[42] Just, F., Özen, Ö., Tortora, S., Riener, R., and Rauter, G. (2017). Feedforward model based arm weight compensation with the rehabilitation robot armin. In *Rehabilitation Robotics (ICORR), 2017 International Conference on*, pages 72–77. IEEE.

[43] Kaczmarek, K. A., Webster, J. G., Bach-y Rita, P., and Tompkins, W. J. (1991). Electrotactile and vibrotactile displays for sensory substitution systems. *IEEE Transactions on Biomedical Engineering*, 38(1):1–16.

[44] Kahn, L. E., Zygman, M. L., Rymer, W. Z., and Reinkensmeyer, D. J. (2006). Robot-assisted reaching exercise promotes arm movement recovery in chronic hemiparetic stroke: a randomized controlled pilot study. *Journal of neuroengineering and rehabilitation*, 3(1):12.

[45] Koenig, A., Novak, D., Omlin, X., Pulfer, M., Perreault, E., Zimmerli, L., Mihelj, M., and Riener, R. (2011). Real-time closed-loop control of cognitive load in neurological patients during robot-assisted gait training. *IEEE Transactions on Neural Systems and Rehabilitation Engineering*, 19(4):453–464.

Francesco Scotto di Luzio

[46] Koritnik, T., Koenig, A., Bajd, T., Riener, R., and Munih, M. (2010). Comparison of visual and haptic feedback during training of lower extremities. *Gait & posture*, 32(4):540–546.

[47] Krebs, H. I., Ladenheim, B., Hippolyte, C., Monterroso, L., and Mast, J. (2009). Robot-assisted task-specific training in cerebral palsy. *Developmental Medicine & Child Neurology*, 51:140–145.

[48] Krebs, H. I., Palazzolo, J. J., Dipietro, L., Ferraro, M., Krol, J., Rannekleiv, K., Volpe, B. T., and Hogan, N. (2003). Rehabilitation robotics: Performance-based progressive robot-assisted therapy. *Autonomous robots*, 15(1):7–20.

[49] Kwakkel, G., Kollen, B. J., and Krebs, H. I. (2008). Effects of robot-assisted therapy on upper limb recovery after stroke: a systematic review. *Neurorehabilitation and neural repair*, 22(2):111–121.

[50] Lam, A. W., HajYasien, A., and Kulic, D. (2014). Improving rehabilitation exercise performance through visual guidance. In *Engineering in Medicine and Biology Society (EMBC), 2014 36th Annual International Conference of the IEEE*, pages 1735–1738. IEEE.

[51] Lambercy, O., Maggioni, S., Lünenburger, L., Gassert, R., and Bolliger, M. (2016). Robotic and wearable sensor technologies for measurements/clinical assessments. In *Neurorehabilitation technology*, pages 183–207. Springer.

[52] Lauretti, C., Cordella, F., Ciancio, A. L., Trigili, E., Catalan, J. M., Badesa, F. J., Crea, S., Pagliara, S. M., Sterzi, S., Vitiello, N., et al. (2018). Learning-by-demonstration for motion planning of upper-limb exoskeletons. *Frontiers in neurorobotics*, 12:5.

[53] Lauretti, C., Cordella, F., di Luzio, F. S., Saccucci, S., Davalli, A., Sacchetti, R., and Zollo, L. (2017a). Comparative performance analysis of m-imu/emg and voice user interfaces for assistive robots. In *Rehabilitation Robotics (ICORR), 2017 International Conference on*, pages 1001–1006. IEEE.

[54] Lauretti, C., Pinzari, G., Ciancio, A. L., Davalli, A., Sacchetti, R., Sterzi, S., Guglielmelli, E., and Zollo, L. (2017b). A vibrotactile stimulation system for improving postural control and knee joint proprioception in lower-limb amputees. In *Robot and Human Interactive Communication (RO-MAN), 2017 26th IEEE International Symposium on*, pages 88–93. IEEE.

[55] Lenzo, B., Fontana, M., Marcheschi, S., Salsedo, F., Frisoli, A., and Bergamasco, M. (2016). Trackhold: a novel passive arm-support device. *Journal of Mechanisms and Robotics*, 8(2):021007.

[56] Li, Z., Milutinovic, D., and Rosen, J. (2015). Spatial map of synthesized criteria for the redundancy resolution of human arm movements. *IEEE Transactions on Neural Systems and Rehabilitation Engineering*, 23(6):1020–1030.

[57] Lum, P. S., Burgar, C. G., Shor, P. C., Majmundar, M., and Van der Loos, M. (2002). Robot-assisted movement training compared with conventional therapy techniques for the rehabilitation of upper-limb motor function after stroke. *Archives of physical medicine and rehabilitation*, 83(7):952–959.

Francesco Scotto di Luzio

[58] Ma, L., Chablat, D., Bennis, F., and Zhang, W. (2009). A new simple dynamic muscle fatigue model and its validation. *International Journal of Industrial Ergonomics*, 39(1):211–220.

[59] Maciejasz, P., Eschweiler, J., Gerlach-Hahn, K., Jansen-Troy, A., and Leonhardt, S. (2014). A survey on robotic devices for upper limb rehabilitation. *Journal of neuroengineering and rehabilitation*, 11(1):3.

[60] Marchal-Crespo, L. and Reinkensmeyer, D. J. (2009a). Review of control strategies for robotic movement training after neurologic injury. *Journal of neuroengineering and rehabilitation*, 6(1):20.

[61] Marchal-Crespo, L. and Reinkensmeyer, D. J. (2009b). Review of control strategies for robotic movement training after neurologic injury. *Journal of neuroengineering and rehabilitation*, 6(1):20.

[62] Marchal-Crespo, L. and Reinkensmeyer, D. J. (2009c). Review of control strategies for robotic movement training after neurologic injury. *Journal of neuroengineering and rehabilitation*, 6(1):20.

[63] Mathiowetz, V., Weber, K., Kashman, N., and Volland, G. (1985). Adult norms for the nine hole peg test of finger dexterity. *The Occupational Therapy Journal of Research*, 5(1):24–38.

[64] McAtamney, L. and Corlett, E. N. (1993). Rula: a survey method for the investigation of work-related upper limb disorders. *Applied ergonomics*, 24(2):91–99.

[65] Mihelj, M., Nef, T., and Riener, R. (2007). A novel paradigm for patient-cooperative control of upper-limb rehabilitation robots. *Advanced Robotics*, 21(8):843–867.

[66] Nordin, N., Xie, S. Q., and Wünsche, B. (2014). Assessment of movement quality in robot-assisted upper limb rehabilitation after stroke: a review. *Journal of neuroengineering and rehabilitation*, 11(1):137.

[67] Novak, D., Mihelj, M., Ziherl, J., Olensek, A., and Munih, M. (2011). Psychophysiological measurements in a biocooperative feedback loop for upper extremity rehabilitation. *IEEE Transactions on Neural Systems and Rehabilitation Engineering*, 19(4):400–410.

[68] Papaleo, E., Zollo, L., Garcia-Aracil, N., Badesa, F., Morales, R., Mazzoleni, S., Sterzi, S., and Guglielmelli, E. (2015a). Upper-limb kinematic reconstruction during stroke robot-aided therapy. In *Medical & Biological Engineering & Computing*, pages 815–828. Springer.

[69] Papaleo, E., Zollo, L., Garcia-Aracil, N., Badesa, F. J., Morales, R., Mazzoleni, S., Sterzi, S., and Guglielmelli, E. (2015b). Upper-limb kinematic reconstruction during stroke robot-aided therapy. *Medical & biological engineering & computing*, 53(9):815–828.

[70] Papaleo, E., Zollo, L., Spedaliere, L., and Guglielmelli, E. (2013). Patient-tailored adaptive robotic system for upper-limb rehabilitation. In *Robotics and Automation (ICRA), 2013 IEEE International Conference on*, pages 3860–3865. IEEE.

[71] Papaleo, E., Zollo, L., Sterzi, S., and Guglielmelli, E. (2012). An inverse kinematics algorithm for upper-limb joint reconstruction during robot-aided motor therapy. In *2012 4th IEEE RAS & EMBS International Conference on Biomedical Robotics and Biomechatronics (BioRob)*, pages 1983–1988. IEEE.

[72] Parker, J., Mountain, G., and Hammerton, J. (2011). A review of the evidence underpinning the use of visual and auditory feedback for computer technology in post-stroke upper-limb rehabilitation. *Disability and rehabilitation: Assistive technology*, 6(6):465–472.

[73] Peternel, L., Tsagarakis, N., Caldwell, D., and Ajoudani, A. (2018). Robot adaptation to human physical fatigue in human–robot co-manipulation. *Autonomous Robots*, 42(5):1011–1021.

[74] Prange, G. B., Jannink, M., Stienen, A., van der Kooij, H., IJzerman, M. J., and Hermens, H. J. (2009). Influence of gravity compensation on muscle activation patterns during different temporal phases of arm movements of stroke patients. *Neurorehabilitation and neural repair*, 23(5):478–485.

[75] Prange, G. B., Kottink, A. I., Buurke, J. H., Eckhardt, M. M., van Keulen-Rouweler, B. J., Ribbers, G. M., and Rietman, J. S. (2015). The effect of arm support combined with rehabilitation games on upper-extremity function in subacute stroke: a randomized controlled trial. *Neurorehabilitation and neural repair*, 29(2):174–182.

[76] Proietti, T., Crocher, V., Roby-Brami, A., and Jarrassé, N. (2016). Upper-limb robotic exoskeletons for neurorehabilitation: a review on control strategies. *IEEE reviews in biomedical engineering*, 9:4–14.

[77] Riener, R., Koenig, A., Bolliger, M., Wieser, M., Duschau-Wicke, A., and Vallery, H. (2009). Bio-cooperative robotics: controlling mechanical, physiological and mental patient states. In *Rehabilitation Robotics, 2009. ICORR 2009. IEEE International Conference on*, pages 407–412. IEEE.

[78] Riener, R. and Munih, M. (2010). Guest editorial special section on rehabilitation via bio-cooperative control. *IEEE Transactions on Neural Systems and Rehabilitation Engineering*, 18(4):337–338.

[79] Riskind, J. H. and Gotay, C. C. (1982). Physical posture: Could it have regulatory or feedback effects on motivation and emotion? *Motivation and Emotion*, 6(3):273–298.

[80] Rodriguez-Guerrero, C., Knaepen, K., Fraile-Marinero, J. C., Perez-Turiel, J., Gonzalez-de Garibay, V., and Lefeber, D. (2017). Improving challenge/skill ratio in a multimodal interface by simultaneously adapting game difficulty and haptic assistance through psychophysiological and performance feedback. *Frontiers in Neuroscience*, 11.

[81] Roh, J., Rymer, W. Z., and Beer, R. F. (2015). Evidence for altered upper extremity muscle synergies in chronic stroke survivors with mild and moderate impairment. *Frontiers in human neuroscience*, 9:6.

[82] Roh, J., Rymer, W. Z., Perreault, E. J., Yoo, S. B., and Beer, R. F. (2012). Alterations in upper limb muscle synergy structure in chronic stroke survivors. *Journal of neurophysiology*, 109(3):768–781.

[83] Rosado, C. and Simone, L. (2007). Translational haptic feedback for post-stroke rehabilitation. In *Bioengineering Conference, 2007. NEBC'07. IEEE 33rd Annual Northeast*, pages 259–260. IEEE.

[84] Runnalls, K. D., Anson, G., and Byblow, W. D. (2015). Partial weight support of the arm affects corticomotor selectivity of biceps brachii. *Journal of neuroengineering and rehabilitation*, 12(1):94.

[85] Sanguineti, V., Casadio, M., Vergaro, E., Squeri, V., Giannoni, P., and Morasso, P. G. (2009). Robot therapy for stroke survivors: proprioceptive training and regulation of assistance. *Stud Health Technol Inform*, 145:126–142.

[86] Santello, M., Baud-Bovy, G., and Jörntell, H. (2013). Neural bases of hand synergies. *Frontiers in computational neuroscience*, 7:23.

[87] Sardini, E., Serpelloni, M., and Pasqui, V. (2014). Wireless wearable t-shirt for posture monitoring during rehabilitation exercises. *IEEE Transactions on Instrumentation and Measurement*, 64(2):439–448.

[88] Sardini, E., Serpelloni, M., Pasqui, V., et al. (2015). Wireless wearable t-shirt for posture monitoring during rehabilitation exercises. *IEEE Trans. Instrumentation and Measurement*, 64(2):439–448.

[89] Scotto di Luzio, F., Cordella, F., Lauretti, C., Simonetti, D., Sterzi, S., Draicchio, F., and Zollo, L. (2019). A bio-cooperative robotic system to ensure ergonomic postures during upper limb rehabilitation in occupational contexts. In *Advances in Intelligent Systems and Computing*, pages 327–336. Springer.

[90] Scotto di Luzio, F., Lauretti, C., Cordella, F., Draicchio, F., and Zollo, L. (2020). Visual vs vibrotactile feedback for posture assessment during upper-limb robot-aided rehabilitation. *Applied ergonomics*, 82:102950.

[91] Scotto di Luzio, F., Simonetti, D., Cordella, F., Carpino, G., Draicchio, F., and Zollo, L. (2018a). An adaptive arm-weight support platform for 3d upper limb robot-aided neuro-rehabilitation. In *2018 7th IEEE International Conference on Biomedical Robotics and Biomechatronics (Biorob)*, pages 426–431. IEEE.

[92] Scotto di Luzio, F., Simonetti, D., Cordella, F., Miccinilli, S., Sterzi, S., Draicchio, F., and Zollo, L. (2018b). Bio-cooperative approach for the human-in-the-loop control of an end-effector rehabilitation robot. *Frontiers in neurorobotics*, 12.

[93] Sigrist, R., Rauter, G., Riener, R., and Wolf, P. (2013). Augmented visual, auditory, haptic, and multimodal feedback in motor learning: a review. *Psychonomic bulletin & review*, 20(1):21–53.

[94] Simonetti, D., Zollo, L., Papaleo, E., Carpino, G., and Guglielmelli, E. (2016). Multimodal adaptive interfaces for 3d robot-mediated upper limb neuro-rehabilitation: An overview of bio-cooperative systems. *Robotics and Autonomous Systems*, 85:62–72.

[95] Simonetti, D., Zollo, L., Papaleo, E., Carpino, G., and Guglielmelli, E. (2017). Reprint of "multimodal adaptive interfaces for 3d robot-mediated upper limb neuro-rehabilitation: An overview of bio-cooperative systems". *Robotics and Autonomous Systems*, 90:86–96.

[96] Singh, R. E., Iqbal, K., White, G., and Hutchinson, T. E. (2018). A systematic review on muscle synergies: From building blocks of motor behavior to a neurorehabilitation tool. *Applied bionics and biomechanics*, 2018.

[97] Song, R., Tong, K.-y., Hu, X., and Zhou, W. (2013). Myoelectrically controlled wrist robot for stroke rehabilitation. *Journal of neuroengineering and rehabilitation*, 10(1):52.

[98] Stienen, A. H., Hekman, E. E., Prange, G. B., Jannink, M. J., van der Helm, F. C., and van der Kooij, H. (2009). Freebal: design of a dedicated weight-support system for upper-extremity rehabilitation. *Journal of medical devices*, 3(4):041009.

[99] Sun, M., Ren, X., and Cao, X. (2010). Effects of multimodal error feedback on human performance in steering tasks. *Journal of Information Processing*, 18:284–292.

[100] Taborri, J., Agostini, V., Artemiadis, P. K., Ghislieri, M., Jacobs, D. A., Roh, J., and Rossi, S. (2018). Feasibility of muscle synergy outcomes in clinics, robotics, and sports: a systematic review. *Applied bionics and biomechanics*, 2018.

[101] Thielman, G. (2010). Rehabilitation of reaching poststroke: a randomized pilot investigation of tactile versus auditory feedback for trunk control. *Journal of Neurologic Physical Therapy*, 34(3):138–144.

[102] Tresch, M. C., Cheung, V. C., and d'Avella, A. (2006). Matrix factorization algorithms for the identification of muscle synergies: evaluation on simulated and experimental data sets. *Journal of neurophysiology*, 95(4):2199–2212.

[103] Valdés, B. A., Glegg, S. M., and Van der Loos, H. M. (2017). Trunk compensation during bimanual reaching at different heights by healthy and hemiparetic adults. *Journal of motor behavior*, 49(5):580–592.

[104] van Vliet, P. and Wulf, G. (2006). Extrinsic feedback for motor learning after stroke: what is the evidence?. *Disability and Rehabilitation*, 28(13–14):831–840.

[105] Veerbeek, J. M., Langbroek-Amersfoort, A. C., Van Wegen, E. E., Meskers, C. G., and Kwakkel, G. (2017). Effects of robot-assisted therapy for the upper limb after stroke: a systematic review and meta-analysis. *Neurorehabilitation and neural repair*, 31(2):107–121.

[106] Wang, Q., Markopoulos, P., Yu, B., Chen, W., and Timmermans, A. (2017). Interactive wearable systems for upper body rehabilitation: a systematic review. *Journal of neuroengineering and rehabilitation*, 14(1):20.

[107] Wells, R., Norman, R., Neumann, P., Andrews, D., Frank, J., Shannon, H., and Kerr, M. (1997). Assessment of physical work load in epidemiologic studies: common measurement metrics for exposure assessment. *Ergonomics*, 40(1):51–61.

[108] Winter, D. A. (2009). *Biomechanics and motor control of human movement*. John Wiley & Sons.

[109] Zariffa, J., Kapadia, N., Kramer, J., Taylor, P., Alizadeh-Meghrazi, M., Zivanovic, V., Willms, R., Townson, A., Curt, A., Popovic, M., et al. (2012). Feasibility and efficacy of upper limb robotic rehabilitation in a subacute cervical spinal cord injury population. *Spinal Cord*, 50(3):220.

[110] Zheng, Y. and Morrell, J. B. (2013). Comparison of visual and vibrotactile feedback methods for seated posture guidance. *IEEE transactions on haptics*, 6(1):13–23.

[111] Zollo, L., Laschi, C., Teti, G., Siciliano, B., and Dario, P. (2001a). Functional compliance in the control of a personal robot. In *Intelligent Robots and Systems, 2001. Proceedings. 2001 IEEE/RSJ International Conference on*, volume 4, pages 2221–2226. IEEE.

[112] Zollo, L., Laschi, C., Teti, G., Siciliano, B., and Dario, P. (2001b). Functional compliance in the control of a rehabilitation robot. In *PROCEEDINGS OF THE ... IEEE/RSJ INTERNATIONAL CONFERENCE ON INTELLIGENT ROBOTS AND SYSTEMS*, pages 2221–2226. IEEE.